Optimization of future projects for the measurement of Cosmic Microwave Background polarization

HOANG Duc-Thuong

The jury:

Francois Couchot	*Rapporteur*
Gérard Rousset	*Examinateur*
Giampaolo Pisano	*Rapporteur*
Sophie Henrot-Versillé	*Examinateur*
Damien Prêle	*Co-encadrant*
Guillaume Patanchon	*Directeur de thèse*

APC, December 17, 2018

Contents

★Systematic effect studies: Bandpass mismatch

★QUBIC's TES array Response to particles

The Universe

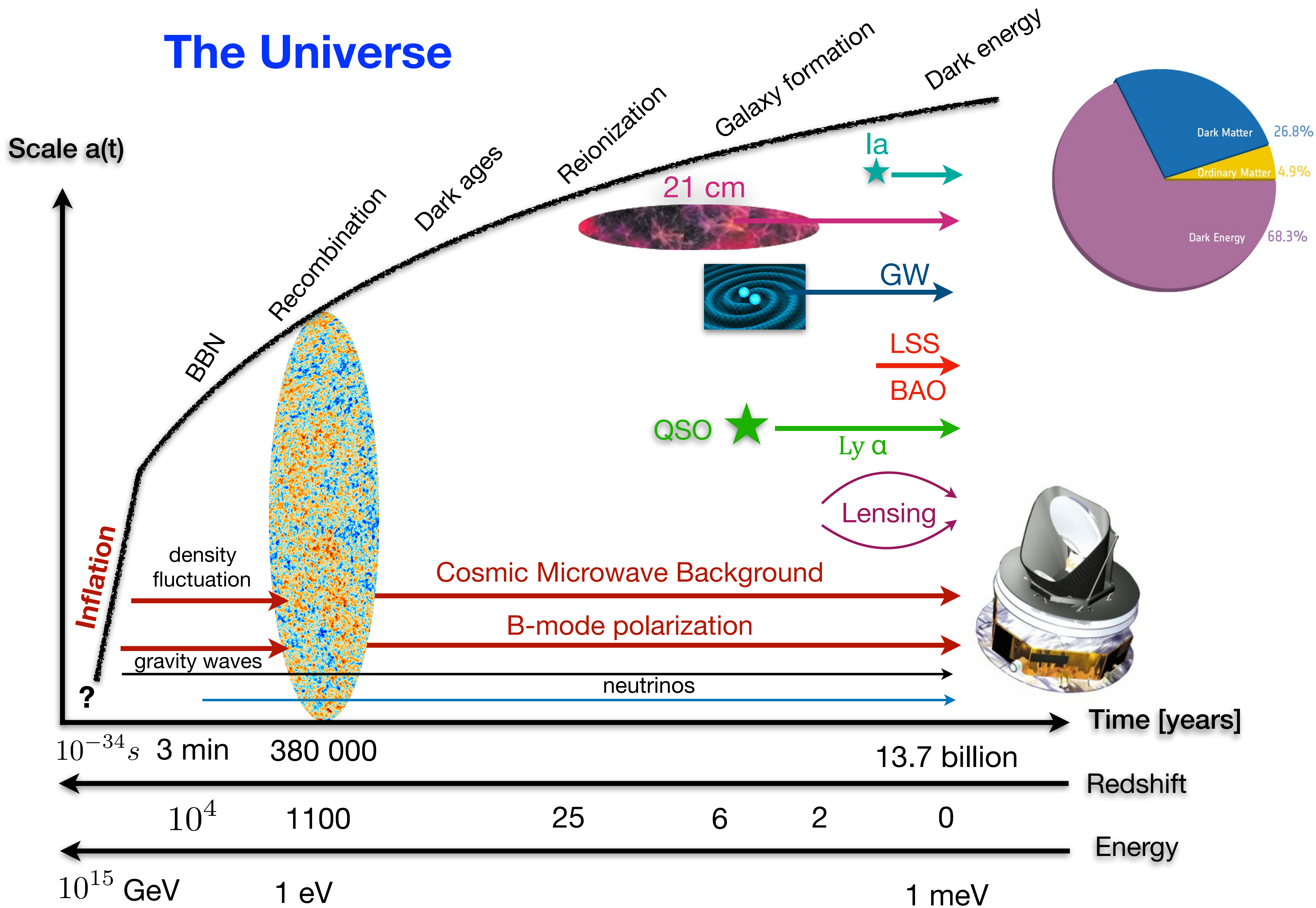

The history and the evolution of the Universe in time and scale factor.

Standard cosmological model

Dynamics

GR, fluid eq.,
Stress-Energy Tensor

$$R_{\mu\nu} - \frac{1}{2}g_{\mu\nu}R - \Lambda g_{\mu\nu} = 8\pi G T_{\mu\nu}$$

Geometry, Structure

Homogeneous and isotropy,
Metric

$$ds^2 = -c^2dt^2 + a^2(t)\left(\frac{dr^2}{1-kr^2} + r^2\left(d\theta^2 + \sin^2\theta d\phi^2\right)\right)$$

Contents

Matter, radiation,
cosmological constant

$$\Omega = \Omega_m + \Omega_r + \Omega_\Lambda$$

Early Universe

Inflation, BBN, CMB

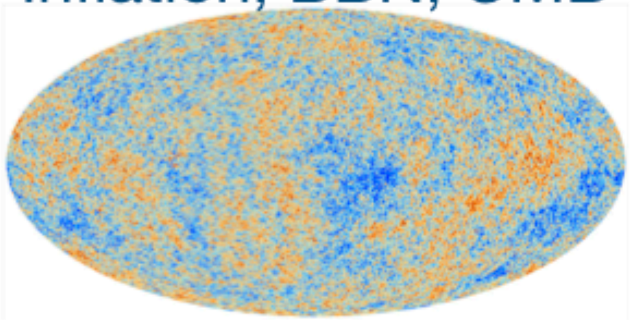

Expansion,

a, H, h, z

$$v = H_0 D$$

Age

H, z

$$\begin{aligned} t_0 &= \frac{2}{3}H_0^{-1} \\ &= 6.51h^{-1} \times 10^9 \quad yrs \end{aligned}$$

Fate

H, z, k, a

$$\Omega - 1 = -\frac{kc^2}{H^2a^2}$$

- **Observational cosmology gives constraint on the ΛCDM cosmological model parameters $\Omega_\Lambda, \Omega_b, \Omega_c, \tau, n_s, A_s, H\ldots$**

Cosmic Microwave Background (CMB)

- **Formation**: CMB is radiation from around 380 000 years after the Universe was born at *recombination epoch*

$$e^- + p \rightleftharpoons H + \gamma$$

-> CMB photons were freely travel to the entire the Universe: *decoupling epoch*

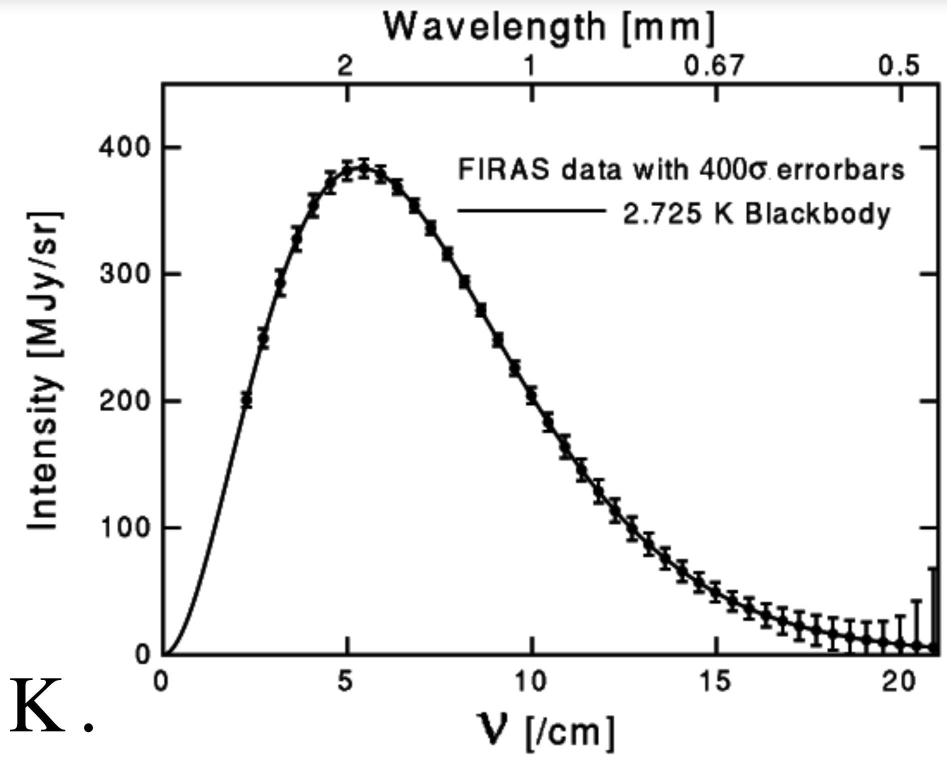

- **Discover: in 1964 by Penzias & Wilson.**
- **CMB spectrum is a black-body (COBE)** $T_{CMB} = 2.725\,\mathrm{K}$.
- **Temperature anisotropies** $10^{-5}\mathrm{K}$ **: Sachs-Wolfe effect, Doppler effect.**
- **~ 10% CMB anisotropies are polarized by free electrons at last scattering surface.**

$\sim 400\,\gamma/\mathrm{cm}^3$

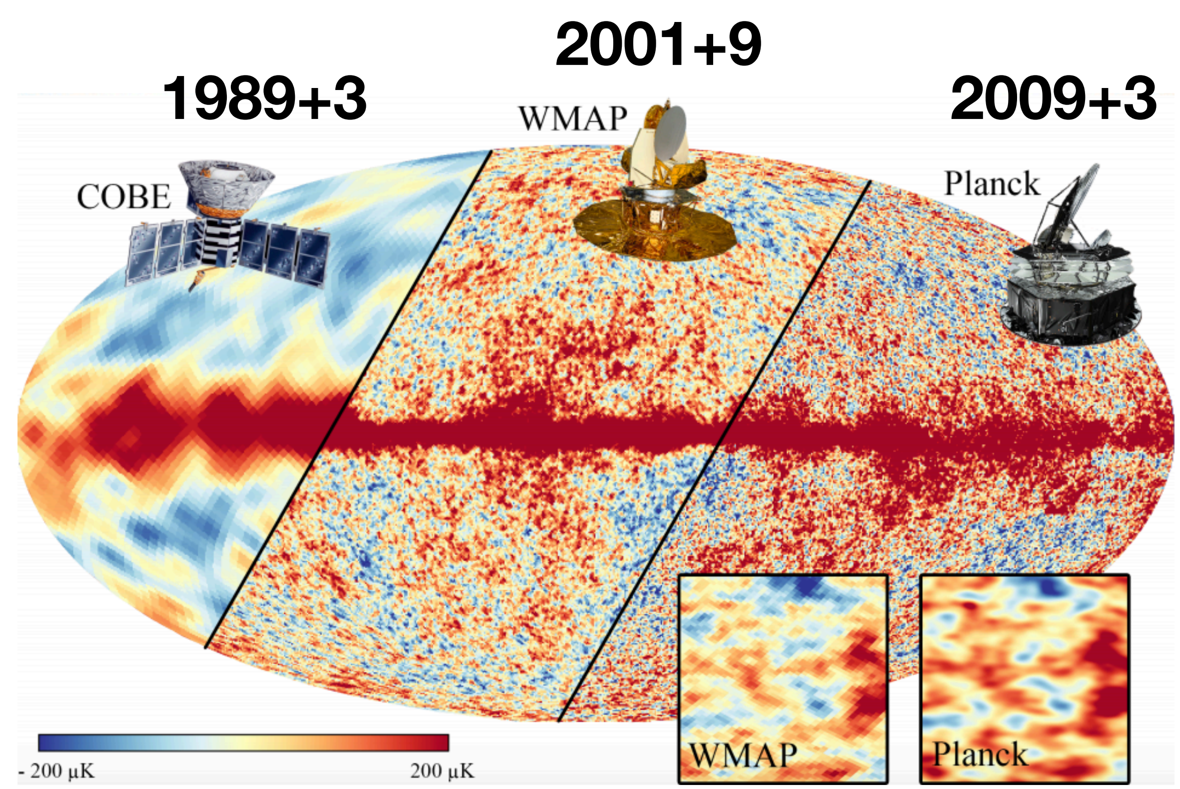

CMB polarization: Stoke parameters

A monochromatic light in z-direction:

$$E_x = E_{0x} \cos\left(\omega_0 t - \theta_x\right); \; E_y = E_{0y} \cos\left(\omega_0 t - \theta_y\right)$$

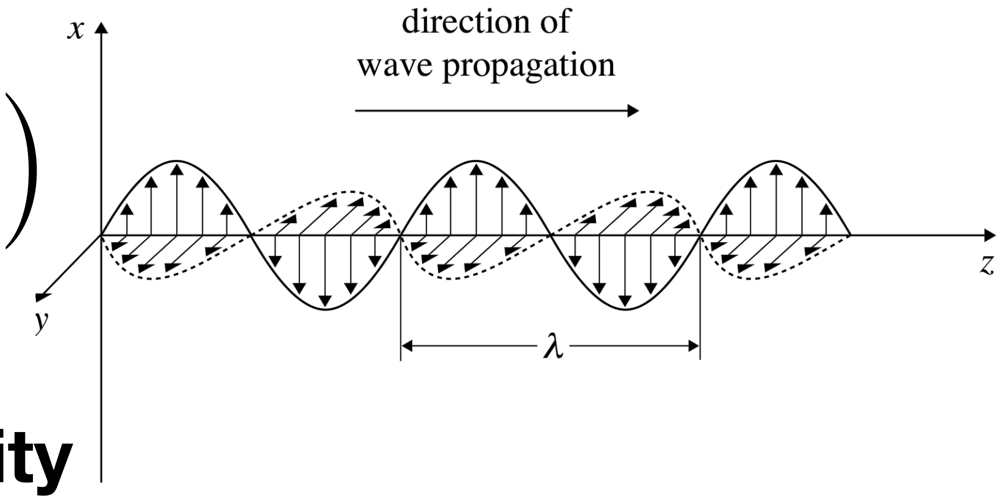

$$I \equiv \langle E_{0x}^2 \rangle + \langle E_{0y}^2 \rangle$$ **Intensity**

$$Q \equiv \langle E_{0x}^2 \rangle - \langle E_{0y}^2 \rangle$$ **Linear polarization**

$$U \equiv \langle 2E_{0x}E_{0y} \cos(\theta_y - \theta_x) \rangle$$ **Linear polarization**

$$V \equiv \langle 2E_{0x}E_{0y} \sin(\theta_y - \theta_x) \rangle$$ **Circular polarization**

In the second-order spin spherical harmonics of degree ℓ and order m:

$$\left(Q \pm iU\right)\left(\theta, \varphi\right) = \sum a_{\pm 2\ell m} Y_{\pm 2\ell m}\left(\theta, \varphi\right)$$

multipoles coefficient

- **Q, U depend on the coordinate system**

CMB polarization (Thomson scattering)

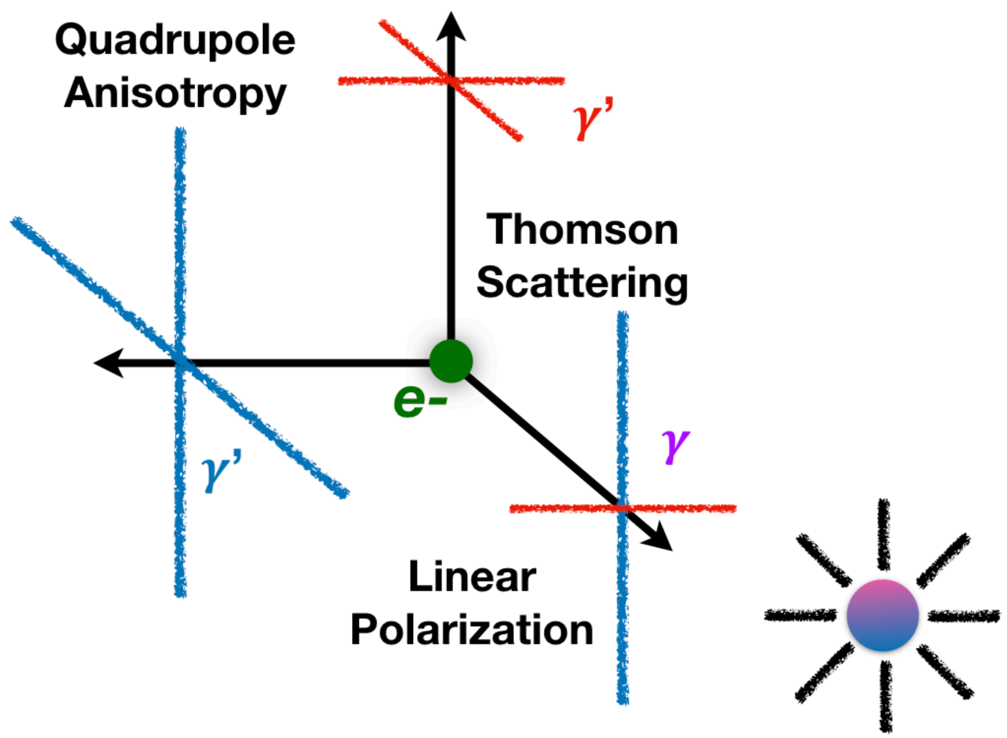

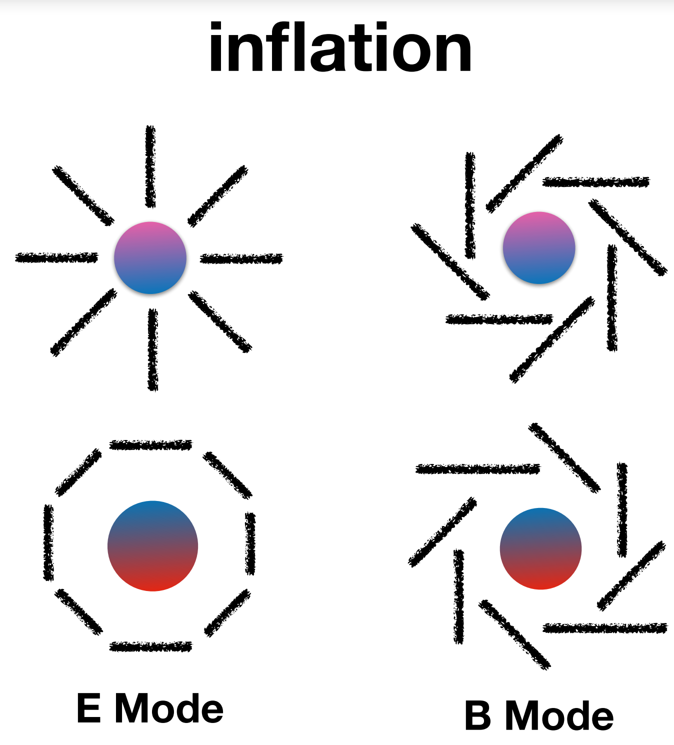

Gravity waves from inflation stretch and squeeze space in orthogonal directions.
Gravity waves from inflation would produce tensor perturbations.
Primordial B-mode is due to only tensor perturbation in inflation!

The polarization pattern can be decomposed into 2 components:

- Curl-free component, called "E-mode" (electric-field) or "gradient-mode"
- Grad-free component, called "B-mode" (magnetic-field) or "curl-mode"

State of the art
After Planck 2018

- **Temperature anisotropies are measured with high accuracy**
- **E-mode polarization is well fit with concordance model (DASI 2002.)**
- **B-mode is not yet measured!**
- **Foreground components challenges**
- **Systematic effects challenges**

Goal: Tensor-to-scalar ratio r

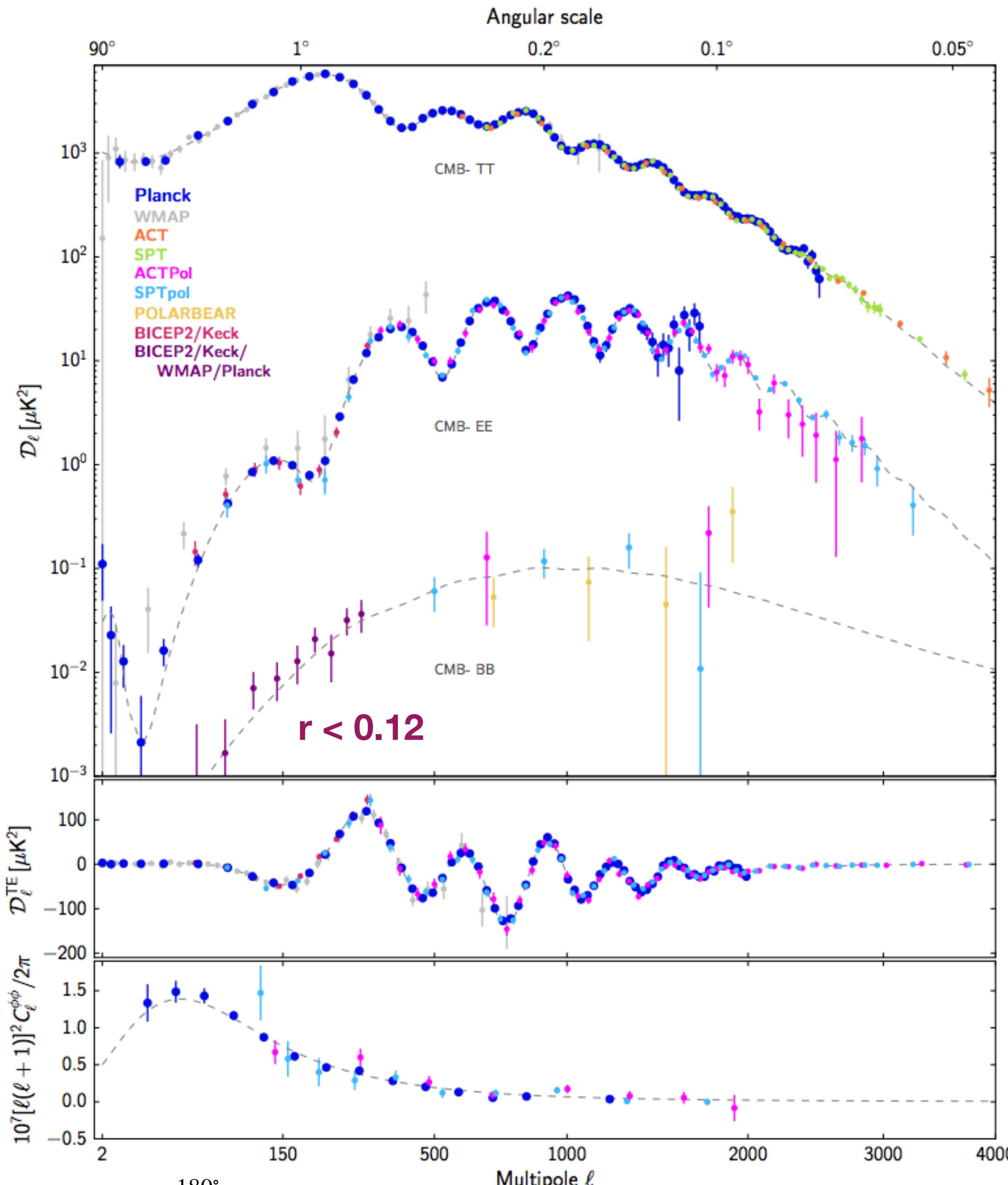

$$\ell = \frac{180^\circ}{\theta}$$

State of the art

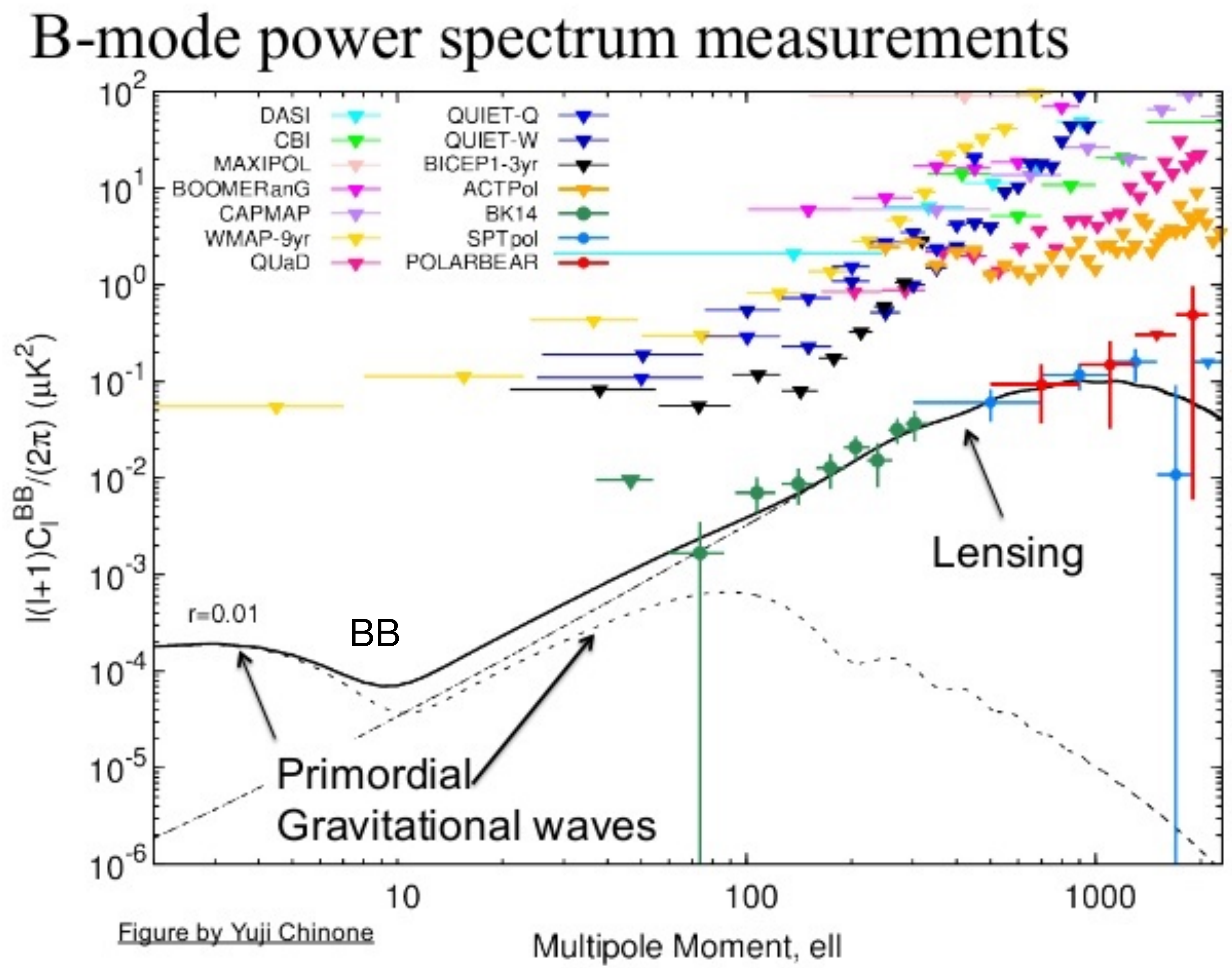

I.1. LiteBIRD science goal

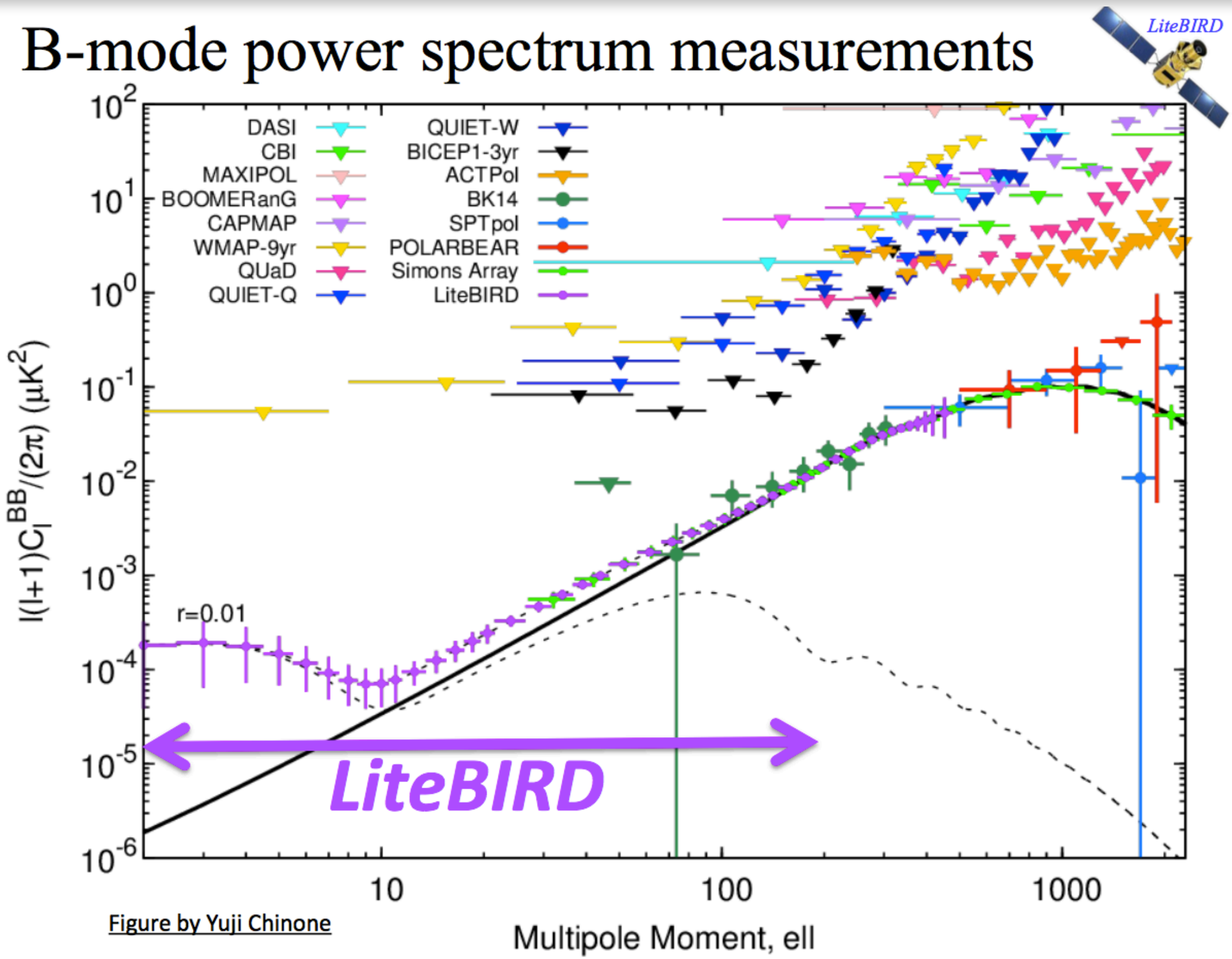

Measurements with r < 0.002 (95% C.L.) for 2 ≤ l ≤ 200 are important

I.1. LiteBIRD Payload module

Phase A1

- Japan: Rocket, Satellite, LFT
- Europe: HFT, sub-Kelvin Cooler
- USA: TES focal plane
- Canada: Warm readout electronics

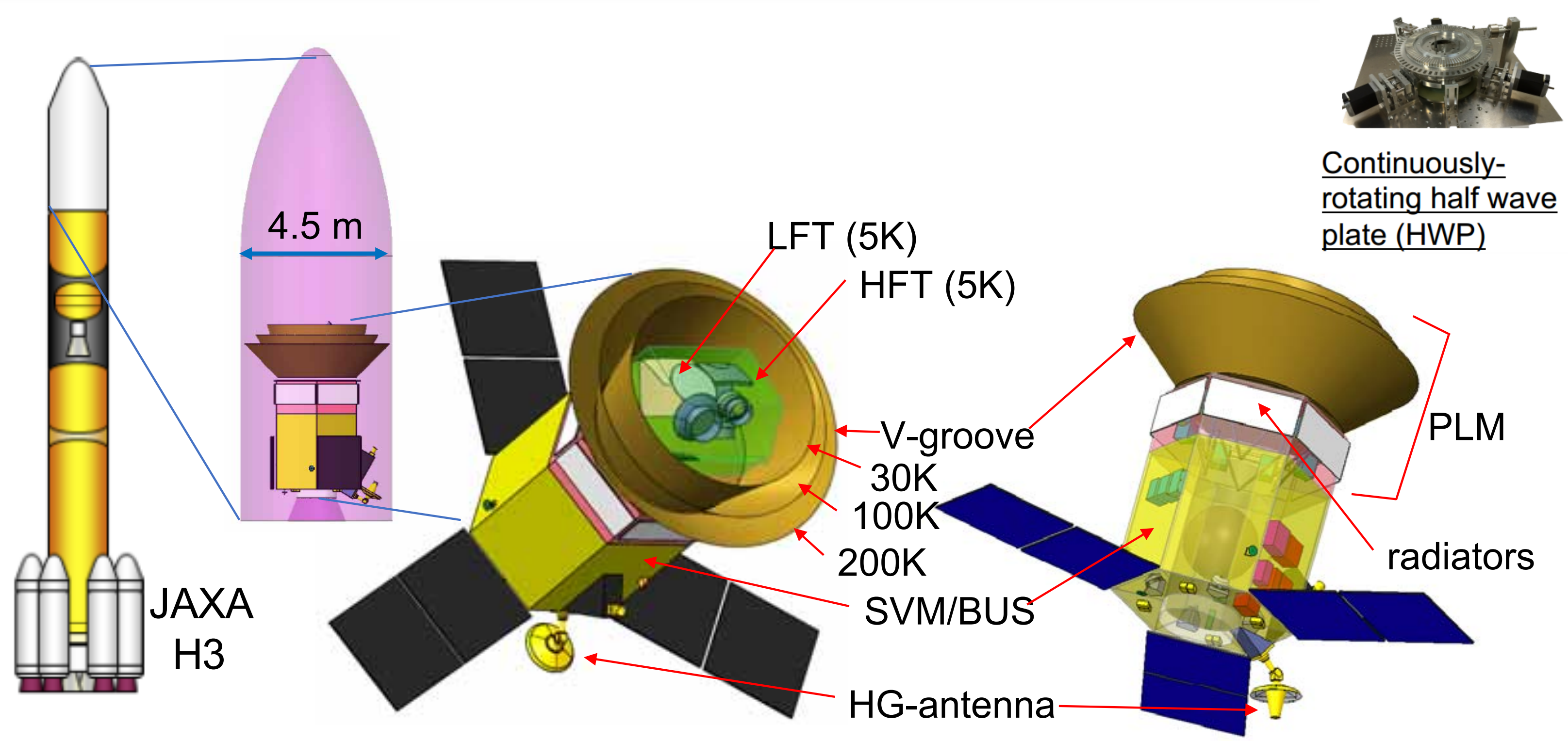

- 3-year at L2 orbit
- Low frequency telescope (40 cm, 20-70 arcmin)
- High frequency telescope (30 cm, 10-40 arcmin)
- Rotating half-wave plate (HWP) modulation
- TES focal plane at 100 mK
- The mass and consumption power 2.6 tons, 3.0 kW

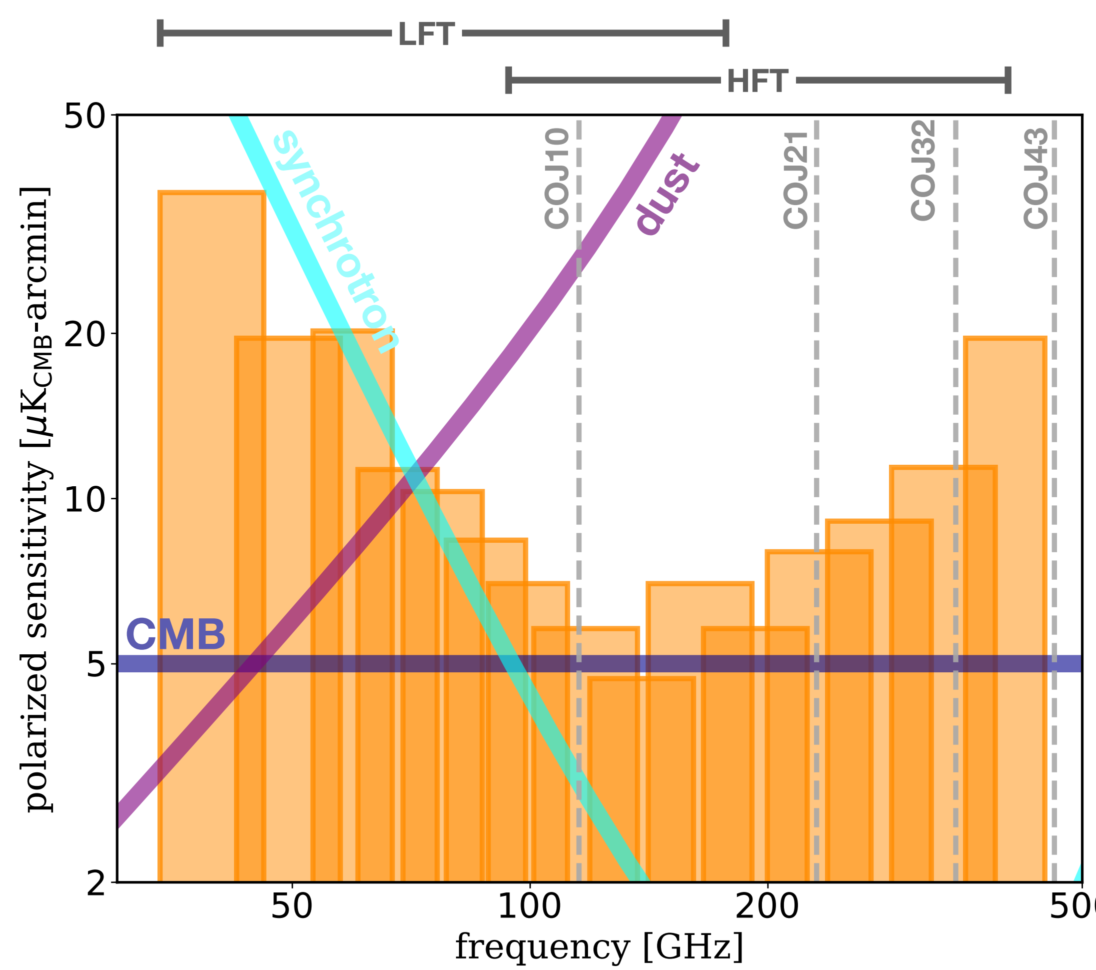

I.1. LiteBIRD Focal plane

High Frequency Telescope (HFT)

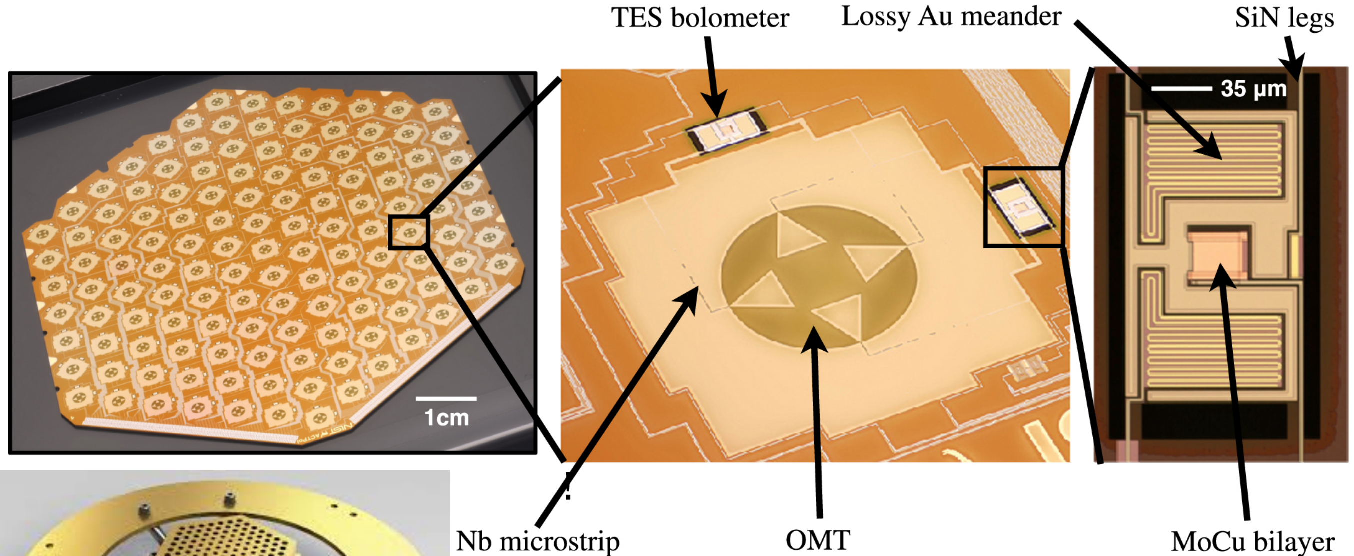

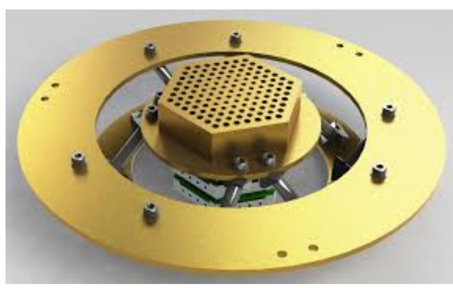

The TES array with corrugated feed horn developed for ABS, ACTpol, SPTpol by UC Boulder, NIST and Stanford

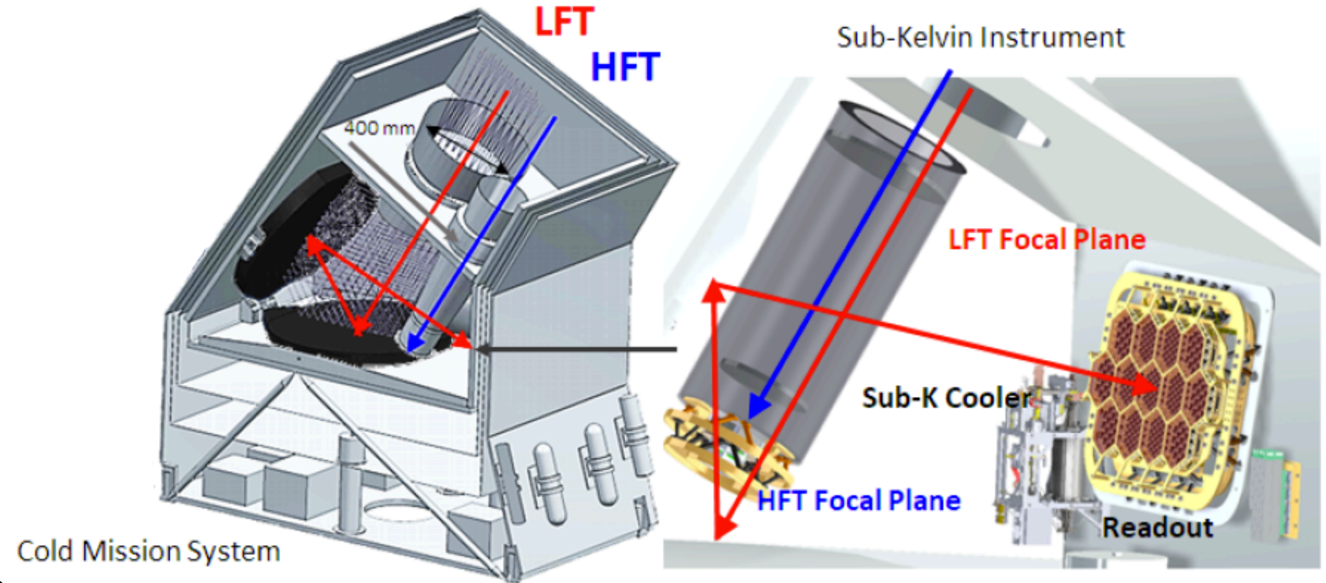

Low Frequency Telescope (LFT)

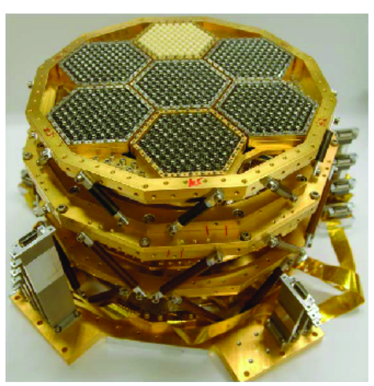

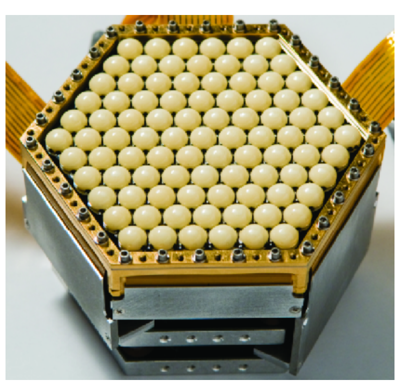

The TES array with a lenslet developed for POLARBEAR by UC Berkeley and UCSD

- LFT 34 GHz ~ 161 GHz: Synchrotron + CMB
- HFT 89 GHz ~ 448 GHz: CMB + Dust

15 frequency bands
> 2000 TES detectors

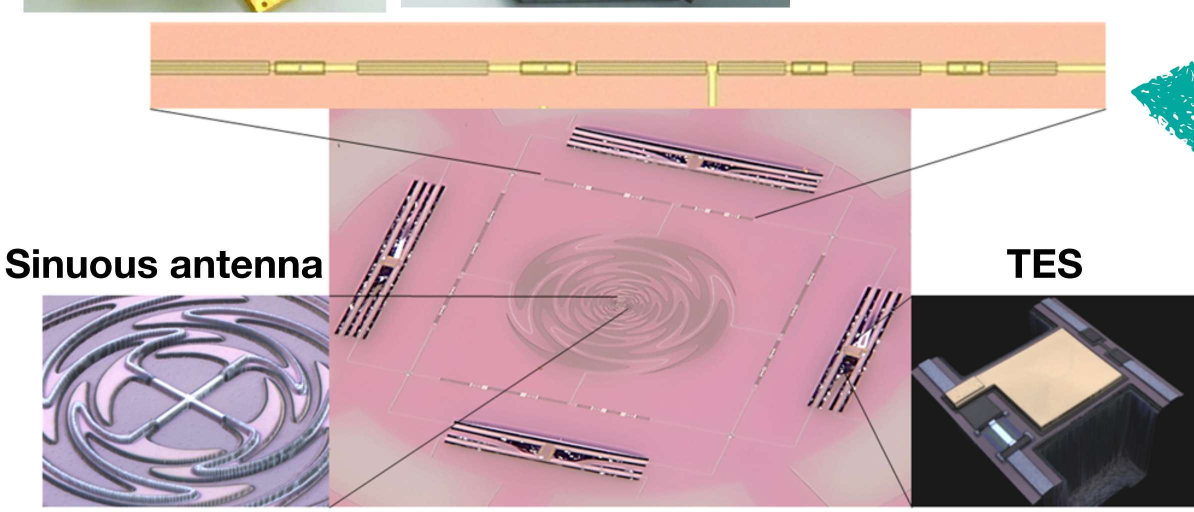

Bandpass filters

I.1. LiteBIRD scanning strategy

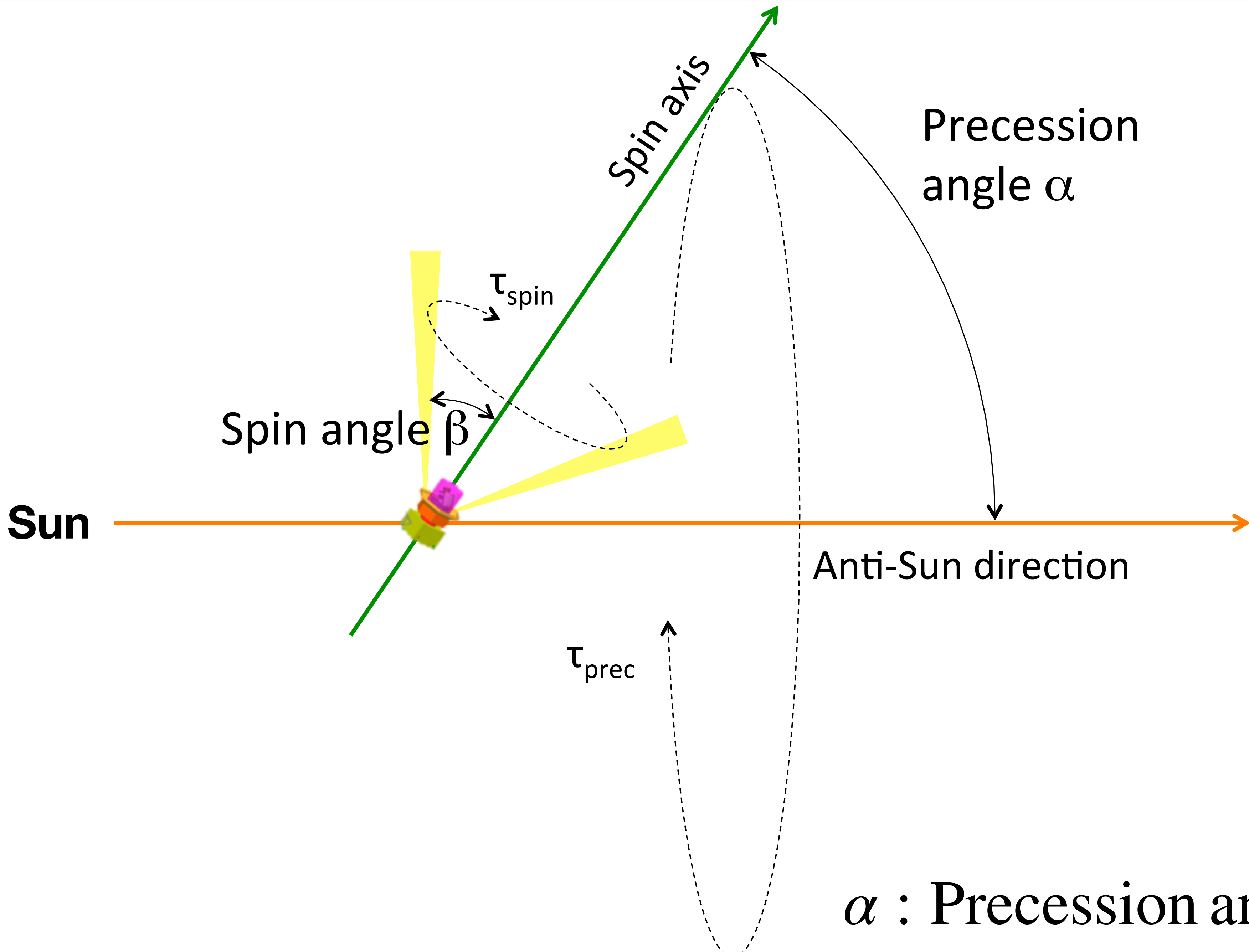

α : Precession angle [deg]

β : Spin angle [deg]

$\tau_{\rm prec}$ or $\omega_{\rm prec}$: Precession spin [time]

$\tau_{\rm spin}$ or $\omega_{\rm spin}$: Rotating spin [rpm]

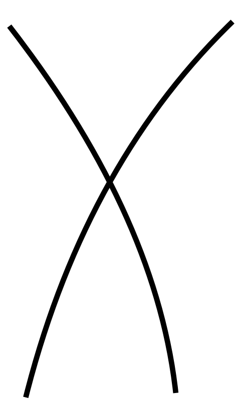

- **Many angles to measure polarization**

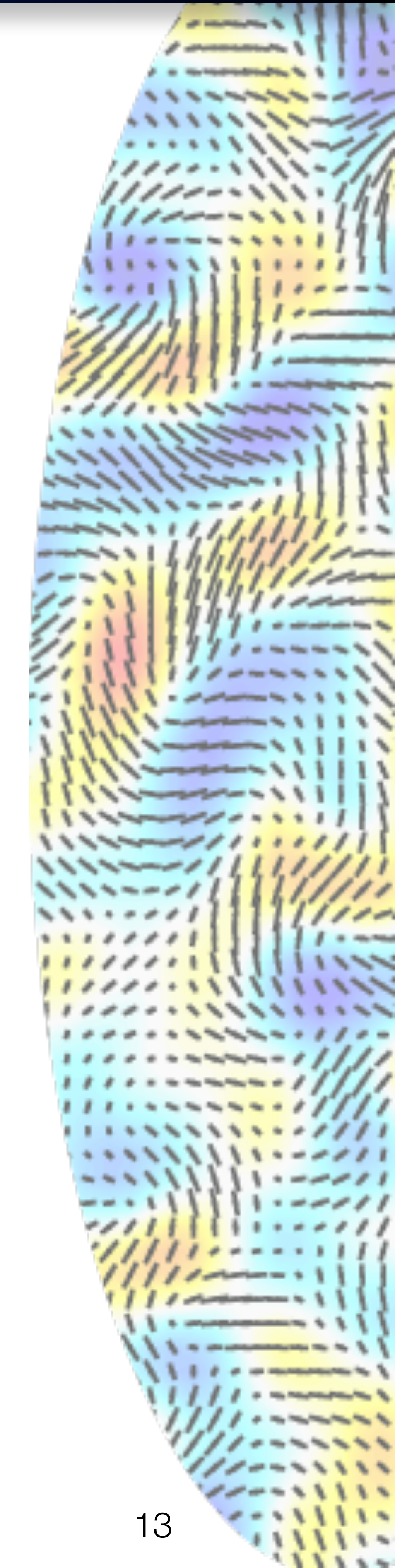

I.1. Foreground components

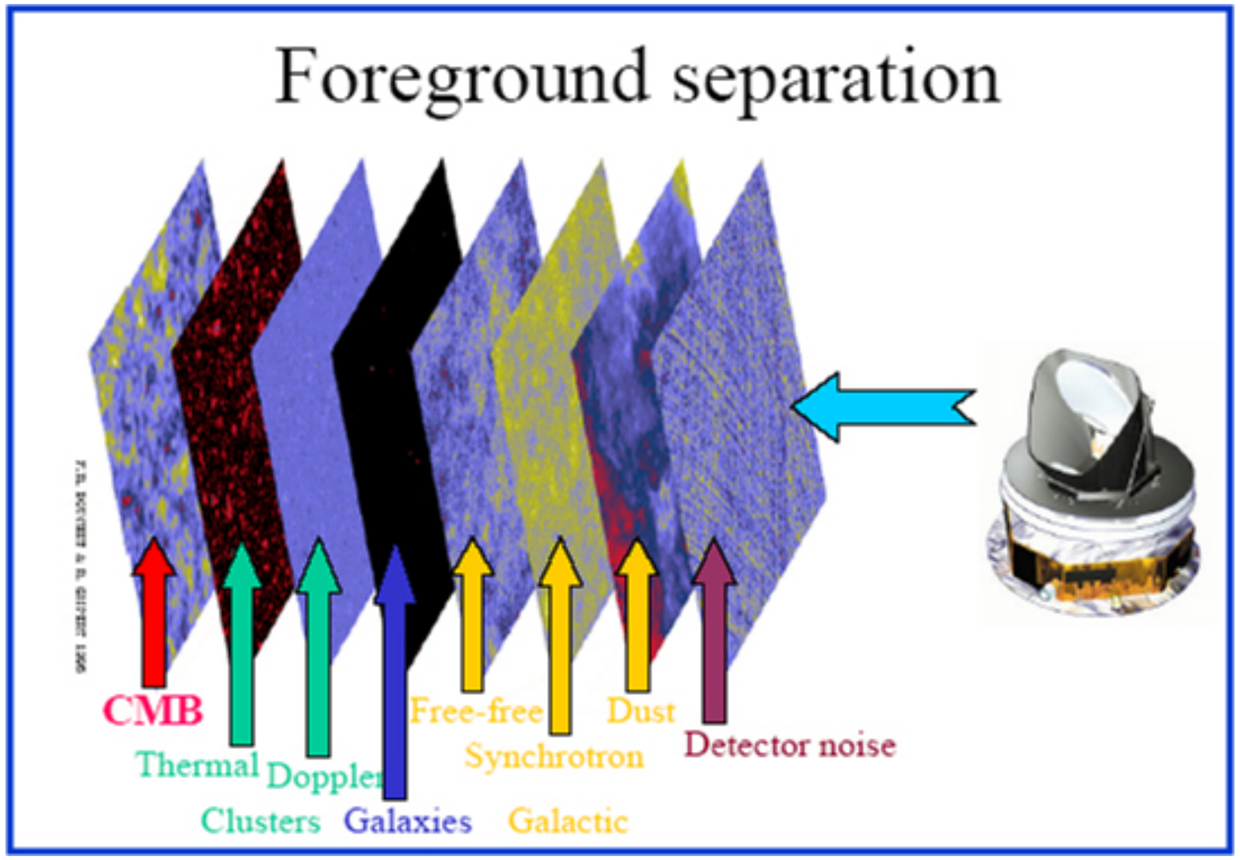

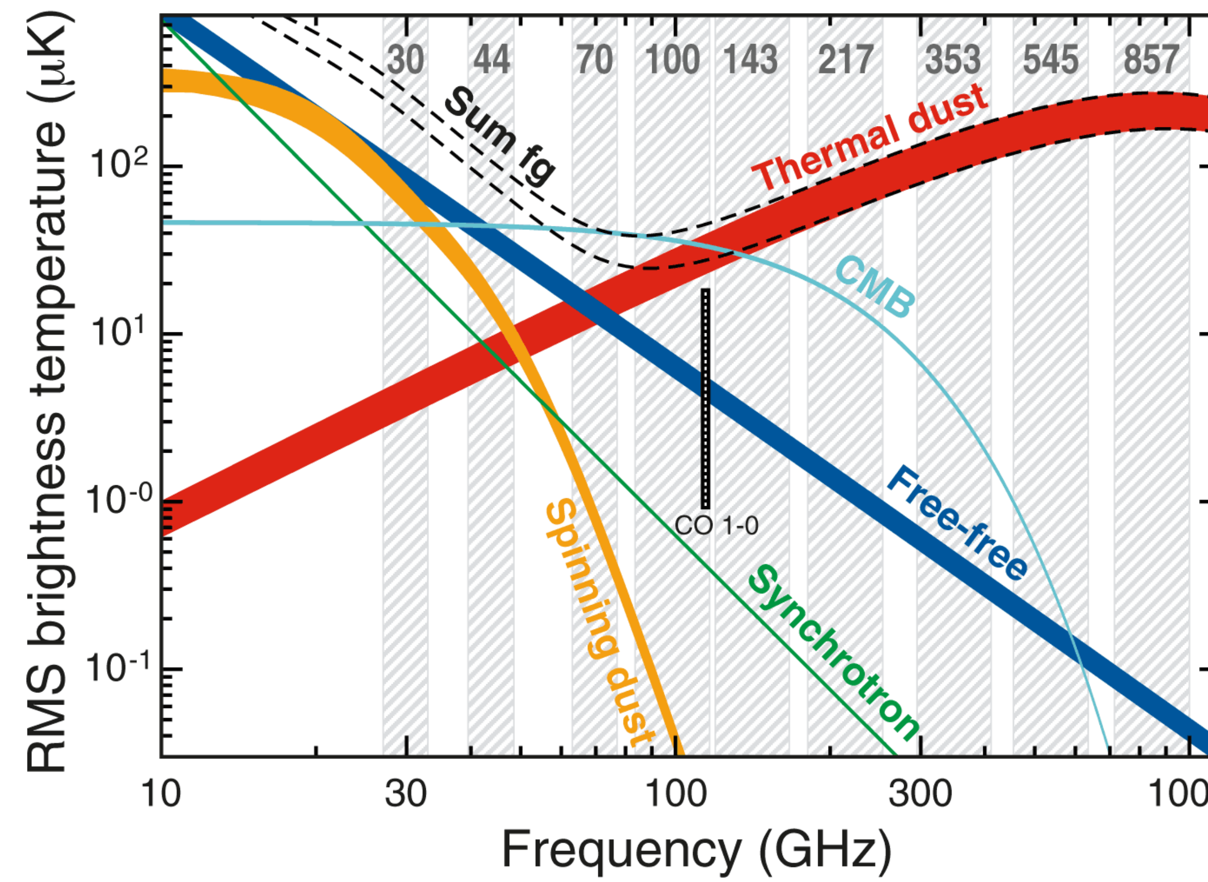

$$S_{sky} = I + Q\cos 2\psi + U\sin 2\psi + n$$

ψ : Polarizer angle

$$I = I_{CMB} + I_{dust} + I_{other\ components}$$

Similar for Q and U.

I, Q, U are Stokes parameters.

I.2. Potential systematic effects

Planck HFI lessons:

- Beam mismatch
- Cosmic rays
- 1/f noise
- ADC non-linearity
- ***Bandpass mismatch***
- Thermal fluctuations

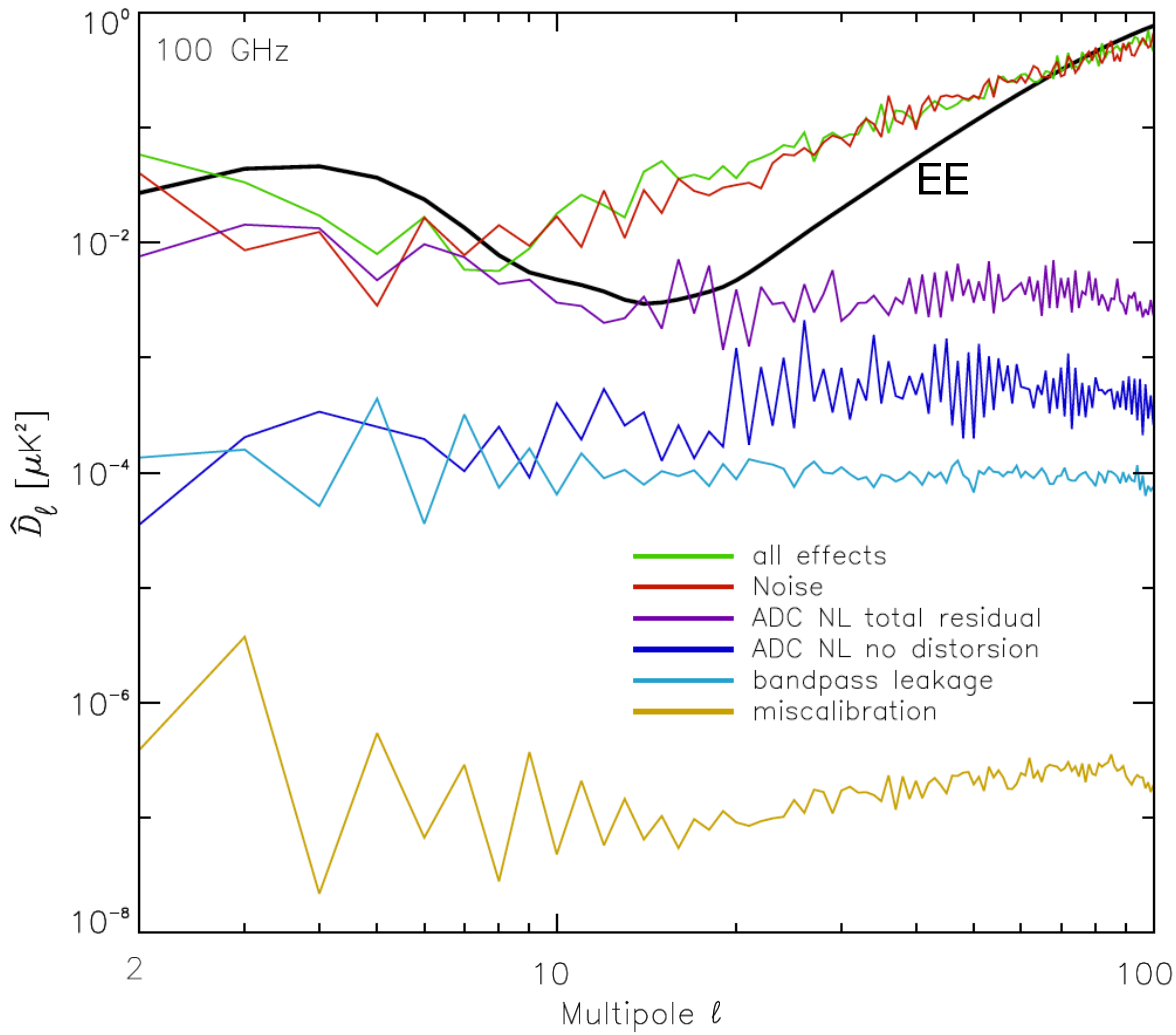

Planck: A&A 596, A107 (2016)

I.2. Bandpass mismatch

Bandpass shape of several Planck-HFI detectors

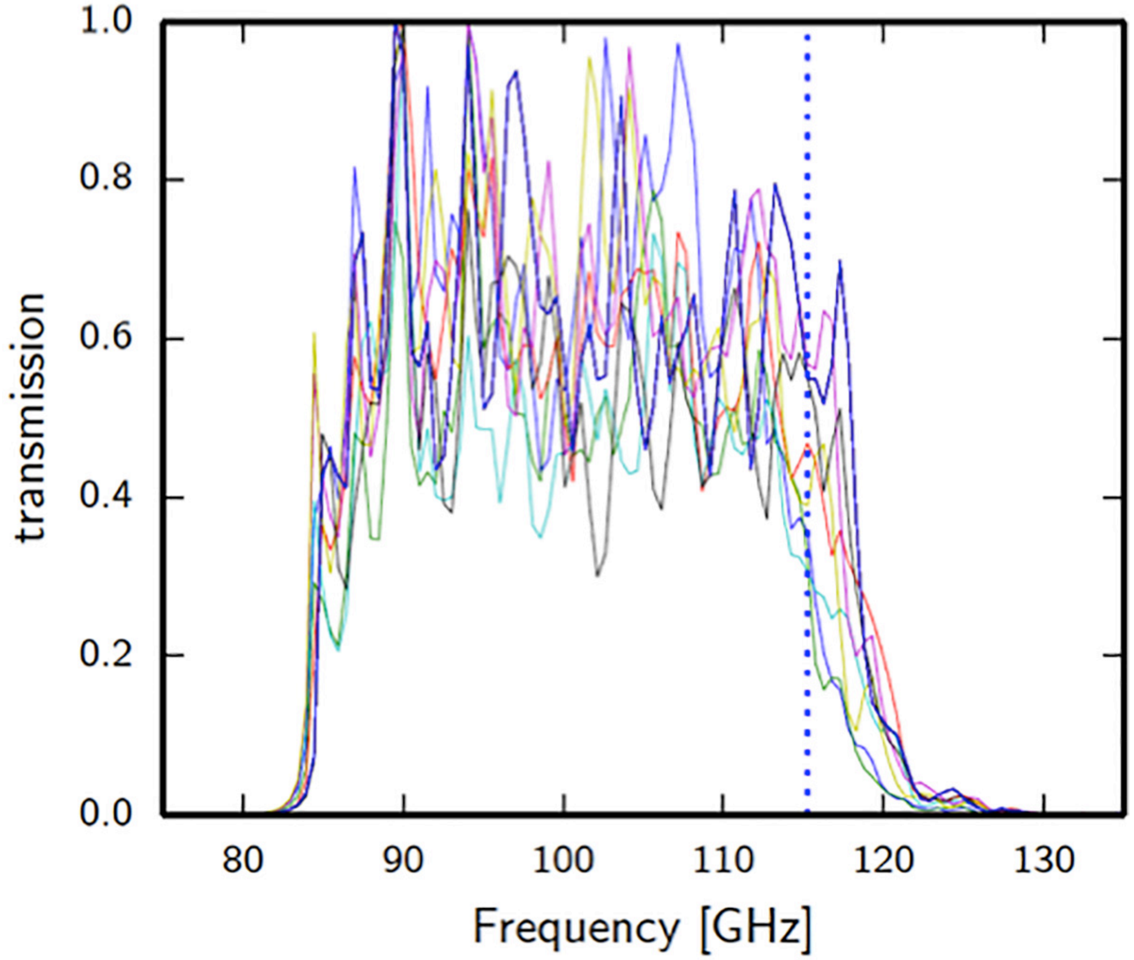

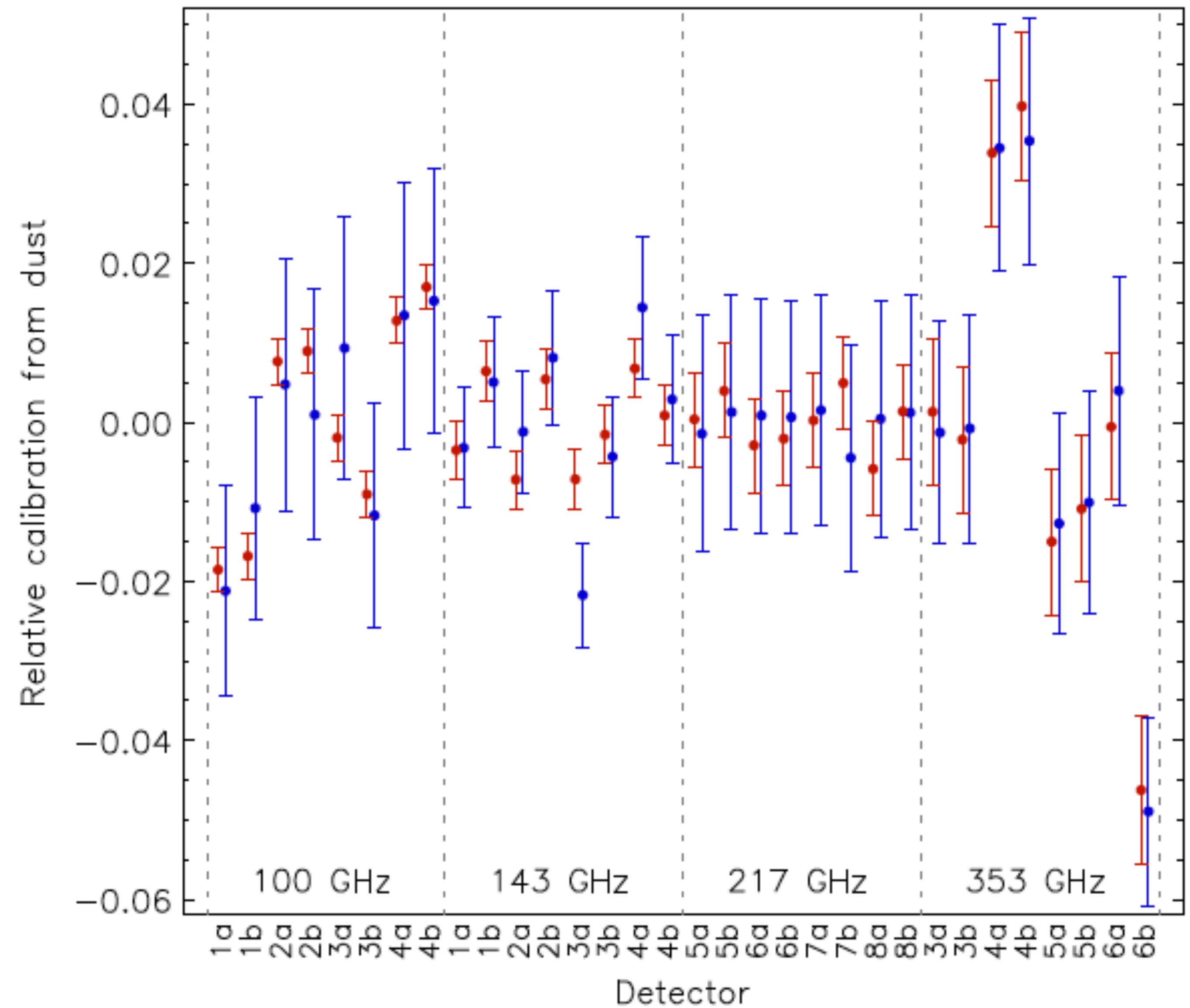

The micro-fabricated technology could contribute to non-ideality of bandpass filters (layer to layer misalignment, dielectric constant, dielectric thickness).

Blue: ground, red: flight

(Planck: A&A 596, A107 (2016))

Leakage from intensity I to polarization Q, U

I.2. Simulation

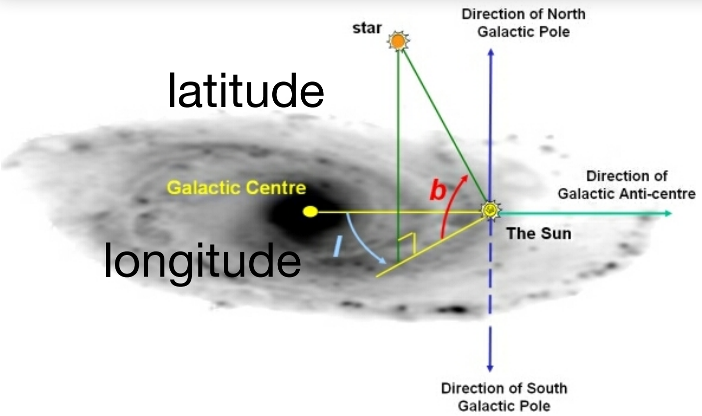

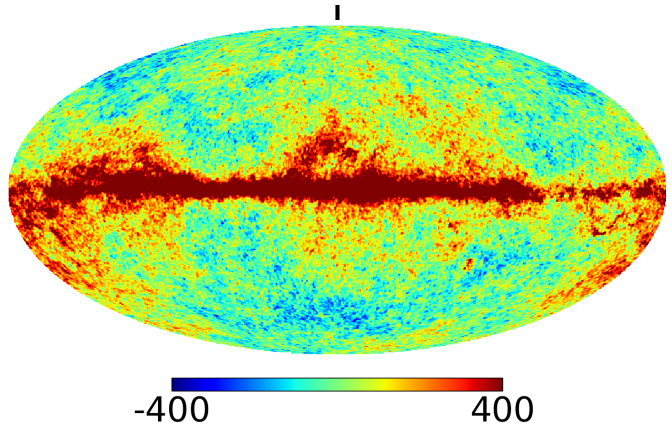

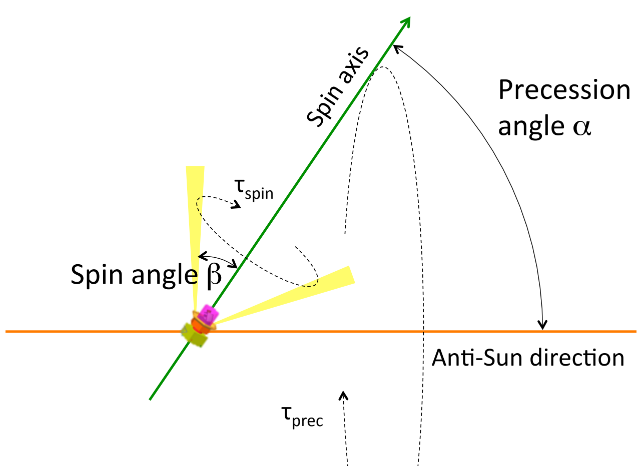

mask 256 galactic

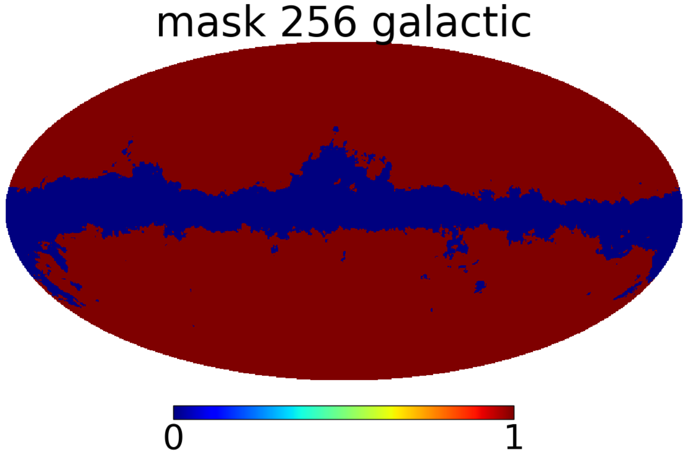

Filter Simulation
γ_d

CMB map → ← Dust map

Data Simulation
$d = I_{CMB} + \gamma_d I_{dust}$

Scanning strategy →

Map Making
$(A^T N^{-1} A)^{-1} A^T N^{-1} d$

← Mask 20%

Angular Power Spectrum
C_l^{BB}, C_l^{EE}

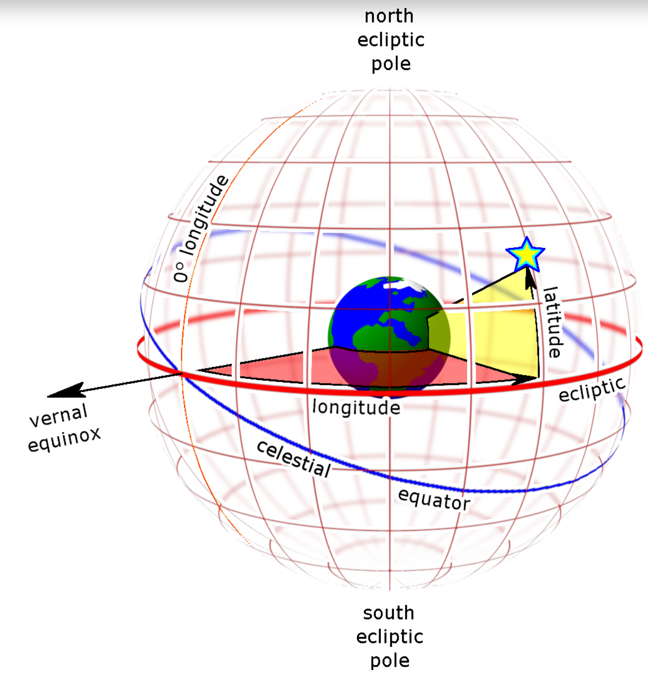

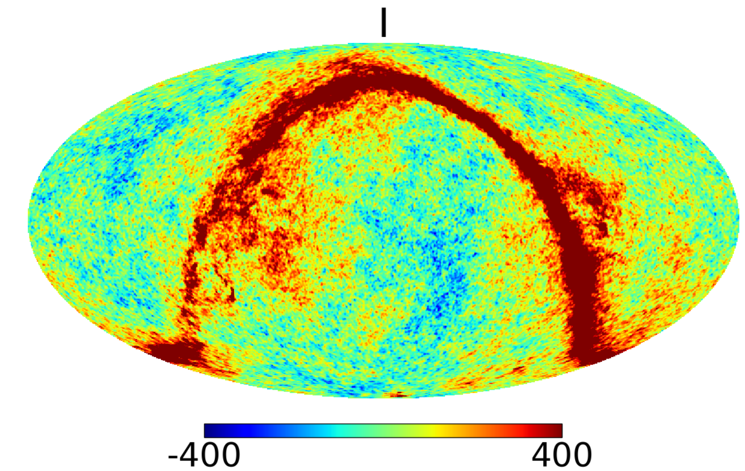

mask 256 ecliptic

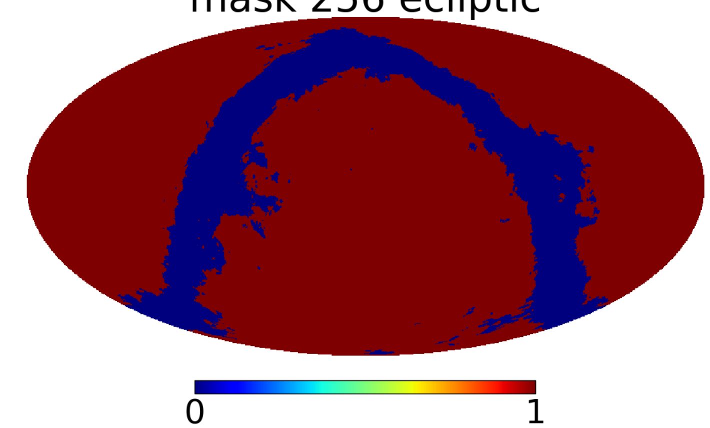

I.2.1. Bandpass mismatch calibration factor

Filters

Dust: Grey body

$$\gamma_d = \left(\frac{\int d\nu \; g_i(\nu) \left(\frac{\nu}{\nu_0}\right)^{\beta} \frac{B(\nu;T_d)}{B(\nu_0;T_d)}}{\int d\nu g_i(\nu) \left(\frac{\partial B(\nu;T)}{\partial T}\right)\Big|_{T_0}} \right) \left(\frac{\partial B(\nu_0;T)}{\partial T}\right)\Big|_{T_0}$$

CMB: Black body

Normalization CMB

$T_0 = T_{CMB} = 2.725$

$T_d = 19\mathrm{K}$

$\beta = 1.62$

$\nu_0 = 140\ \mathrm{GHz}$

Planck's law $B(\nu, T) = \frac{2h\nu^3}{c^2} \frac{1}{e^{\frac{h\nu}{k_B T}} - 1}$

$\gamma_{\mathrm{s}}, \gamma_{\mathrm{f}}, \gamma_{\mathrm{spin}}$

I.2.1. Bandpass filter

Planck-like errors
(1 % vary on edges)

Typical measurement errors
(1GHz top-hat)

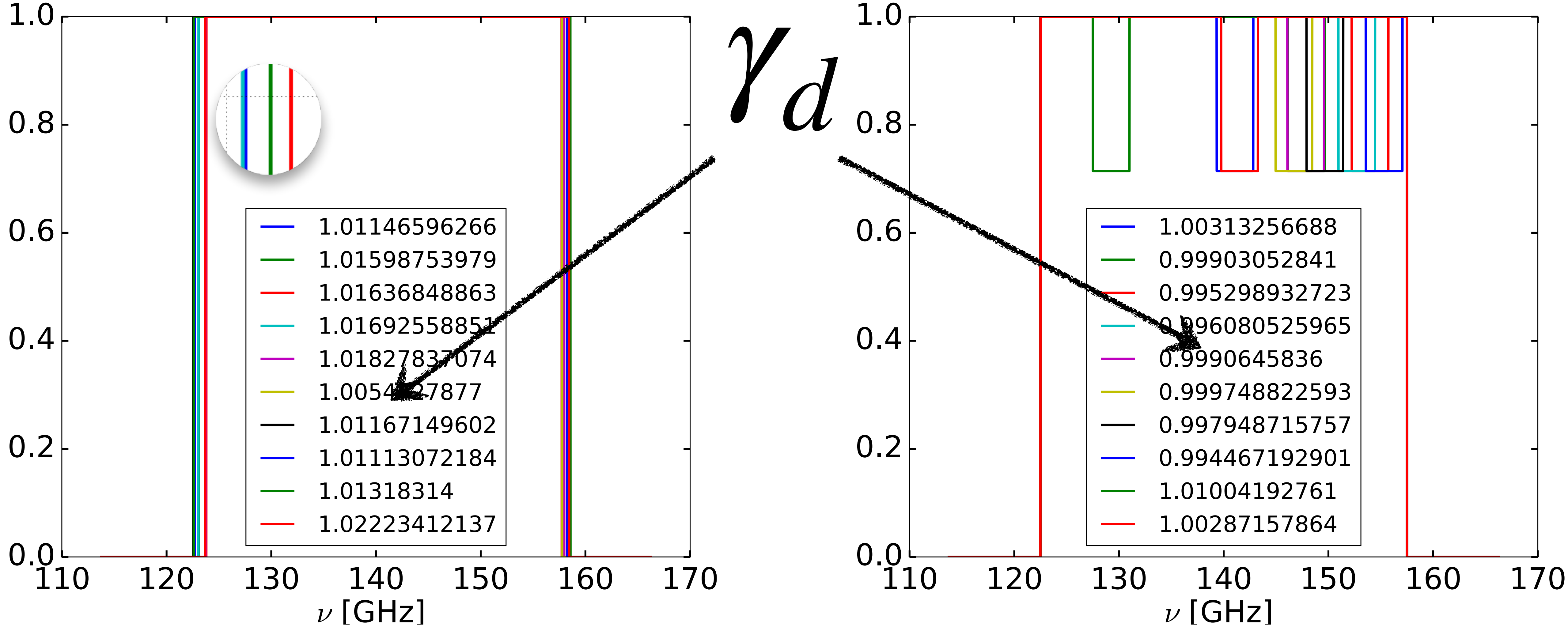

Standard derivation: 0.00626

Standard derivation: 0.005975

Half of a percent from detector to detector

→ **Calibration detectors by** γ_d

I.2.2. Time order data (TOD) simulation

- In order to observe leakage: The effect of intensity I to polarization Q, U
- Data simulation: $\mathbf{S}_{\text{sky}} = \mathbf{I}_{\text{CMB}} + \gamma_{\text{d}}\mathbf{I}_{\text{dust}} + \gamma_{\text{s}}\mathbf{I}_{\text{synchrotron}} + \ldots$
- No polarization
- No noise or white noise
- Same pixelization between input and output map
- Simulation at 140 GHz used different scanning strategy configurations
- The focal plane and polarizer orientations for LiteBIRD

The map of intensity I and polarization Q, and U is $\mathbf{m} = \begin{pmatrix} \mathbf{I} \\ \mathbf{Q} \\ \mathbf{U} \end{pmatrix}$,

the map-making solution:

$$\mathbf{m} = \left[\mathbf{A}^{\text{T}}\mathbf{N}^{-1}\mathbf{A}\right]^{-1}\mathbf{A}^{\text{T}}\mathbf{N}^{-1}\mathbf{S}_{\text{sky}}$$

The pointing matrix for pixel p: $\mathbf{A} = \begin{pmatrix} 1 & \cos(2\psi) & \sin(2\psi) \end{pmatrix}_{\text{p}}$

I.2.3. Results (1) -> Leakage maps

Galactic coordinate

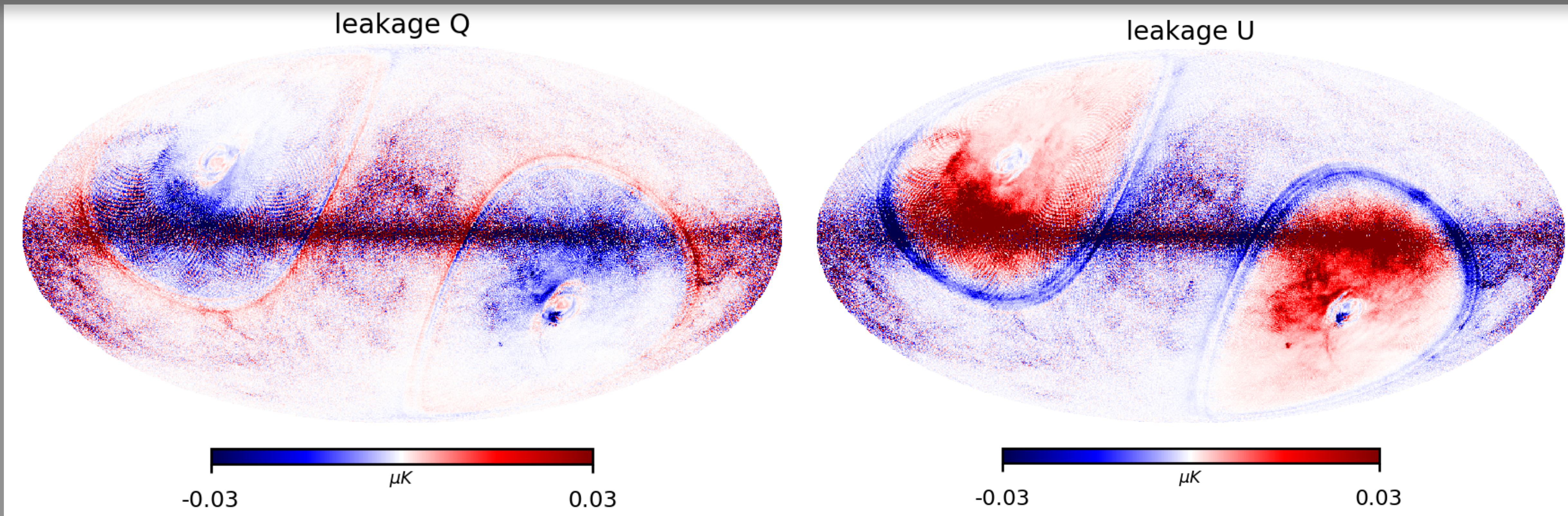

222 detectors and 365 days observation, 140 GHz

Ecliptic coordinate

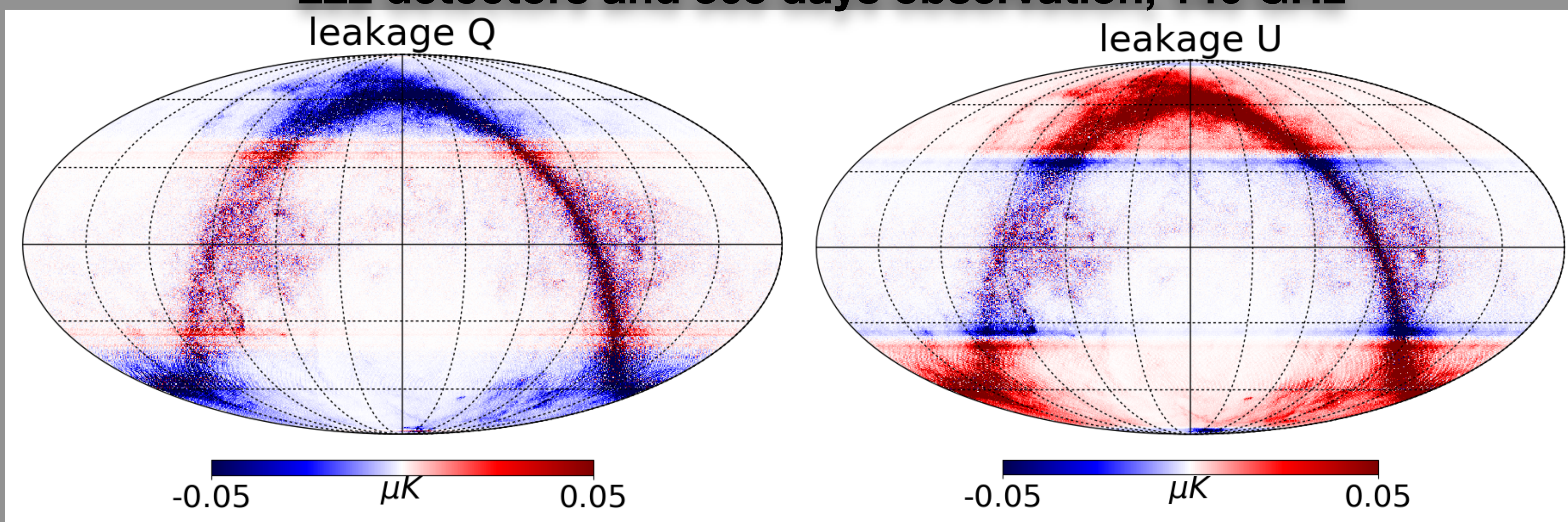

$$\alpha = 65^\circ, \beta = 30^\circ, \tau_{\mathrm{prec}} = 96.1803\,\mathrm{minutes}, \omega_{\mathrm{spin}} = 0.1\,\mathrm{rpm}$$

- **In ecliptic coordinate: Symmetric patterns around the pole.**

I.2.3. Results (2) -> Analytic estimation

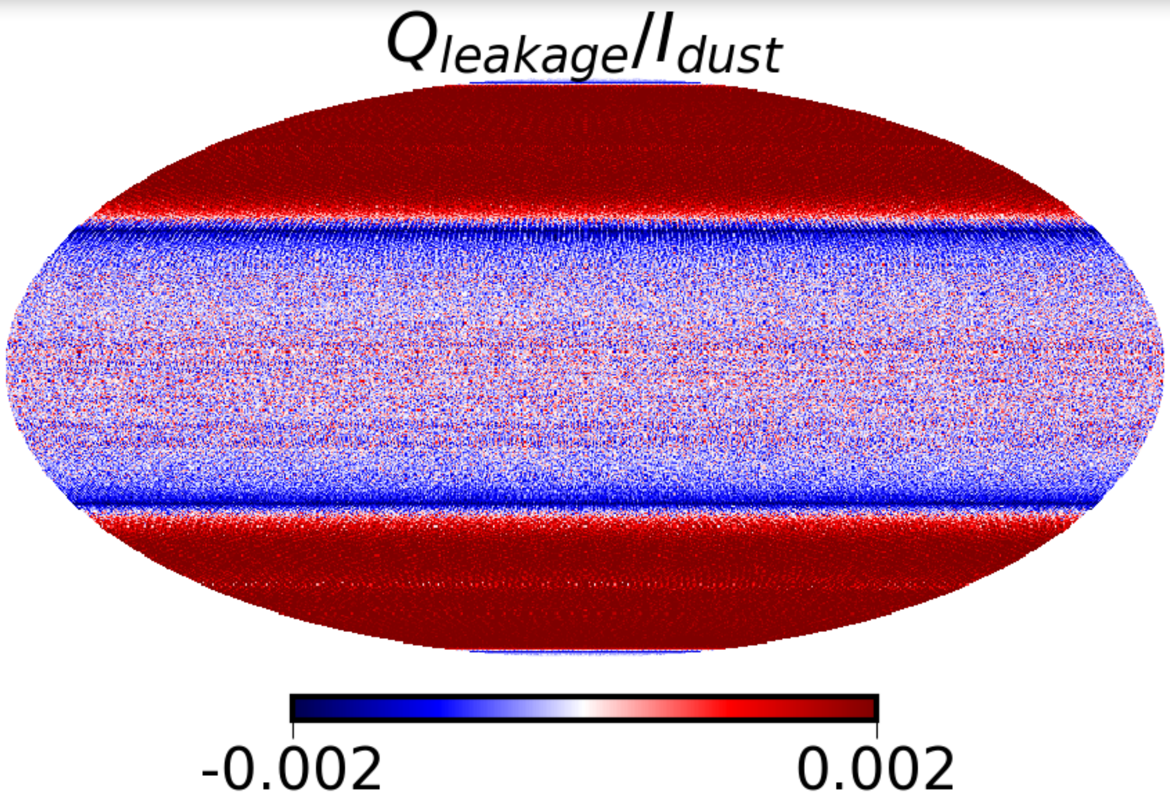

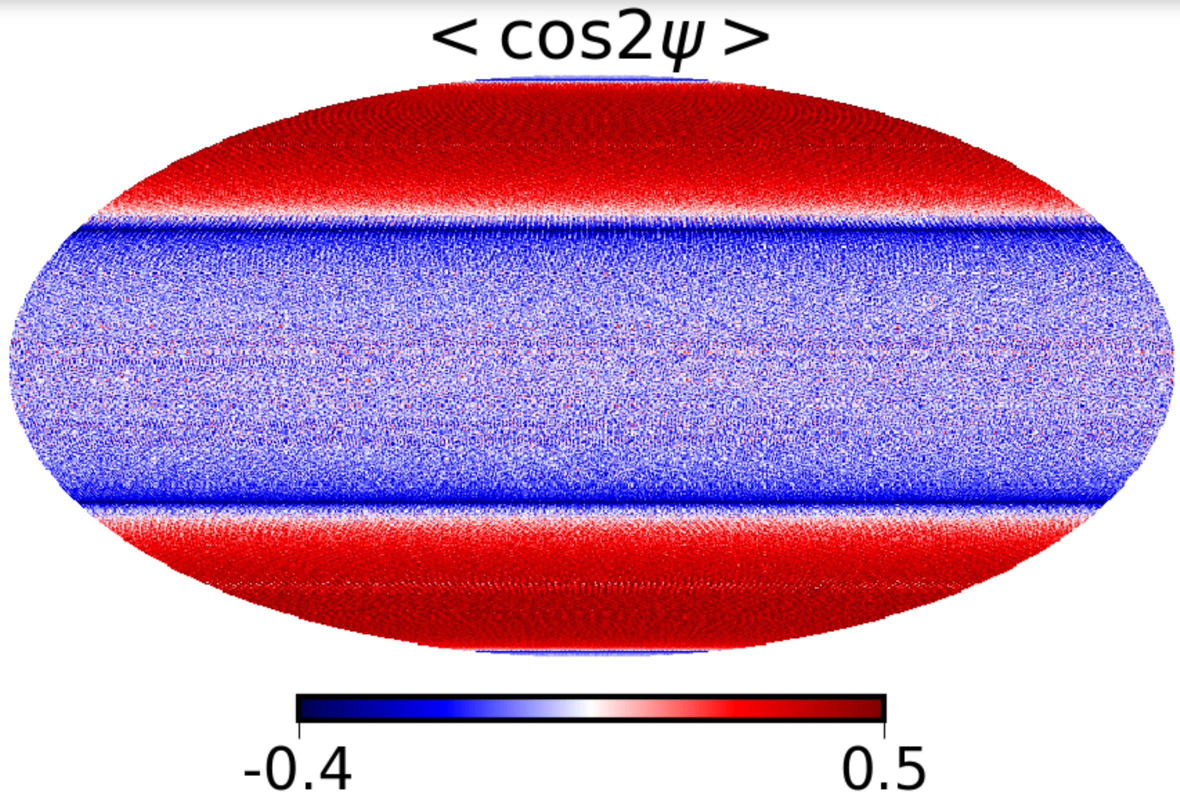

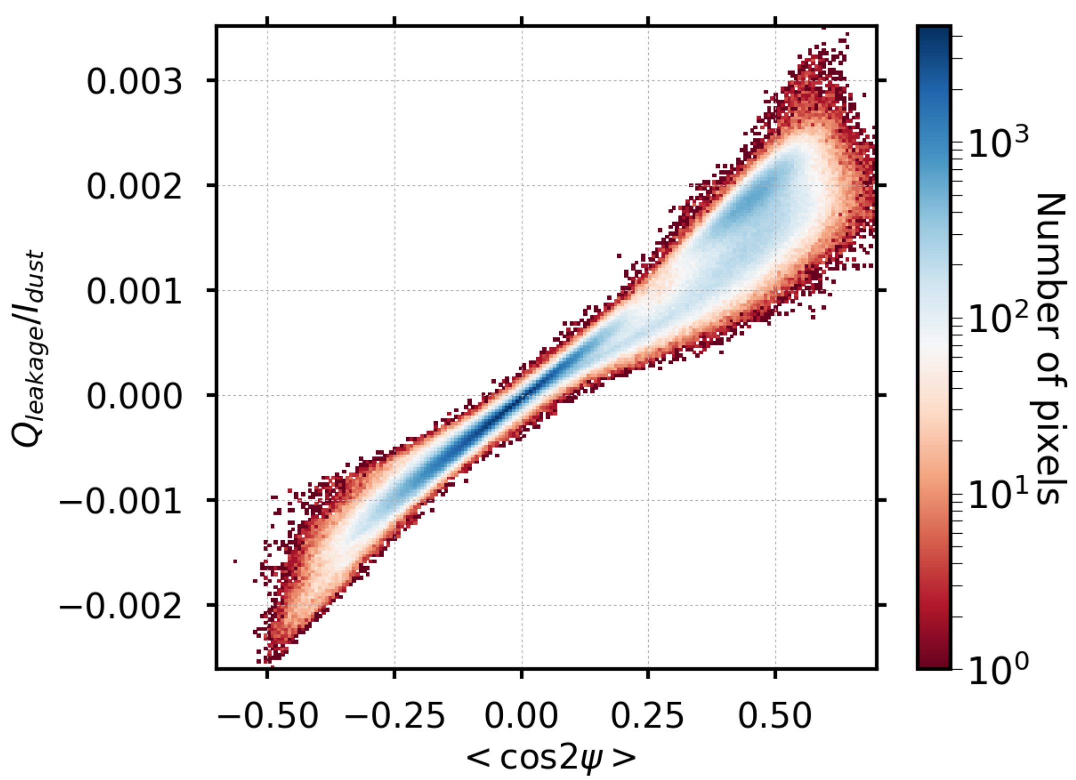

a pair detector

$$\begin{pmatrix} \frac{\delta Q_p}{I_{\mathrm{Gal};p}} \\ \frac{\delta U_p}{I_{\mathrm{Gal};p}} \end{pmatrix} = \left(\gamma^a_{\mathrm{Gal}} - \gamma^b_{\mathrm{Gal}}\right) \begin{pmatrix} \langle \cos 2\psi \rangle \\ \langle \sin 2\psi \rangle \end{pmatrix}$$

leakage maps **crossing moment**

- **Tight correlation between the relative leakage and the crossing moment.**

I.2.3. Results (3) -> 1 / N detectors

20% masked galactic plane, 74 and 222 detectors and 365 days observation, 10 sims

$$\frac{1}{N_{det}}$$

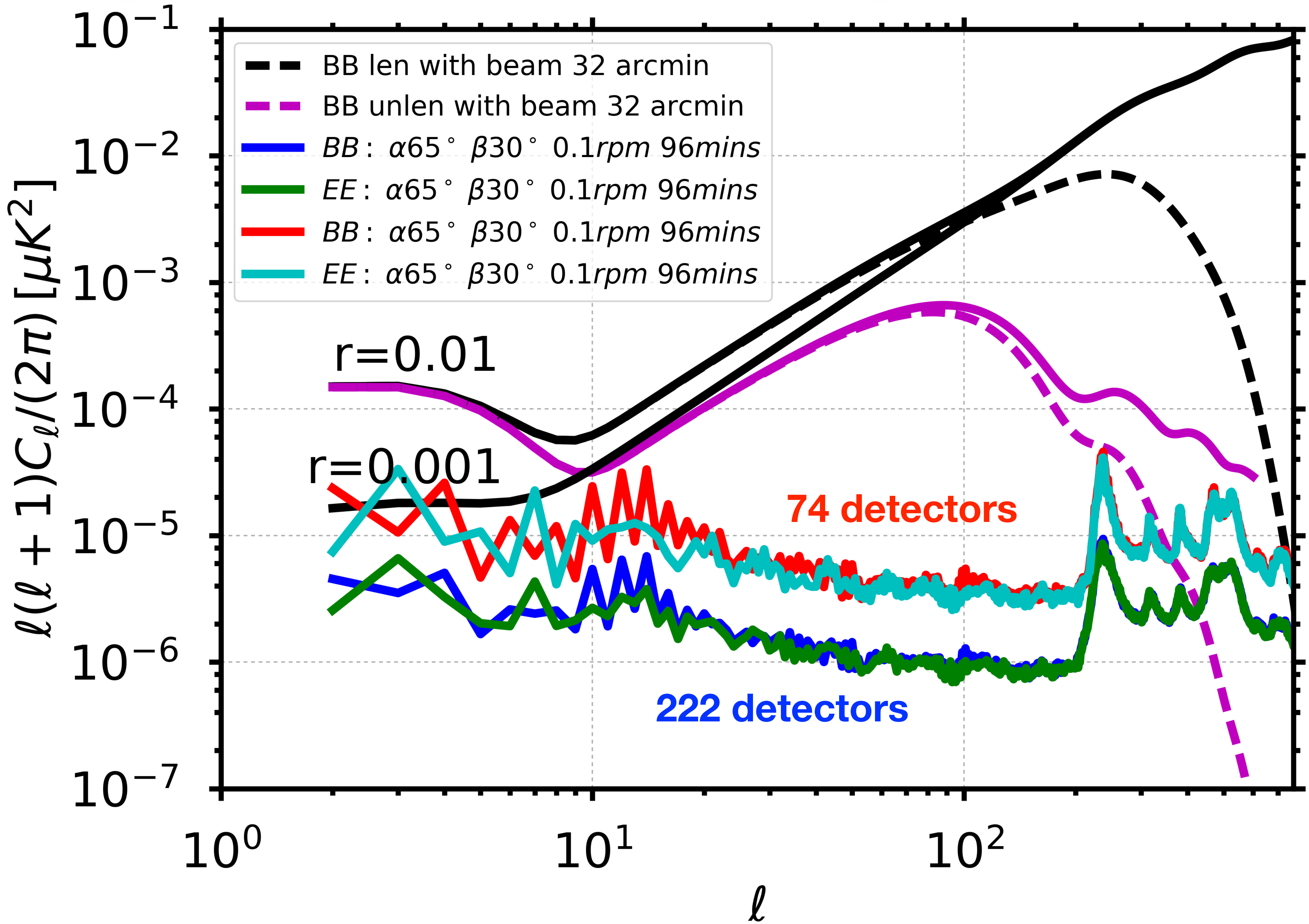

$$\alpha = 65^{\circ}, \beta = 30^{\circ}, \tau_{\mathrm{prec}} = 96.1803\,\mathrm{minutes}, \omega_{\mathrm{spin}} = 0.1\,\mathrm{rpm}$$

I.2.3. Results (4) -> scanning strategies

20% masked galactic plane, 222 detectors and 365 days observation, 10 sims

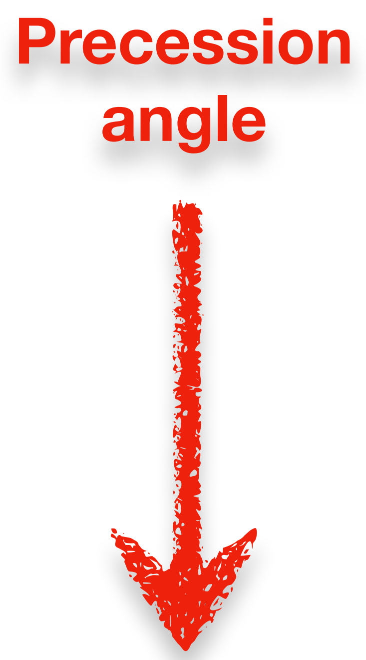

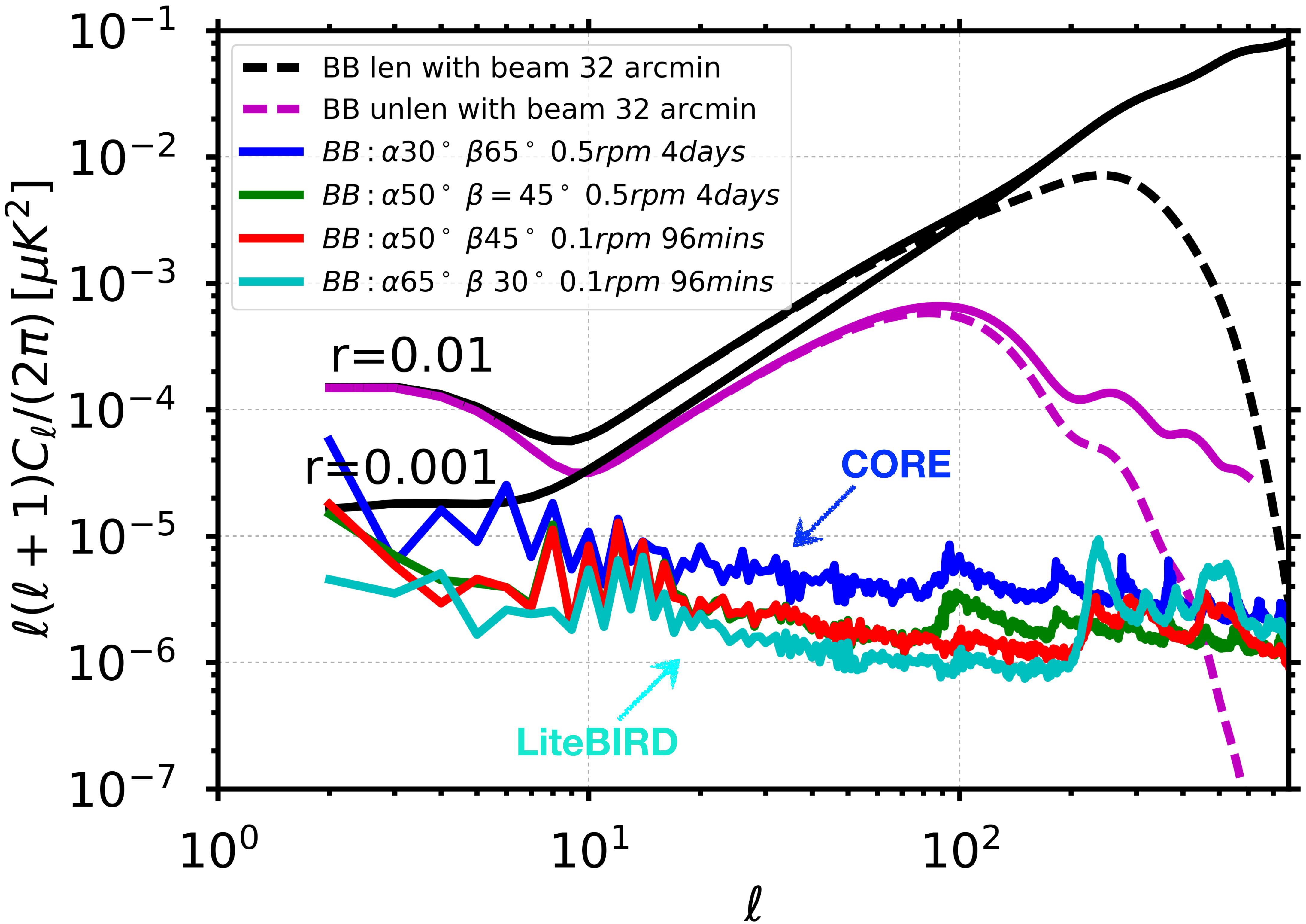

- **Scanning strategies with larger precession angle produce less leakage because of homogeneous scan angle per pixel.**

I.2.3. Results (5) -> An ideal Half Wave Plate 88 rpm

20% masked galactic plane, 50 detectors and 180 days observation

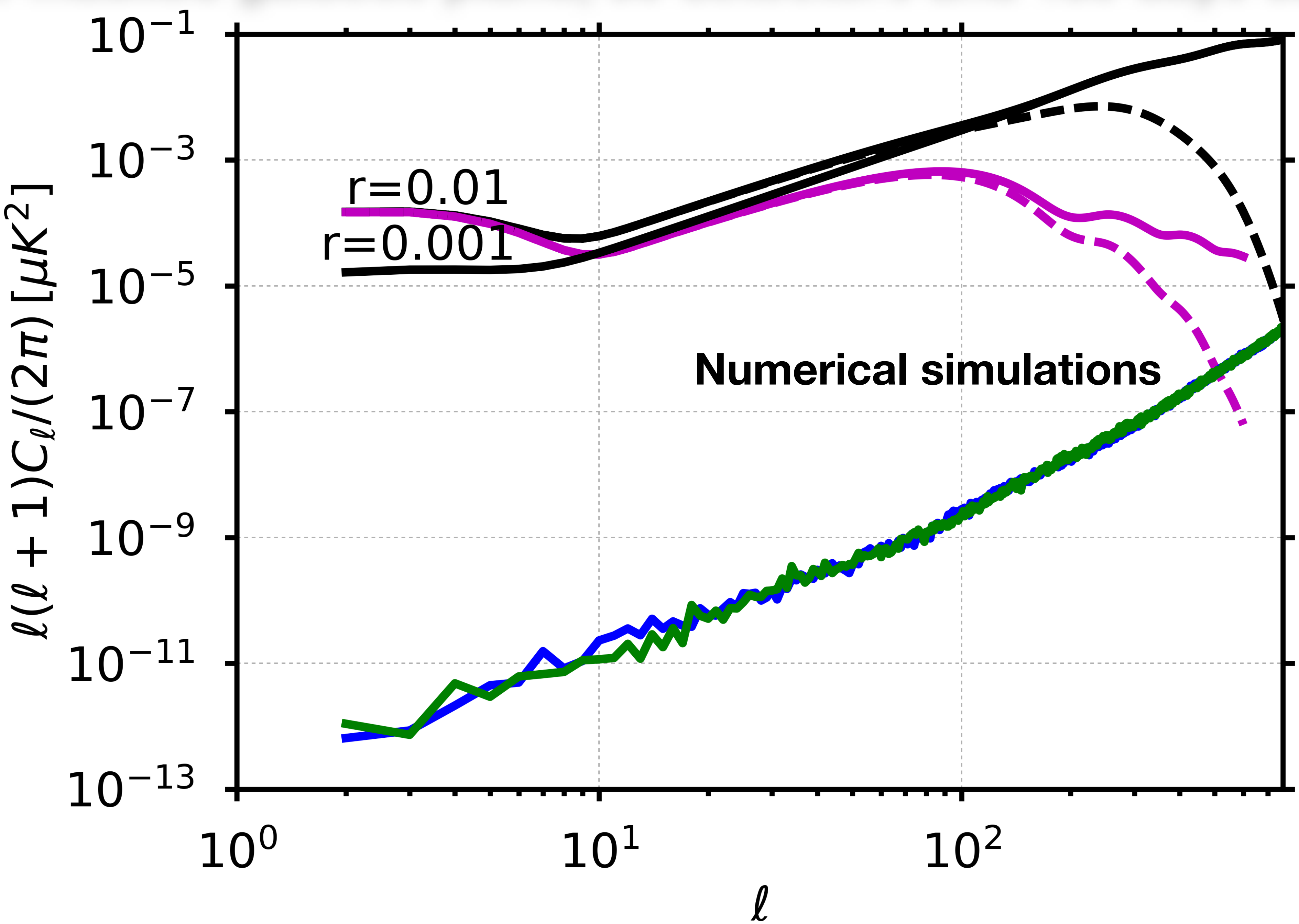

$$\alpha = 65^\circ, \beta = 30^\circ, \tau_{\text{prec}} = 93\,\text{minutes}, \omega_{\text{spin}} = 0.1\,\text{rpm}$$

- **An rotating HWP mitigates bandpass leakage by homogenizing the angular coverage each pixel.**

I.2.3. Results (6) -> precession and spin

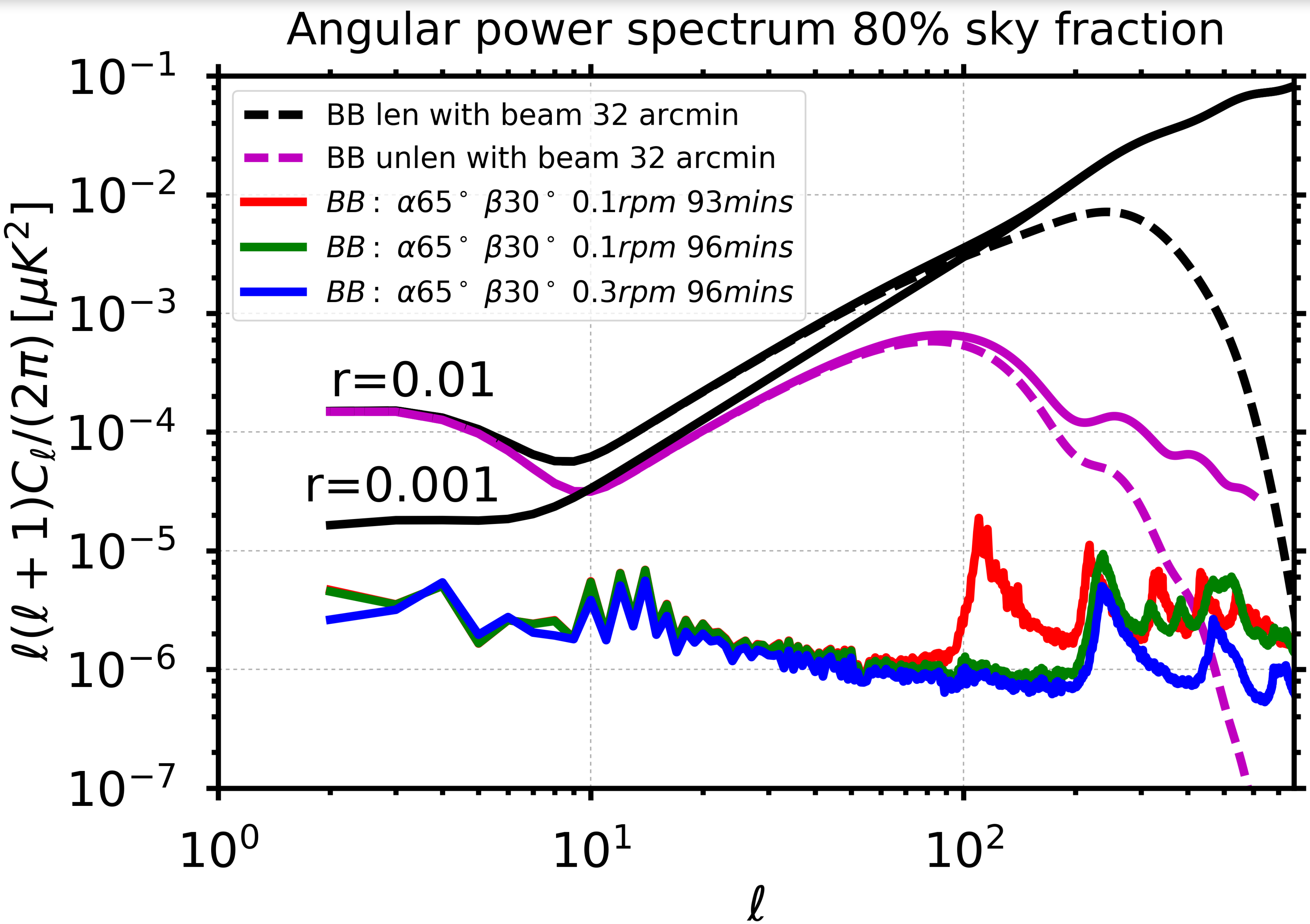

$$\alpha = 65^\circ, \beta = 30^\circ$$

- precession 93 minutes, spin 0.1 rpm
- precession 96.1803 minutes, spin 0.1 rpm
- precession 96.1803 minutes, spin 0.3 rpm

- **The location of the peaks depends on the ratio** $\tau_{\text{prec}}/\tau_{\text{spin}}$

20% masked galactic plane, 222 detectors and 365 days observation

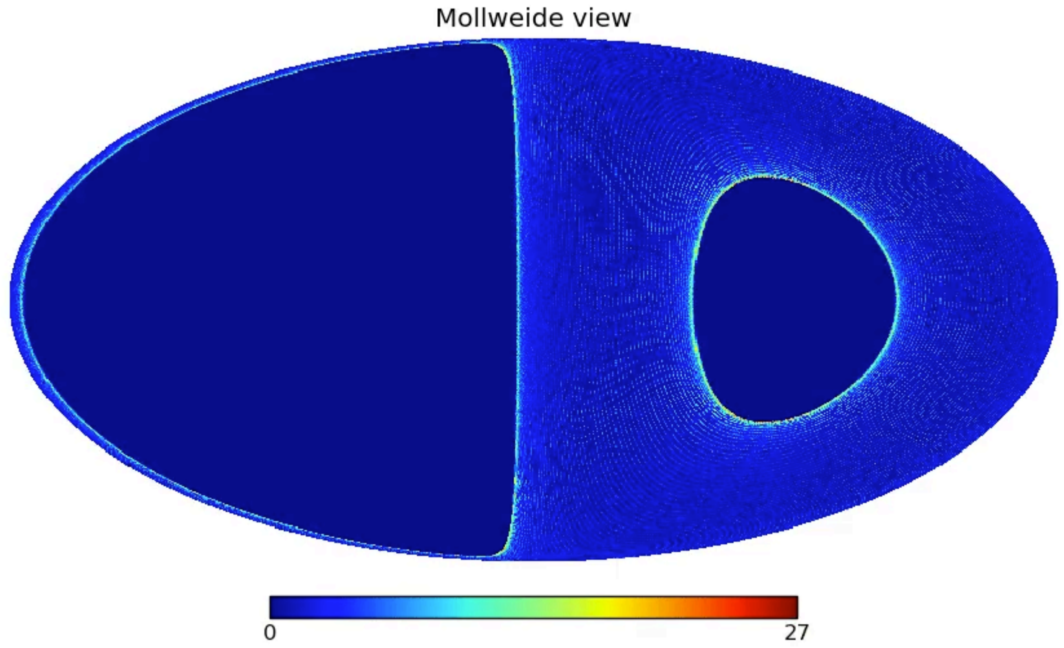

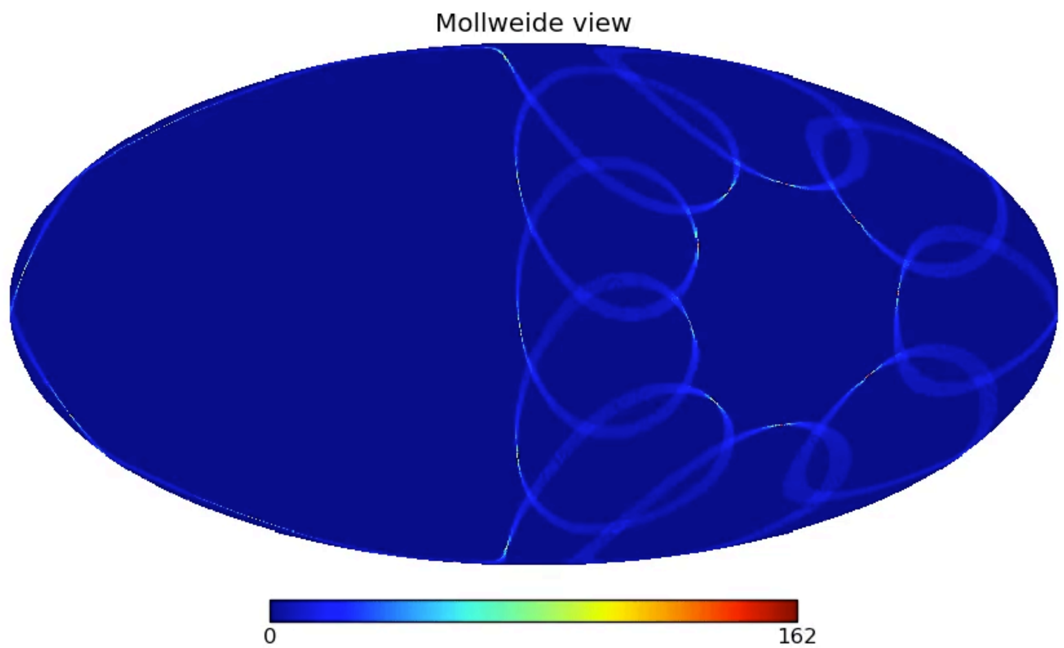

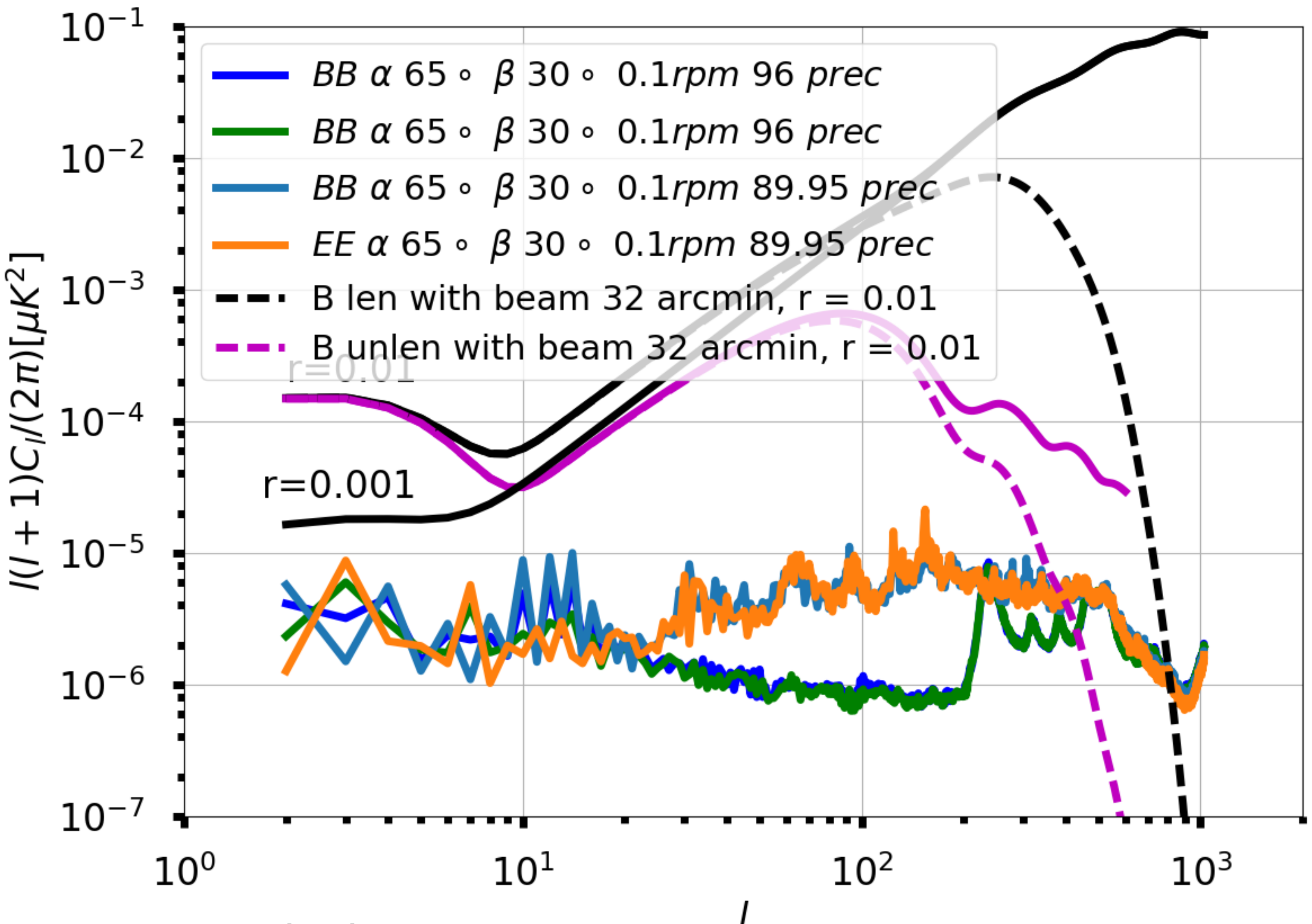

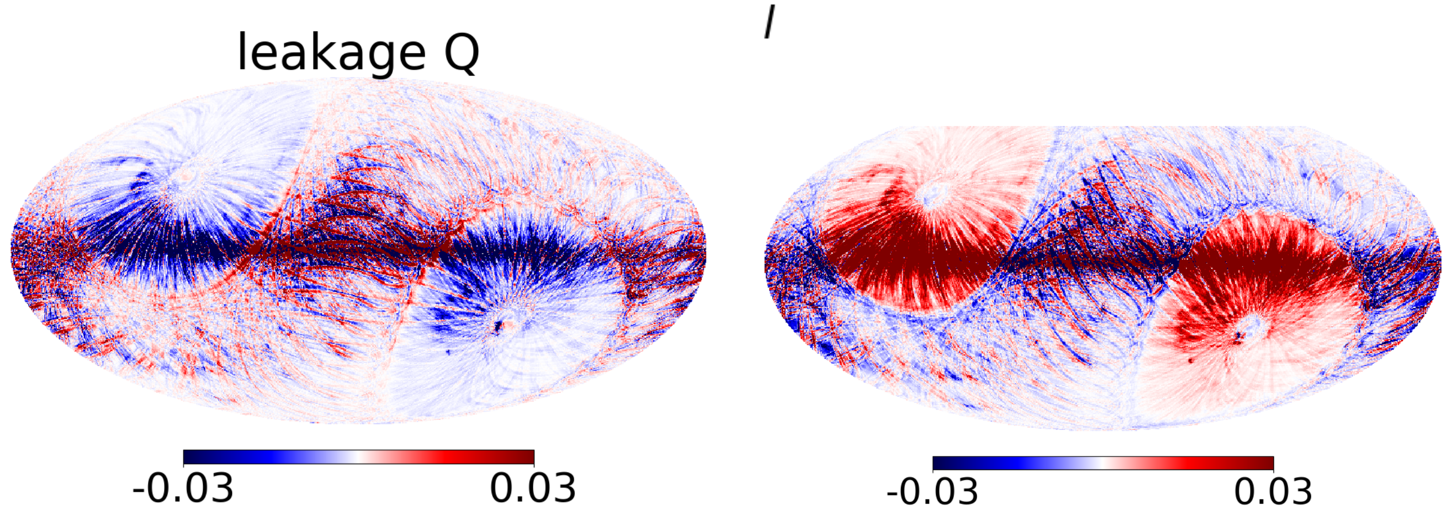

- **Effects on intermediate angular power spectrum**

I.2.3. Results (8) -> Vary scanning strategy params

20% masked galactic, 222 detectors and 365 days observation

Amplitudes are rescaled

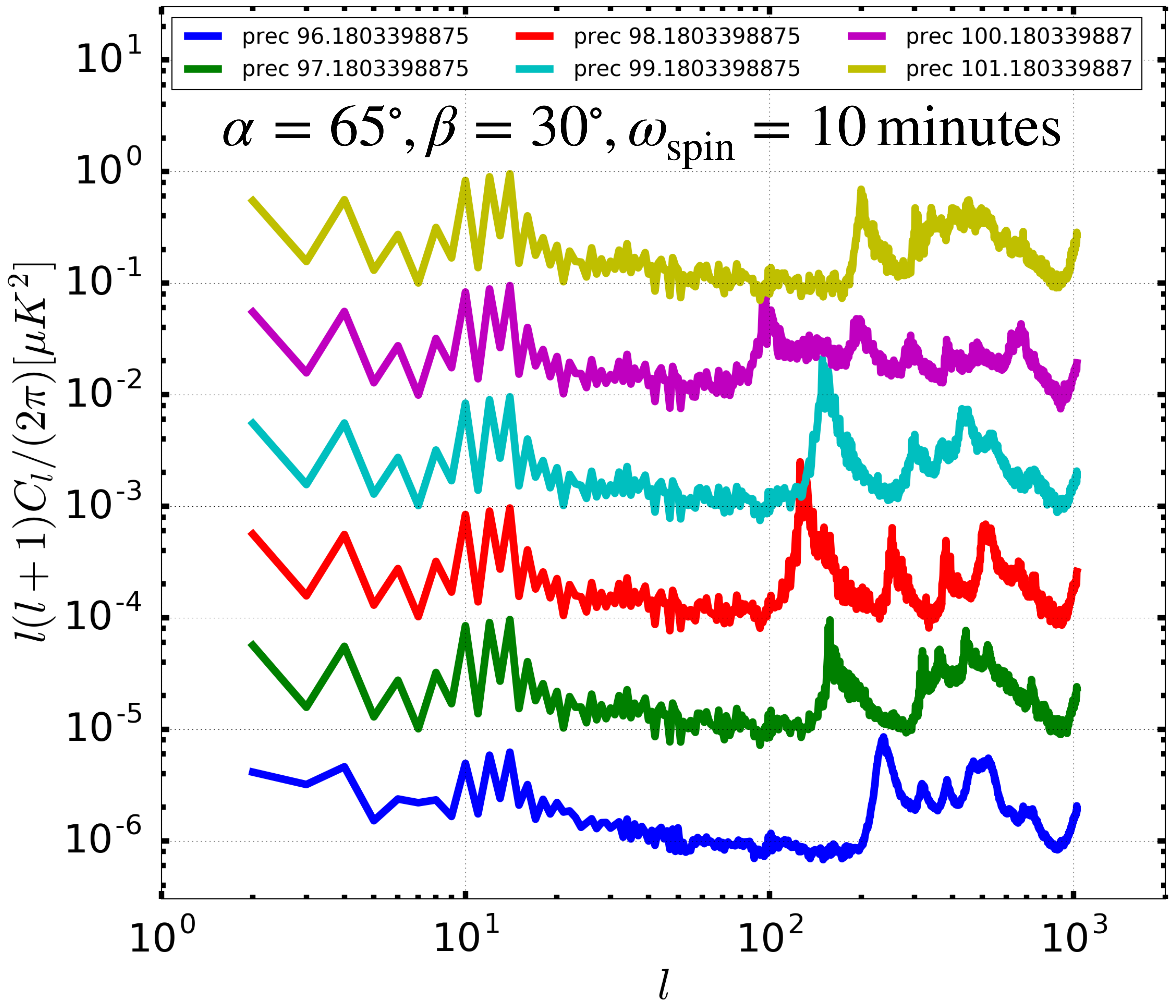

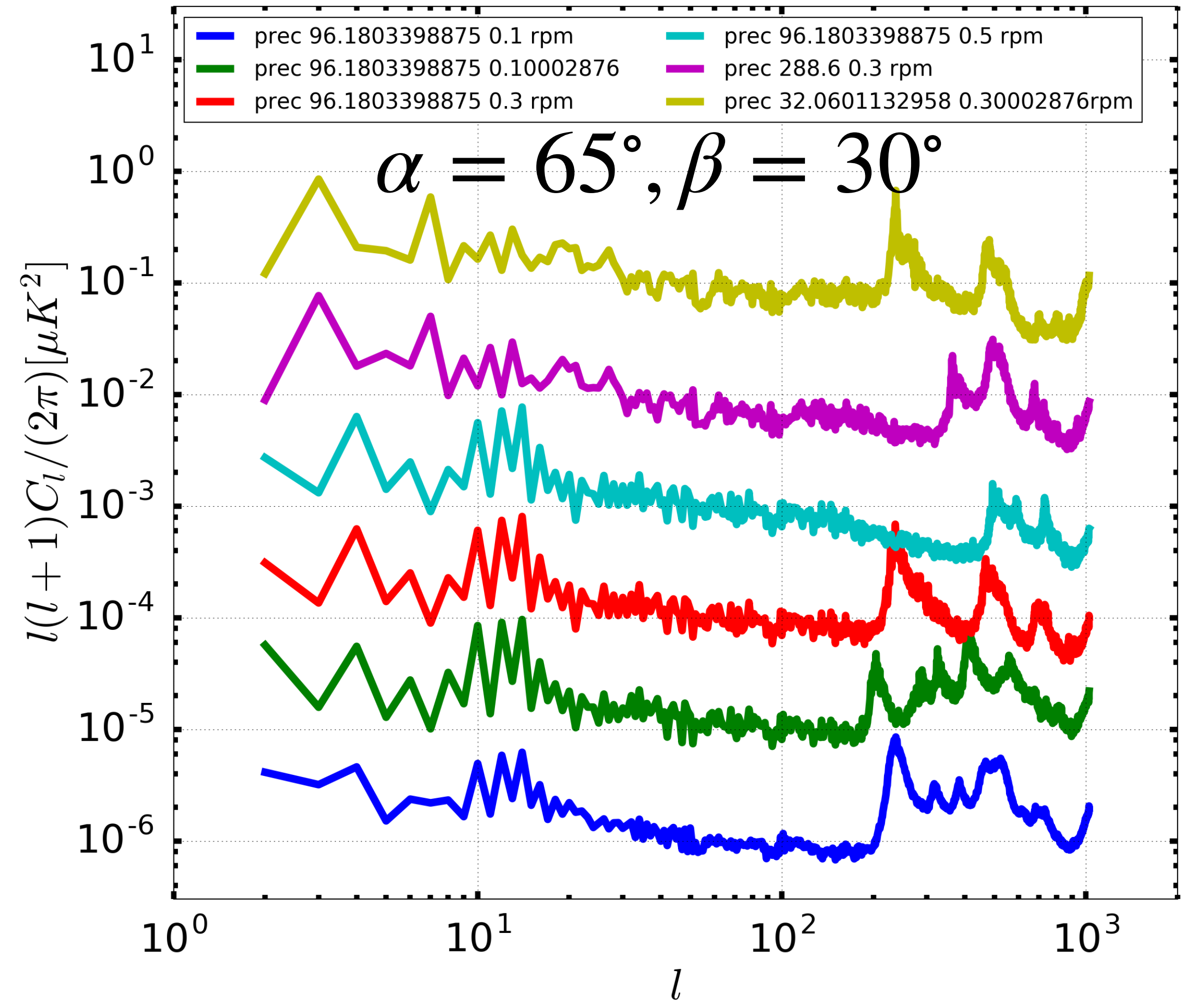

- **The location of the peaks changes**
- **The location of the peaks depends on the ratio** $\tau_{\rm prec}/\tau_{\rm spin}$

I.3. A correction method: A pair detector

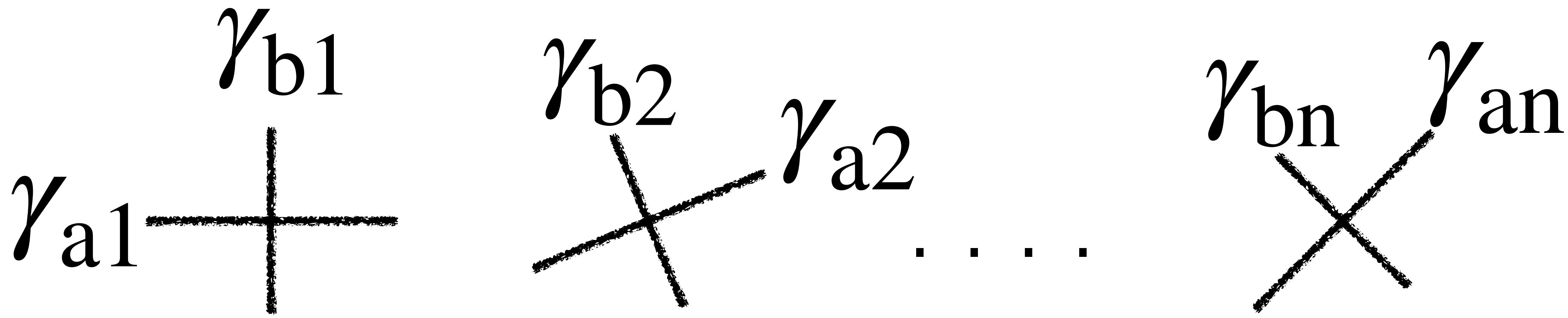

1st pair 2nd pair 111th pair

- **Detector pair subtraction**

$$S_a = \gamma_a I + Q \cos 2\psi_a + U \sin 2\psi_a$$

$$S_b = \gamma_b I - Q \cos 2\psi_a - U \sin 2\psi_a$$

$$\frac{S_a - S_b}{2} = \frac{\left(\gamma_a - \gamma_b\right) I}{2} + Q \cos 2\psi_a + U \sin 2\psi_a$$

I.3. A correction method: A pair detector

- **In case of leakage: The covariant matrix:**

$$\mathrm{Cov}_{3;\mathrm{p}} = (\mathbf{A}^{\mathrm{T}}\mathbf{N}^{-1}\mathbf{A})^{-1} = \frac{\sigma_{\mathrm{n}}}{\mathrm{N_p}} \times \begin{pmatrix} 1 & \langle \cos 2\psi \rangle & \langle \sin 2\psi \rangle \\ \langle \cos 2\psi \rangle & \dfrac{1 + \langle \cos 4\psi \rangle}{2} & \dfrac{\langle \sin 4\psi \rangle}{2} \\ \langle \sin 2\psi \rangle & \dfrac{\langle \sin 4\psi \rangle}{2} & \dfrac{1 - \langle \cos 4\psi \rangle}{2} \end{pmatrix}^{-1}.$$

- **In case of no leakage: The sub-matrix covariance**

$$\mathrm{Cov}_{2;\mathrm{p}} = \sigma_{\mathrm{n}} \times \begin{pmatrix} \dfrac{1 + \langle \cos 4\psi \rangle}{2} & \dfrac{\langle \sin 4\psi \rangle}{2} \\ \dfrac{\langle \sin 4\psi \rangle}{2} & \dfrac{1 - \langle \cos 4\psi \rangle}{2} \end{pmatrix}^{-1}.$$

  - **We study the loss of accuracy in two cases numerically.**

I.3. A correction method: A pair detector

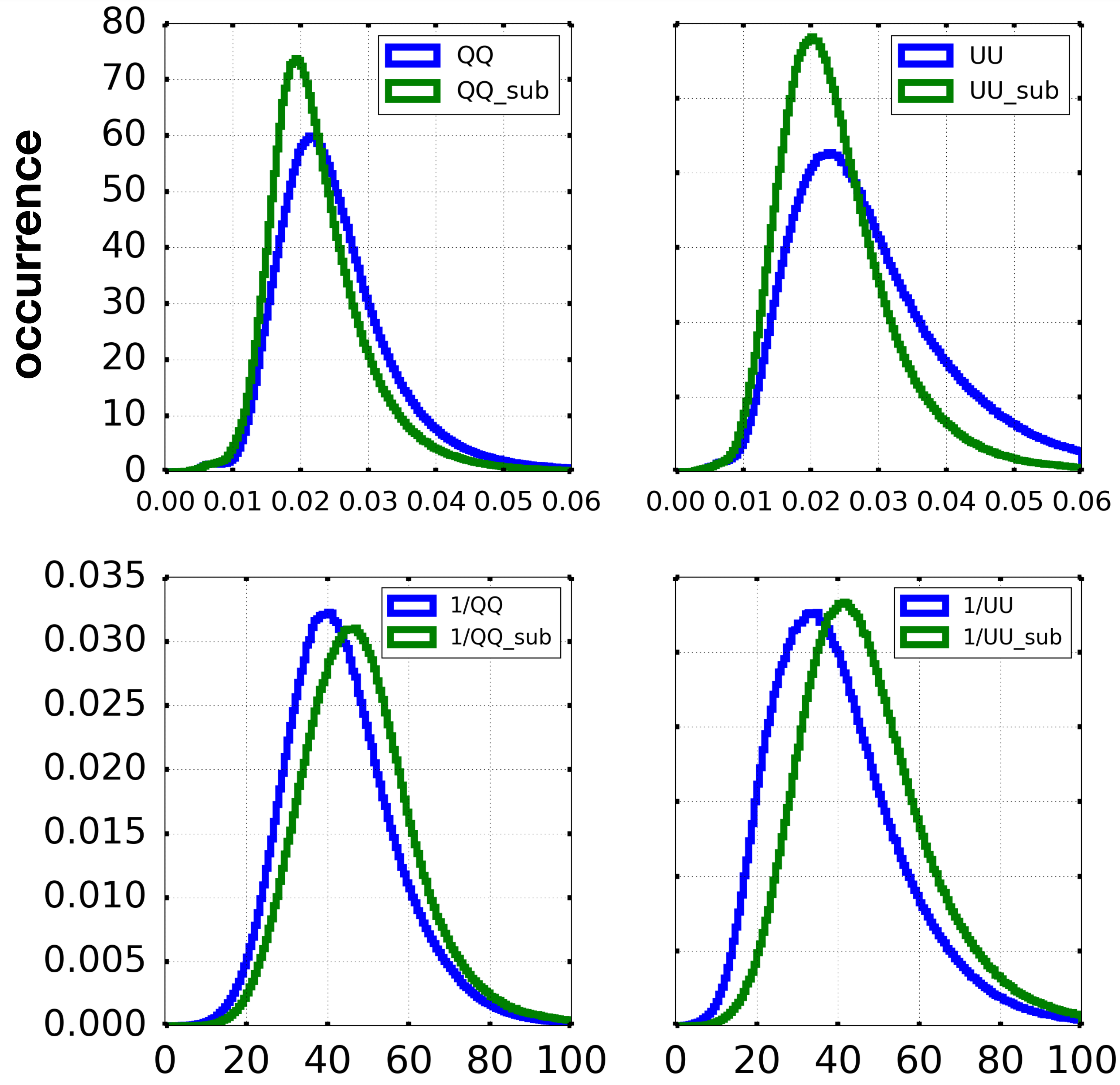

$$\alpha = 65^\circ, \beta = 30^\circ, \tau_{\mathrm{prec}} = 96.1803\,\text{minutes}, \omega_{\mathrm{spin}} = 0.1\,\text{rpm}$$

- **The loss accuracy of the Q component is of the order of 10% for a given detector pair**

Conclusions

222 detectors and 365 days observation, τ = 0.055 +/- 0.009	$2 \leq \ell \leq 10$	$10 \leq \ell \leq 200$
$\alpha = 30°; \beta = 65°; \tau_{\rm prec} = 4\,{\rm days}; \omega_{\rm spin} = 0.5\,{\rm rpm}$	1.83×10^{-3}	9.32×10^{-5}
$\alpha = 50°; \beta = 45°; \tau_{\rm prec} = 4\,{\rm days}; \omega_{\rm spin} = 0.5\,{\rm rpm}$	6.49×10^{-4}	4.66×10^{-5}
$\alpha = 50°; \beta = 45°; \tau_{\rm prec} = 96\,{\rm min}; \omega_{\rm spin} = 0.1\,{\rm rpm}$	6.32×10^{-4}	3.08×10^{-5}
$\alpha = 65°; \beta = 30°; \tau_{\rm prec} = 93\,{\rm min}; \omega_{\rm spin} = 0.1\,{\rm rpm}$	3.29×10^{-4}	7.61×10^{-5}
$\alpha = 65°; \beta = 30°; \tau_{\rm prec} = 96\,{\rm min}; \omega_{\rm spin} = 0.1\,{\rm rpm}$	3.27×10^{-4}	2.11×10^{-5}
$\alpha = 65°; \beta = 30°; \tau_{\rm prec} = 96\,{\rm min}; \omega_{\rm spin} = 0.3\,{\rm rpm}$	3.03×10^{-4}	1.77×10^{-5}

1. Bandpass mismatch is the non-negligible systematic effect.
2. An optimal scanning strategy for future CMB polarization satellite.
3. Tensor-to-scalar r is of the order of 10^{-3} in reionization bump.
4. Tight correlation between leakage maps and cross linking moment.
5. 1/N detectors dependence of the level of the power spectra => increase number of detectors.
6. An ideal half wave plate mitigates the bandpass mismatch effect.
7. Bandpass mismatch error for satellite CMB experiments II: Correction effect, Ranajoy et al., [*in preparation*].

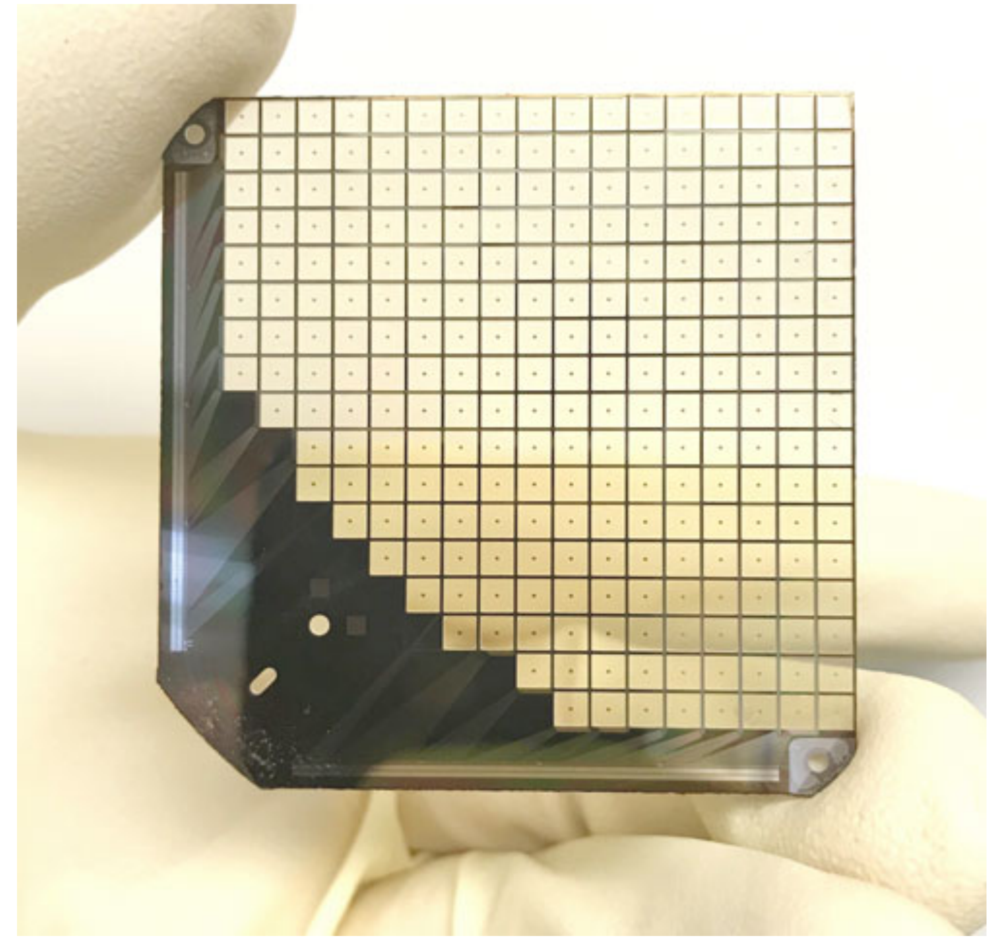

II. Interaction of particles with a 256 Transition Edge Sensor (TES) array of the QUBIC experiment.

HOANG Duc-Thuong

APC, December 17, 2018

The Q & U Bolometric Interferometer for Cosmology

22 labs
> 130 persons

APC Paris, France
C2N Orsay, France
CSNSM Orsay, France
IRAP Toulouse, France
Maynooth University, Ireland
Università di Milano-Bicocca, Italy
Università degli studi, Milano, Italy
Università La Sapienza, Roma, Italy
University of Manchester, UK
Richmond University, USA
Brown University, USA
University of Wisconsin, USA
NIKHEF, The Netherlands
GEMA, Argentina
Centro Atómico Cóntituyentes, Argentina
Comisión Nacional de Energía Atómico, Argentina
Facultad de CS Astronómicas y Geofísicas, Argentina
Centro Atómico Bariloche and Instituto Balseiro, Argentina
Instituto de Tecnologías en detección y Astropartículas, Argentina
Instituto Argentino de Radio Astronomía, Argentine

II.1. QUBIC science goal & Instrument

Self-calibration: Open/close horn couple

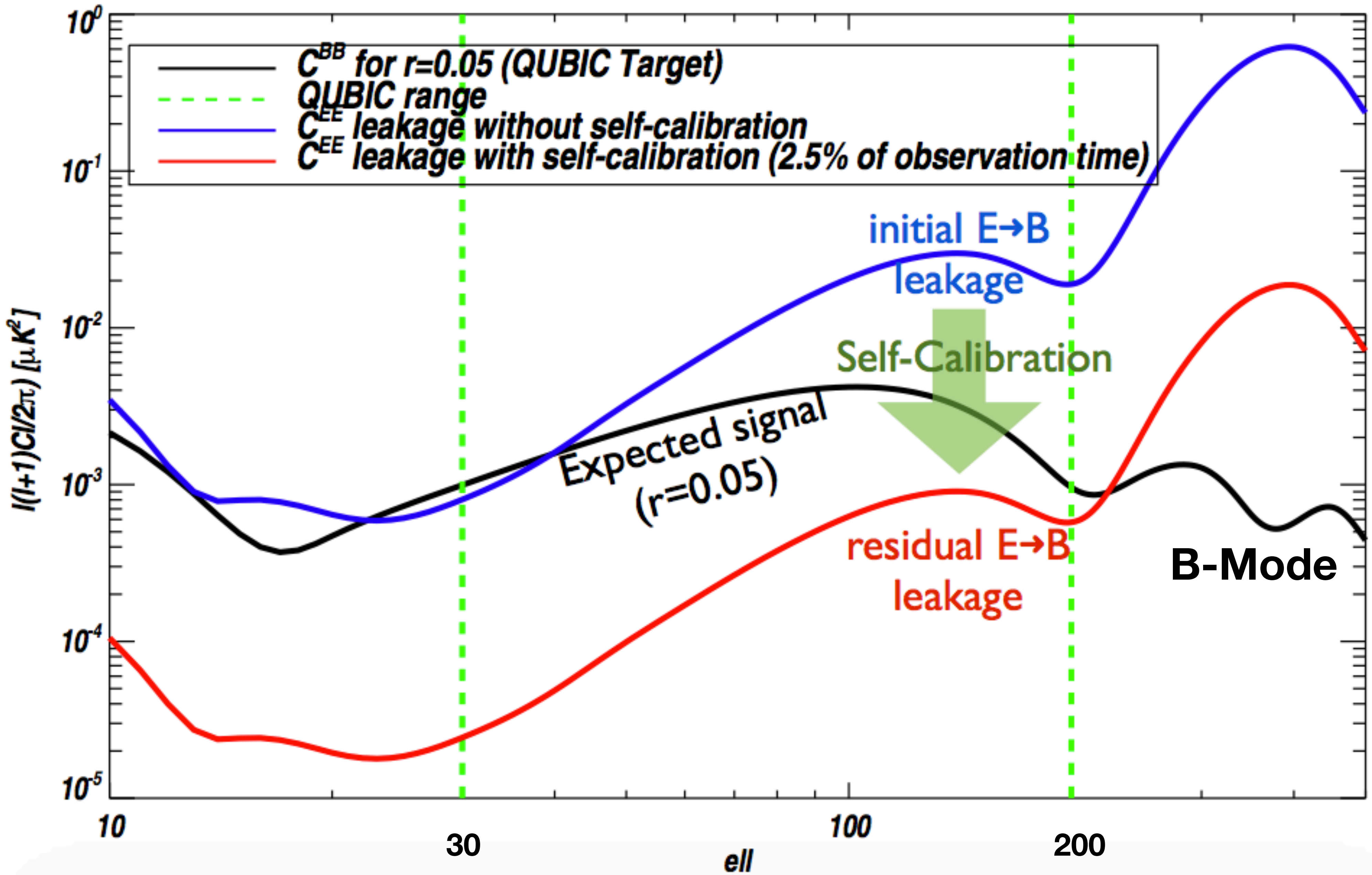

arXiv:1209.4905

$\sigma(r)$ goal: no foreground: 0.006, with foreground 0.01

QUBIC in a Nutshell

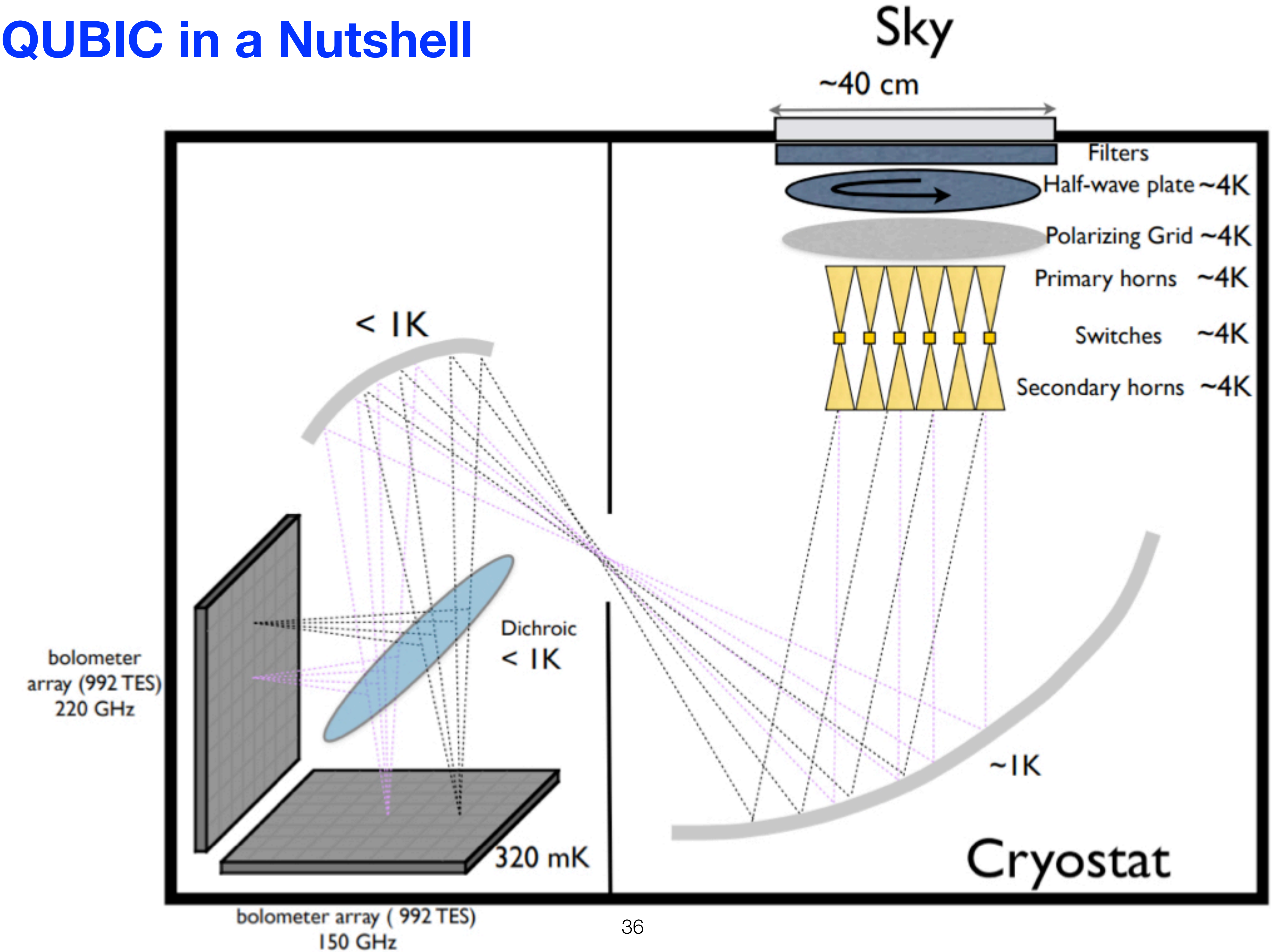

QUBIC in a Nutshell

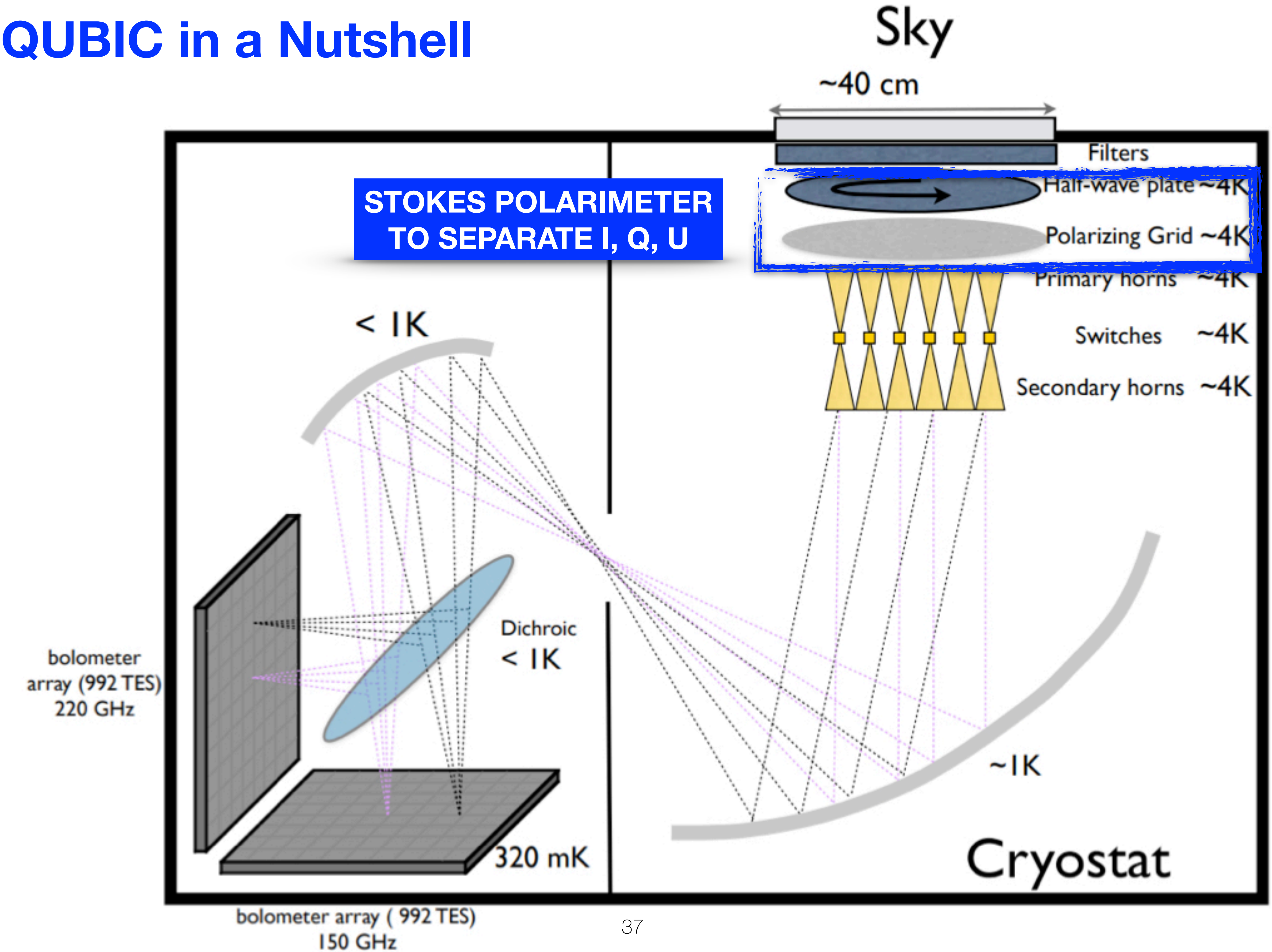

QUBIC in a Nutshell

400 BACK TO BACK HORNS SWITCHES TO OPEN/CLOSE A HORNS COUPLE: BASELINE.

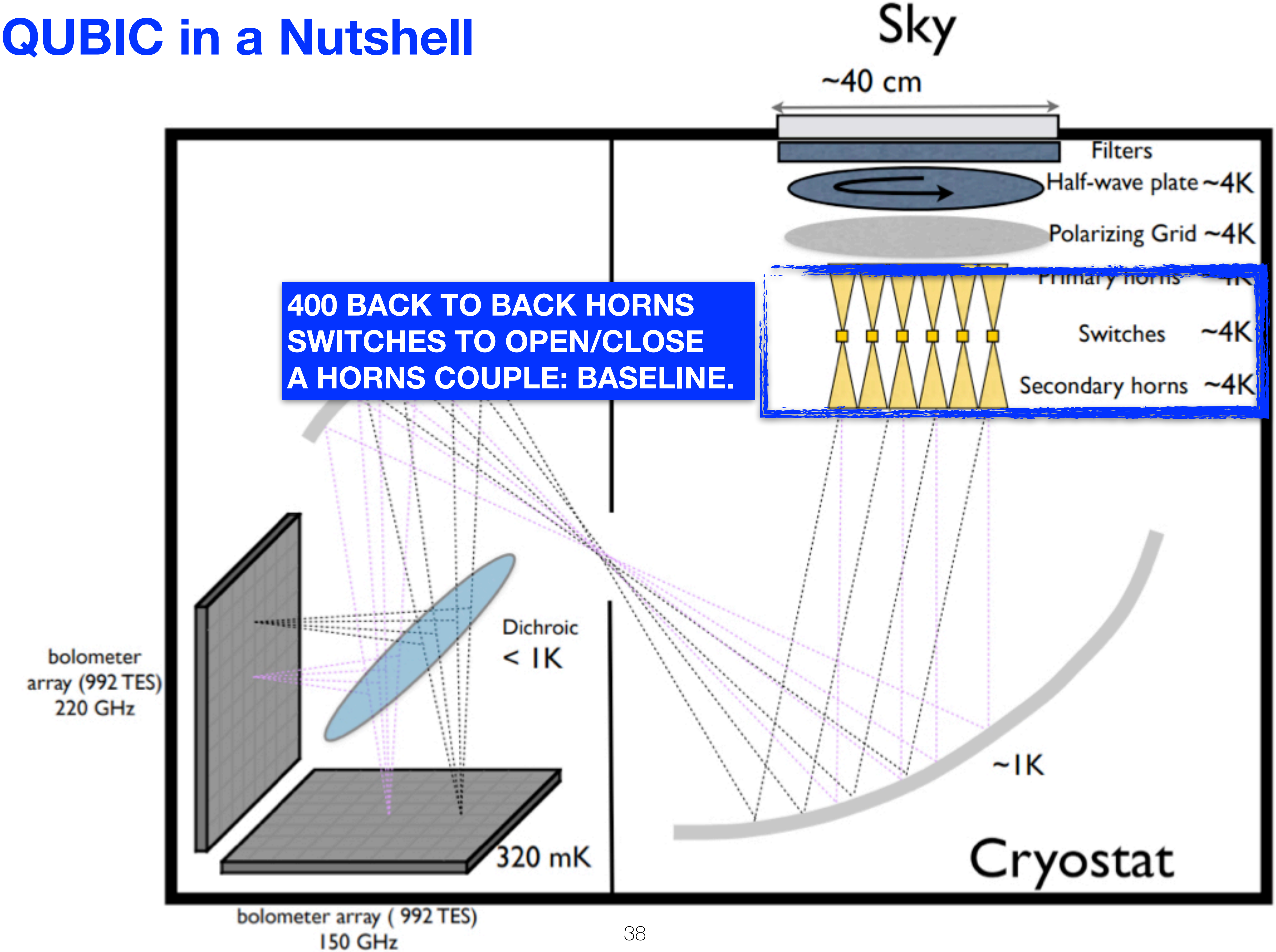

QUBIC in a Nutshell

MIRRORS MADE A FIZEAU INTERFEROMETER. OPENING AND CLOSING THE SWITCHES. WE CAN CHANGE THE INTERFEROMETRIC FRINGES ON THE FOCAL PLANE.

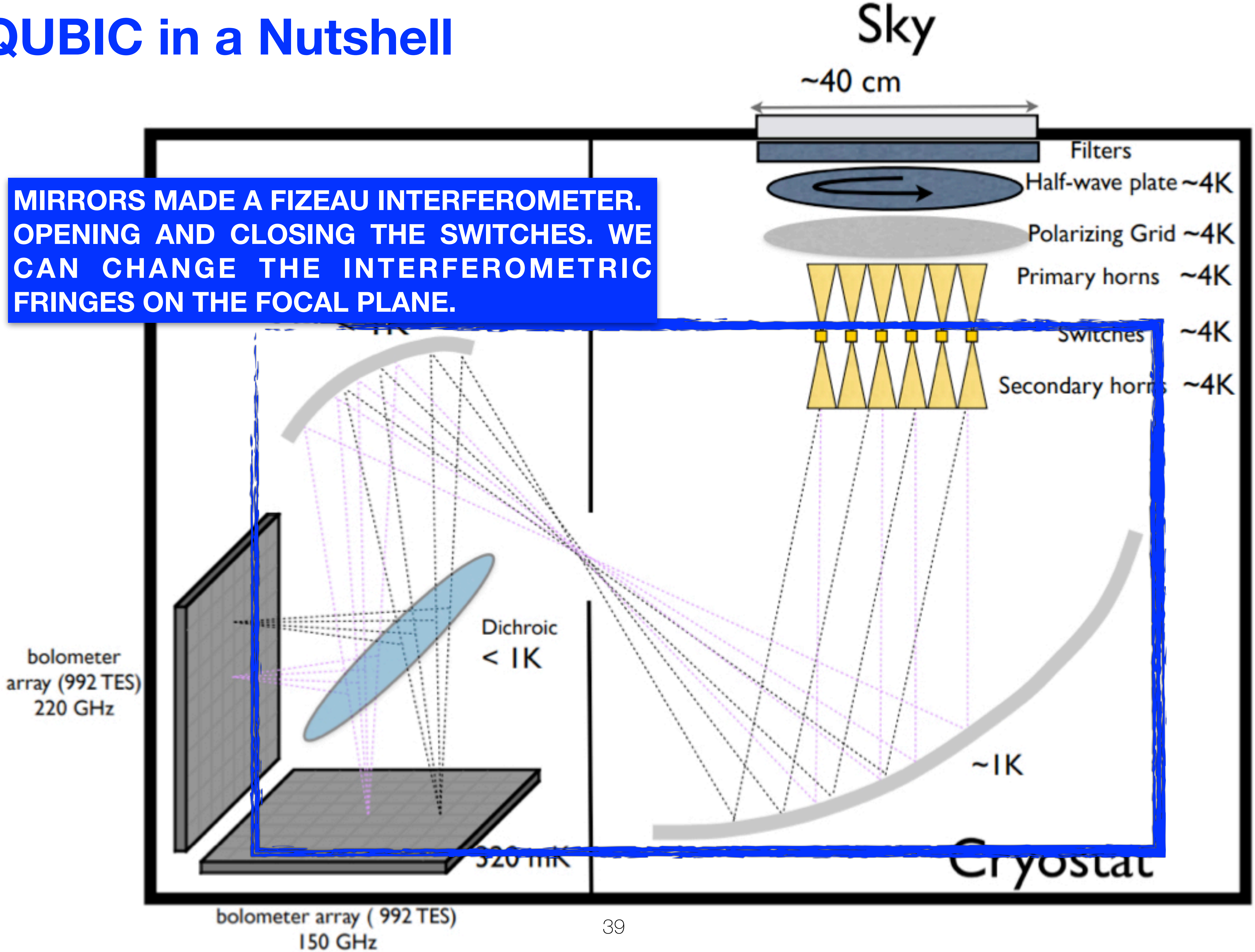

QUBIC in a Nutshell

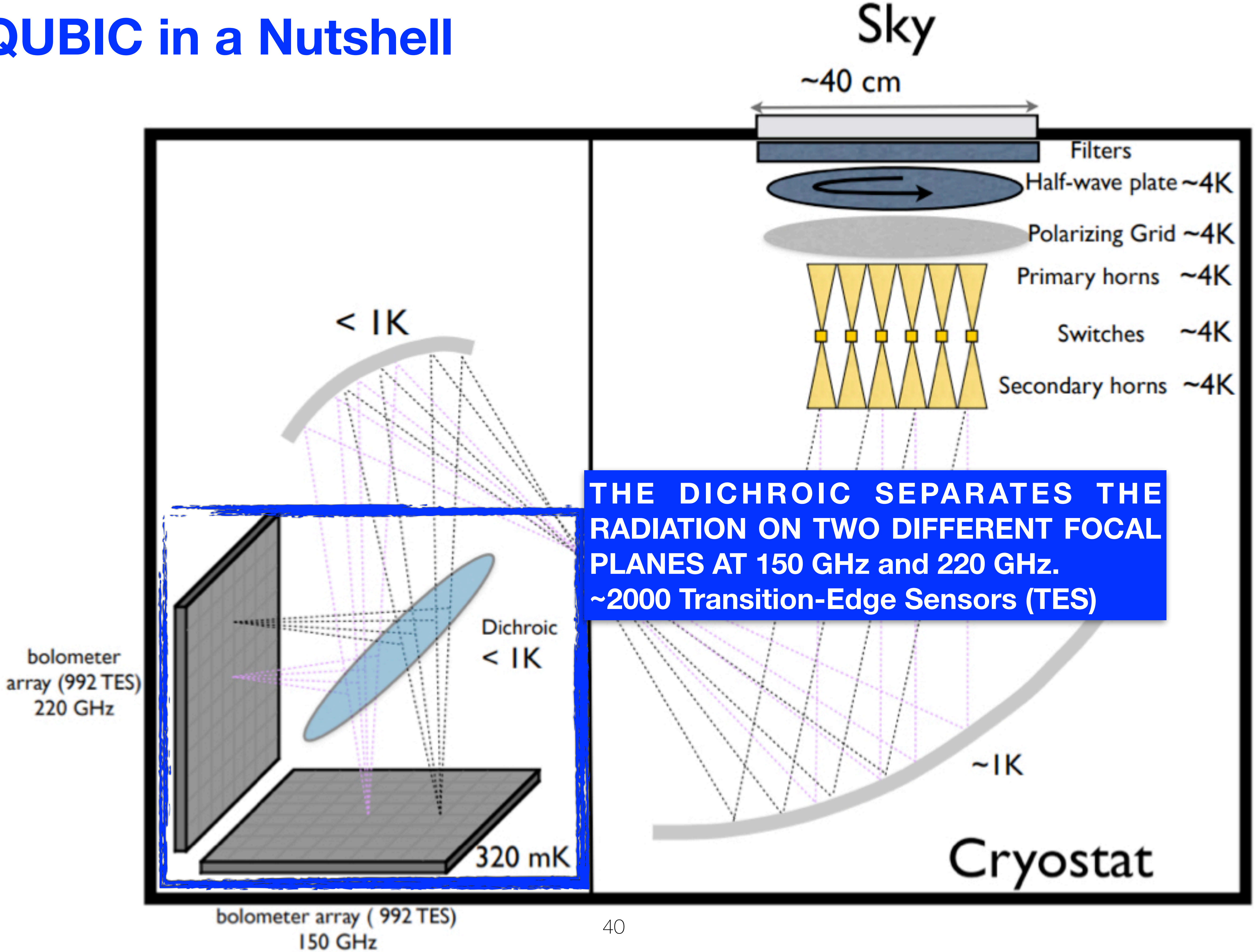

THE DICHROIC SEPARATES THE RADIATION ON TWO DIFFERENT FOCAL PLANES AT 150 GHz and 220 GHz. ~2000 Transition-Edge Sensors (TES)

II.1. QUBIC's Cryostat

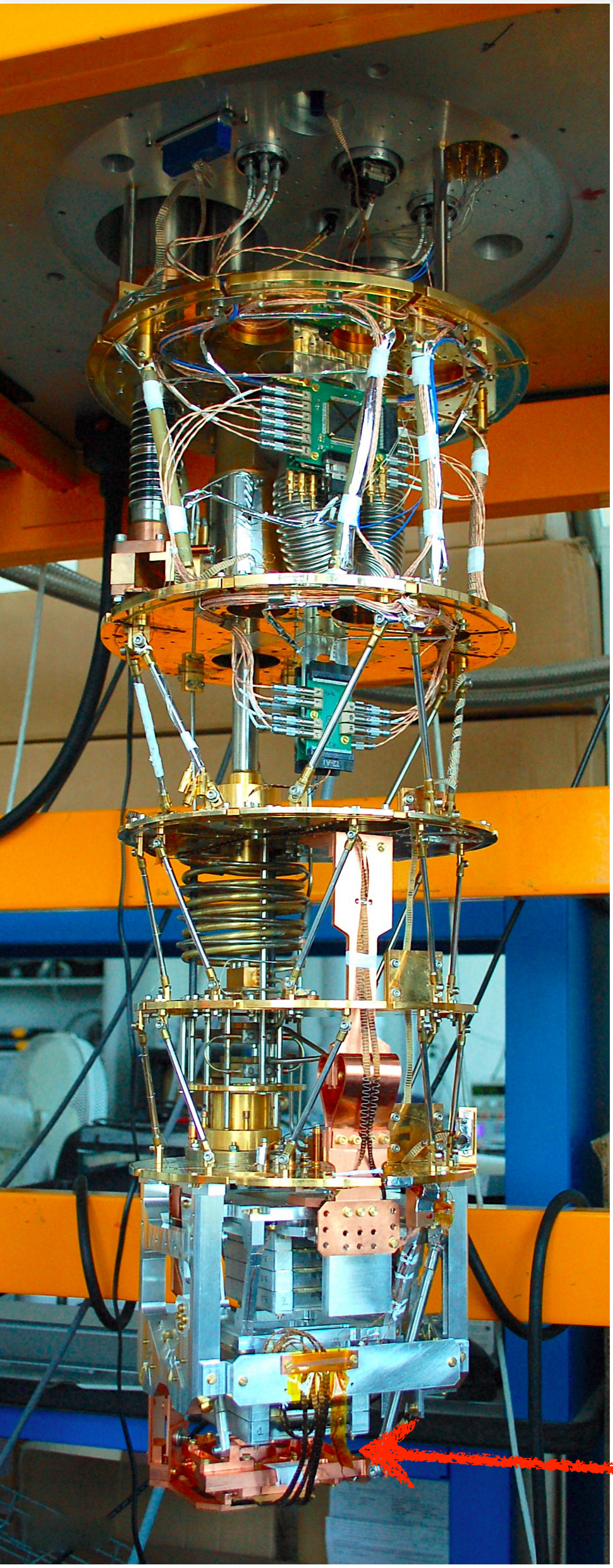

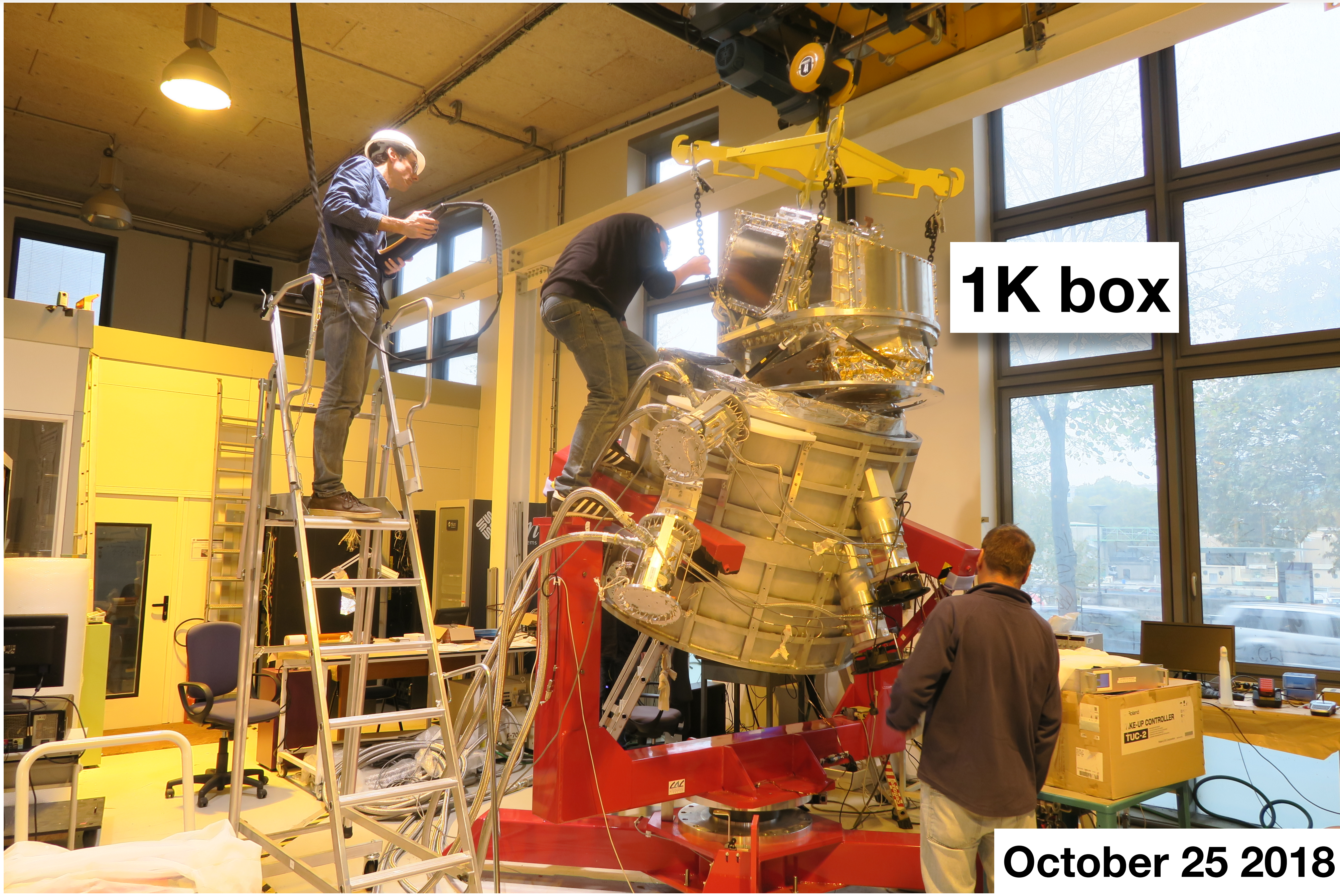

- QUBIC cryostat at APC 1.6 m x 1.8 m
- 10 days need to cool down to mK
- Transition Edge Sensor (TES) focal plane

Lab cryostat: Triton 200/400

II.2. Transition Edge Sensor (TES)

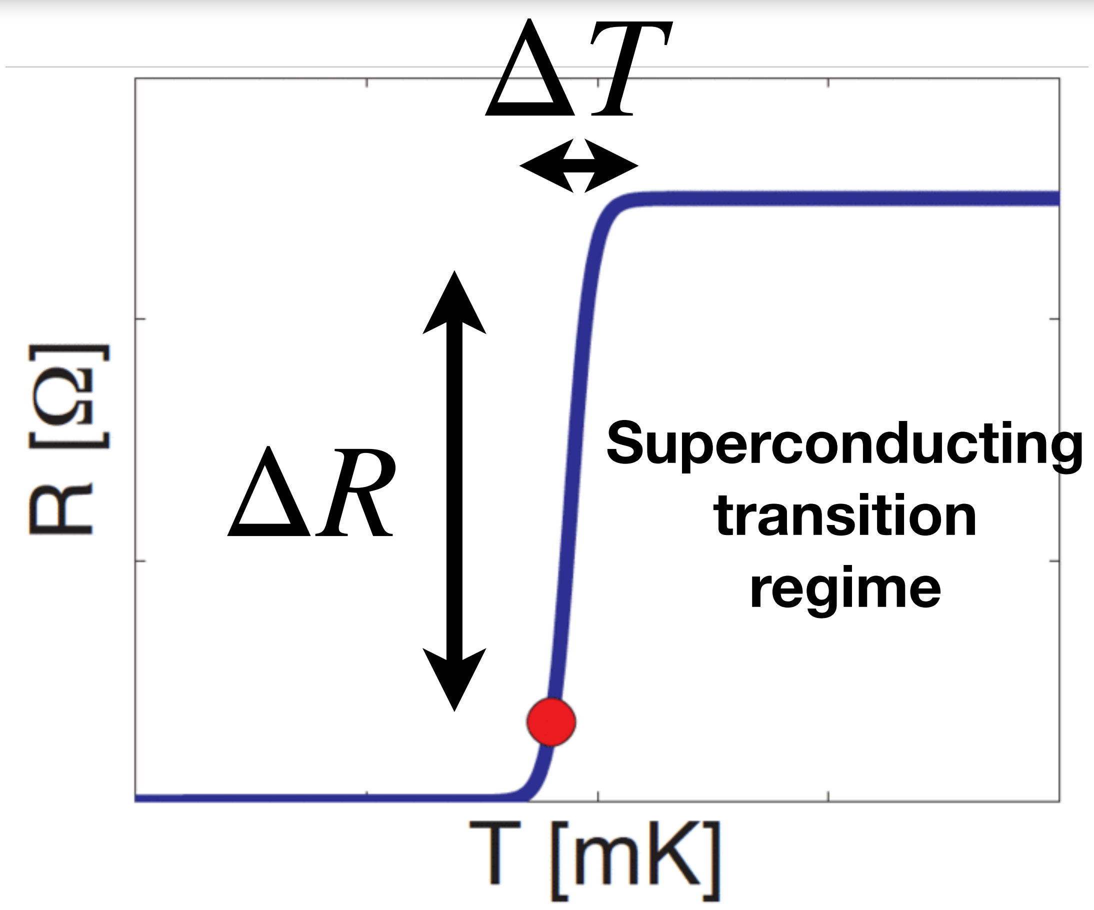

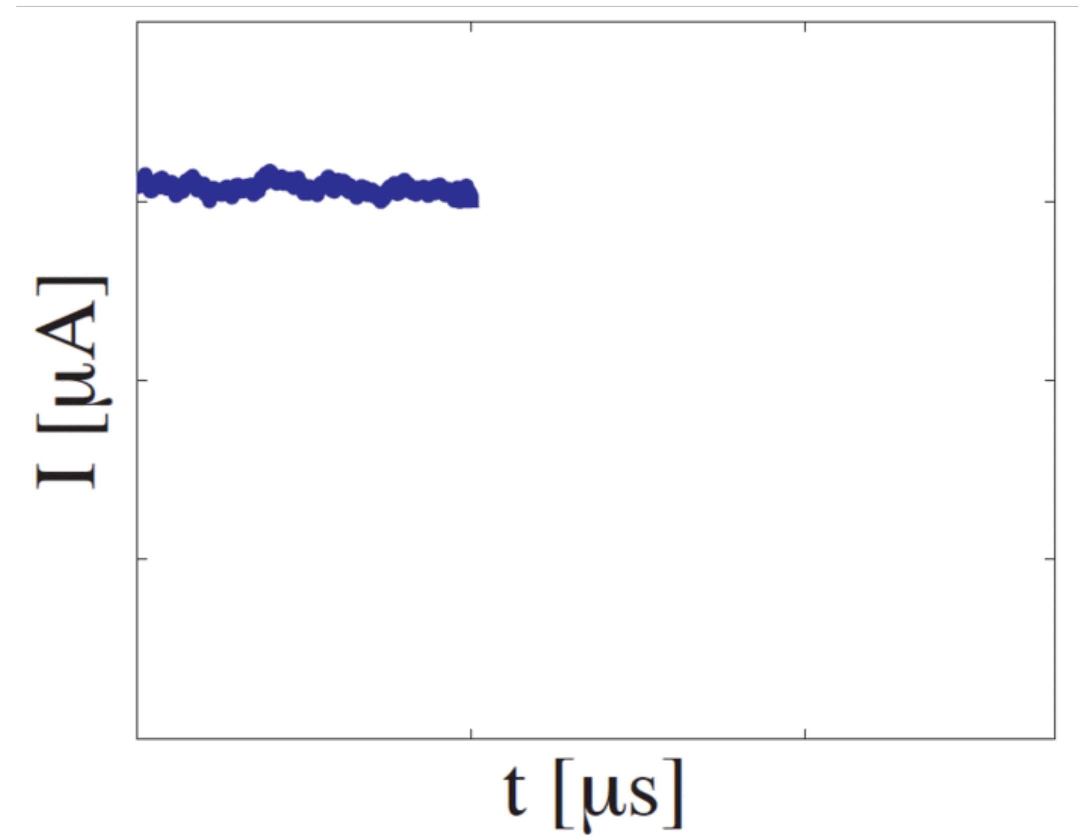

- A strong negative ElectroThermal Feedback (ETF) speeds the detector by the loop gain parameter $\tau_{thermal} = \frac{C}{G(\mathscr{L}+1)}$, $\mathscr{L} = 10 - 100$
- In a voltage-bias mode: TES is self-calibrating in its transition temperature. $P_j = \frac{V_{bias}^2}{R_{TES}}$.
  =>TES array
- Linear response, the current responsivity is $-\frac{1}{V_{bias}}$.

- An array of 256-TES
- 4x32 SQUIDs read out signal
- 128:1 Time Domain Multiplexing
- 2-ASIC
- FPGA (PID controller)
- QUBIC studio interface

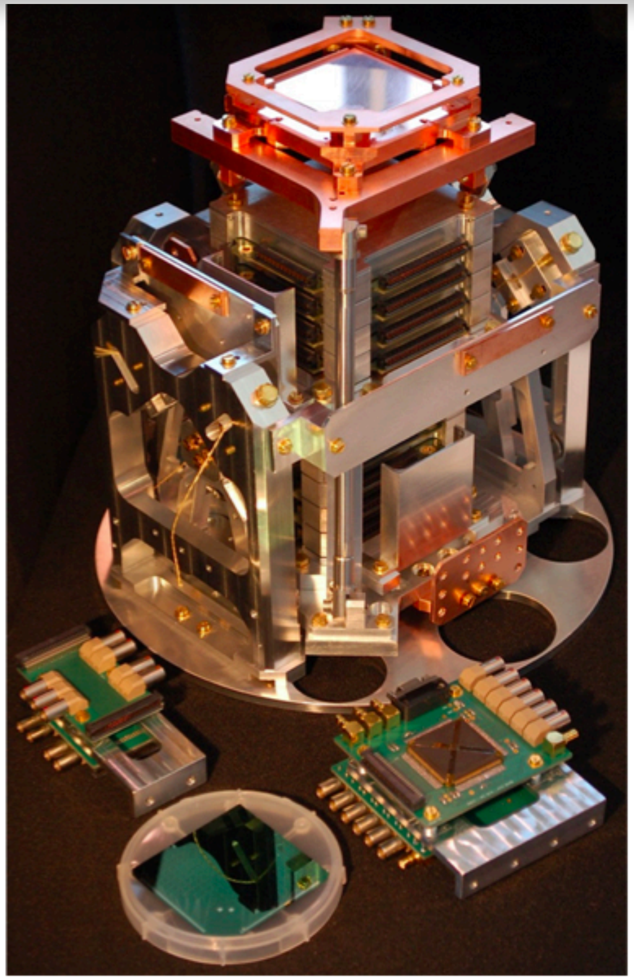

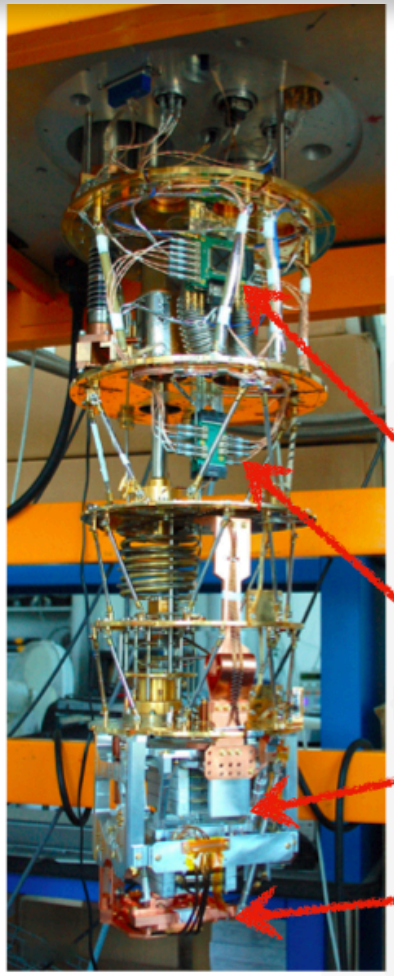

Cryostat wiring for 256 TESs warm readout FPGA & QUBIC studio

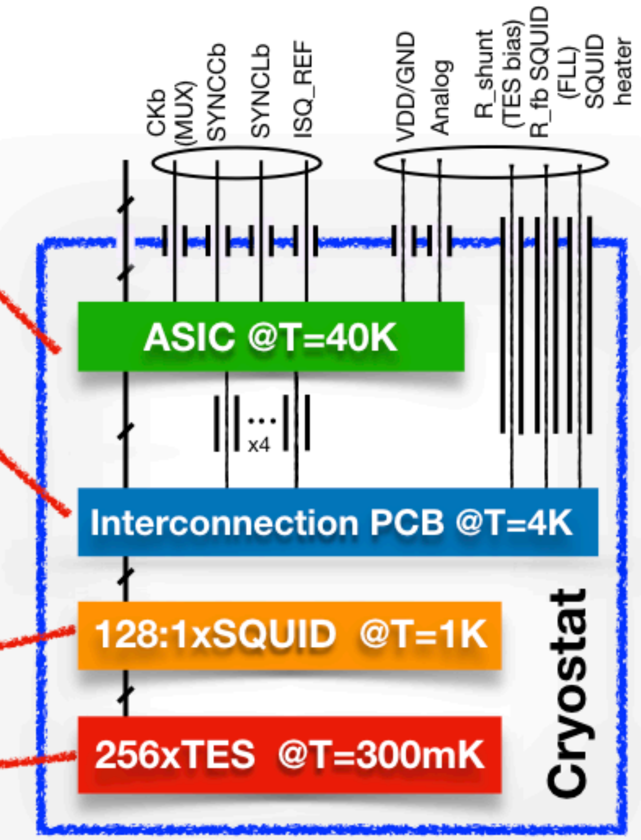

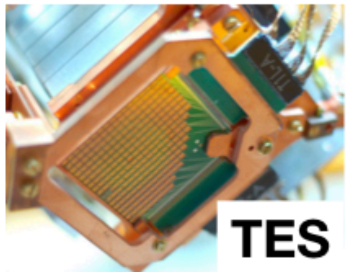

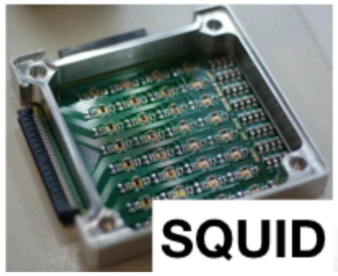

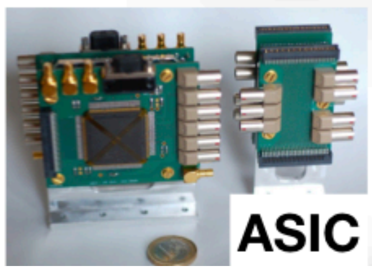

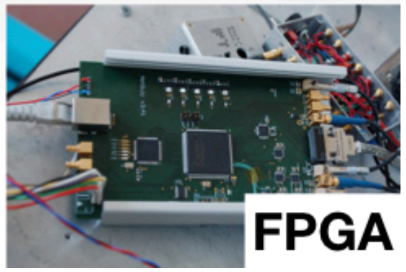

- Electronic readout chain time constant:

$$\tau_{\text{elec}} = \frac{R_{\text{fb}}}{H_{\text{SQ}} G_{\text{gain}} M_{\text{fb}} K_{\text{I}}}$$

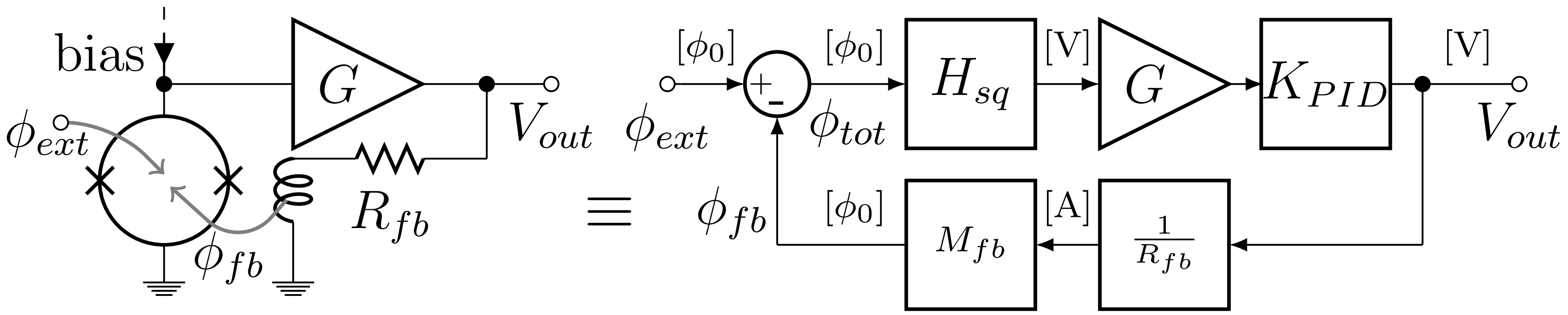

II.2. IV curves measurement

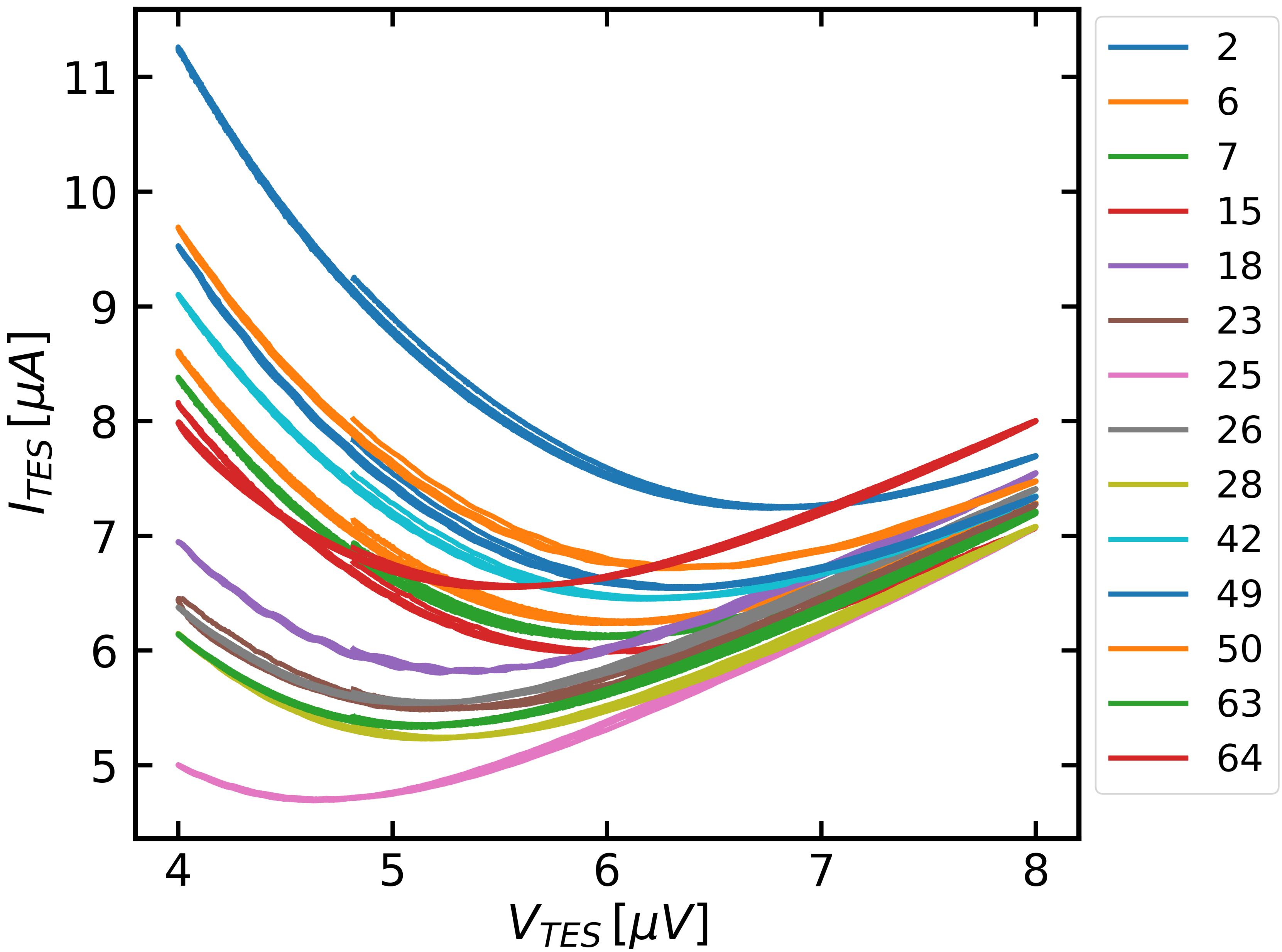

- **Superconducting regime   Transition regime   Normal regime**
- **IV curves help us to determine TES behavior and calibrate.**
- **Determine position of radioactive source.**

II.3. Radioactive source 241Am

Study TES behavior

- 241 Am:
  - 5.4 MeV alpha particles
  - 80 keV gamma rays
  - 8 particles per second
- 5 mm from detector
- In front of the pixel 88

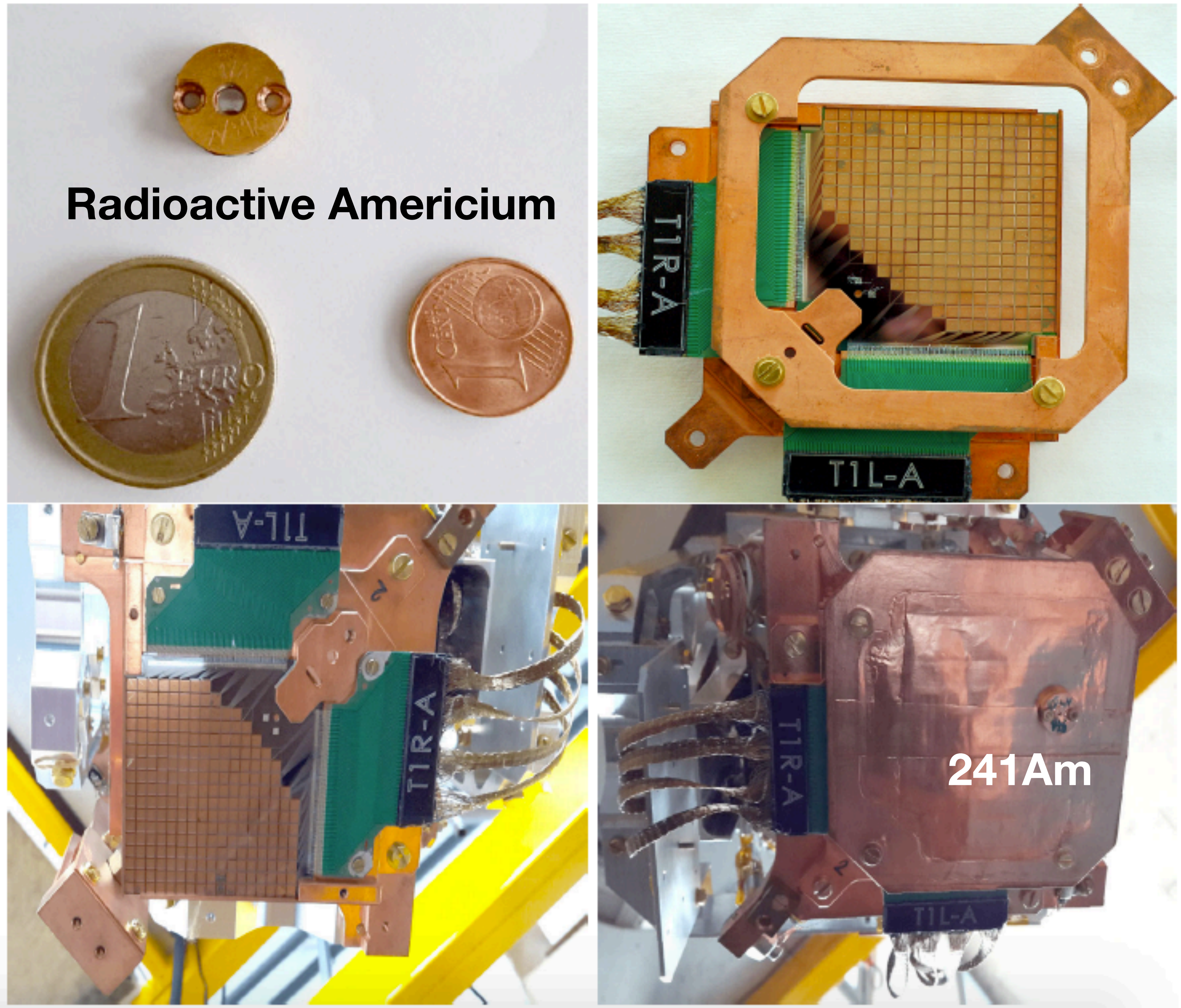

II.4. Glitches data analysis

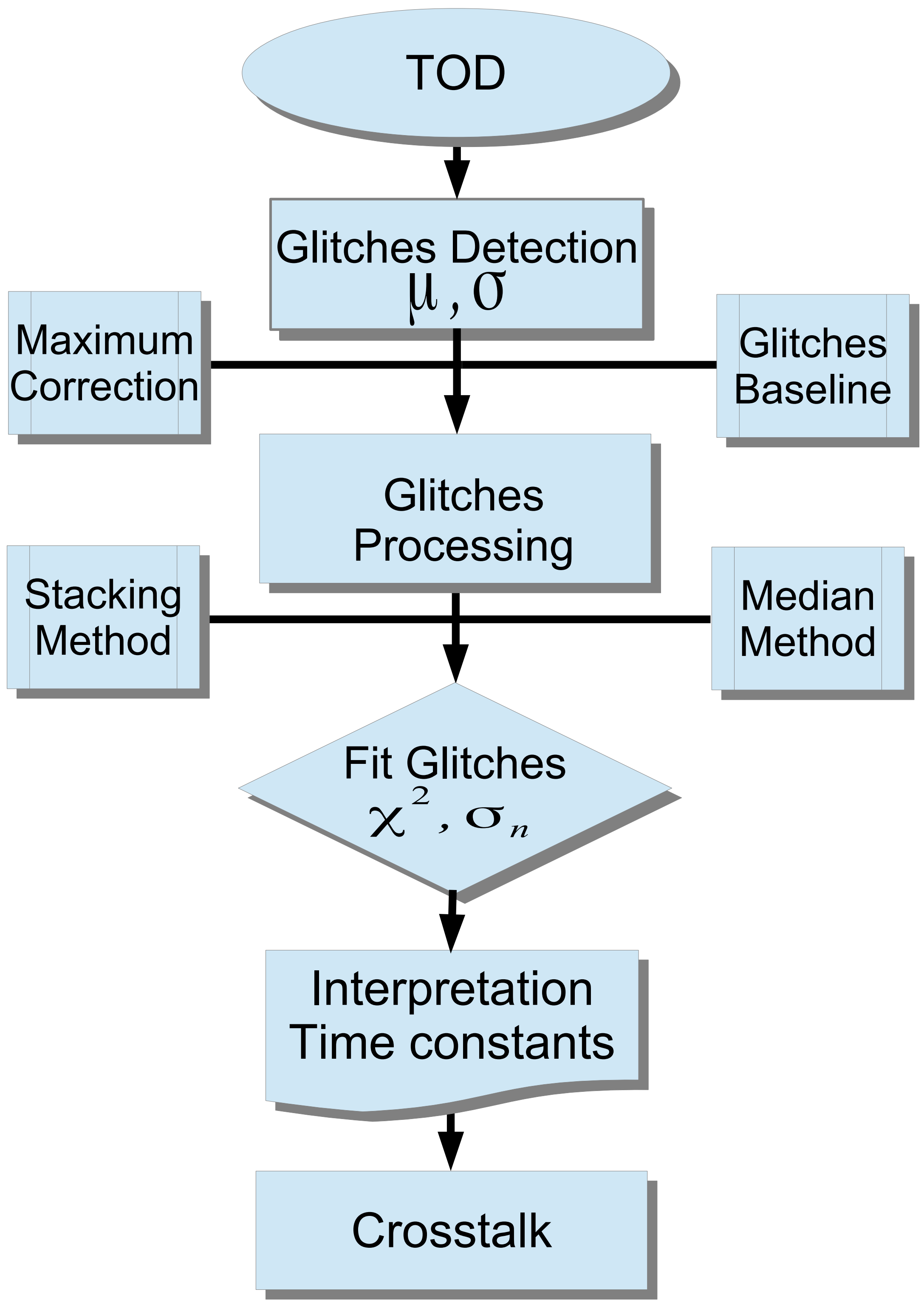

~ 10 minutes

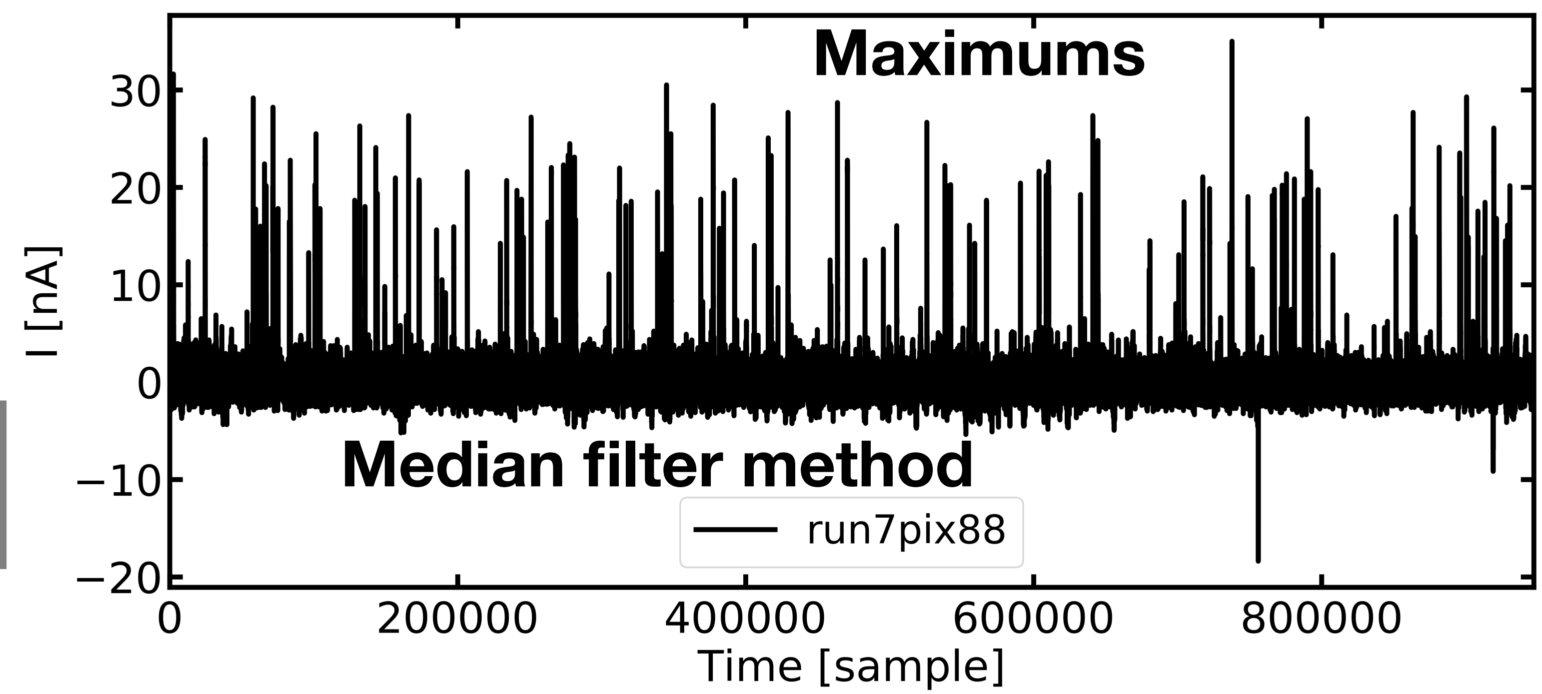

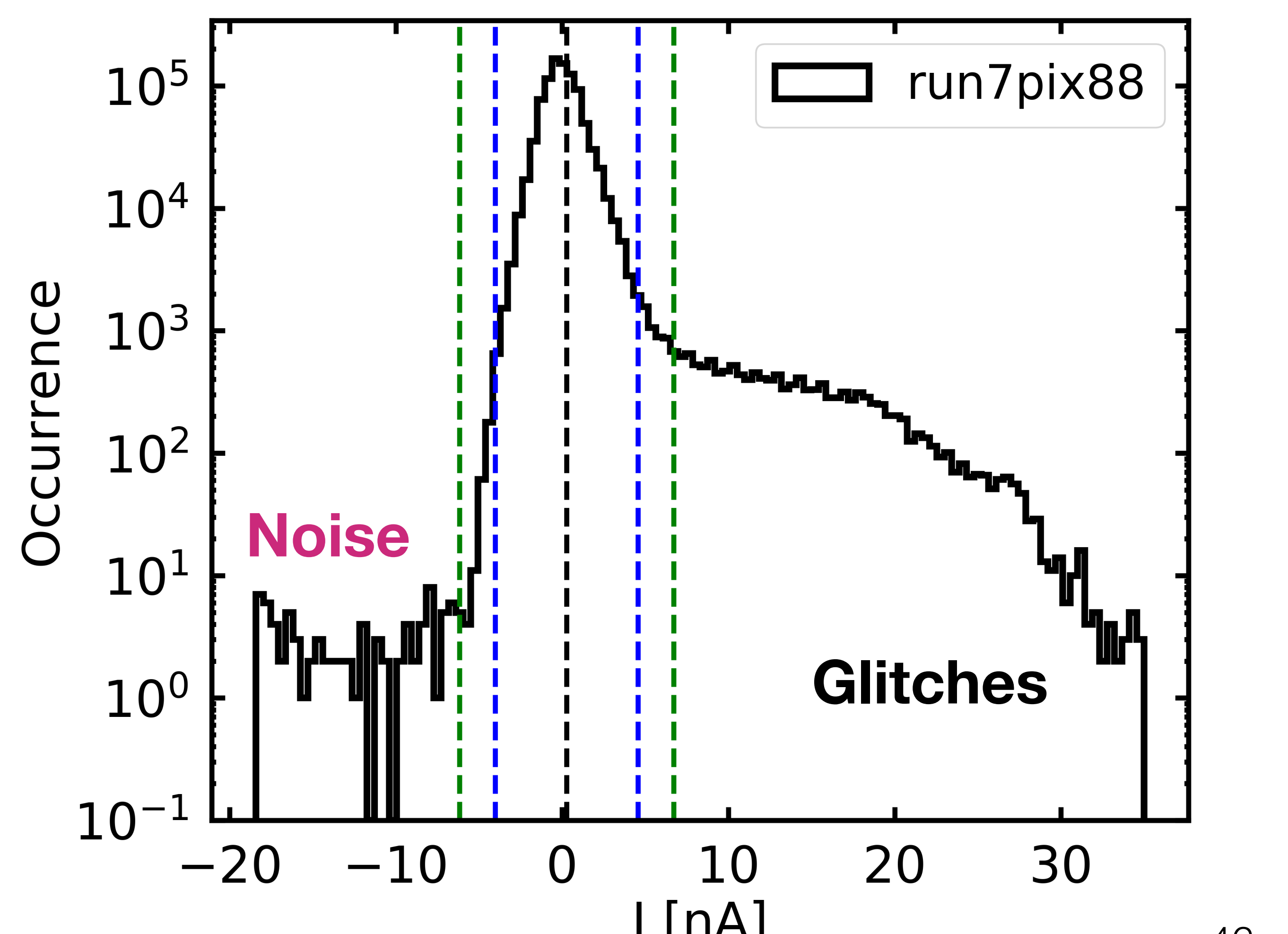

II.4. Glitches detection & processing

Glitches detection:

- A Glitch: 750 bins sample (200+550)

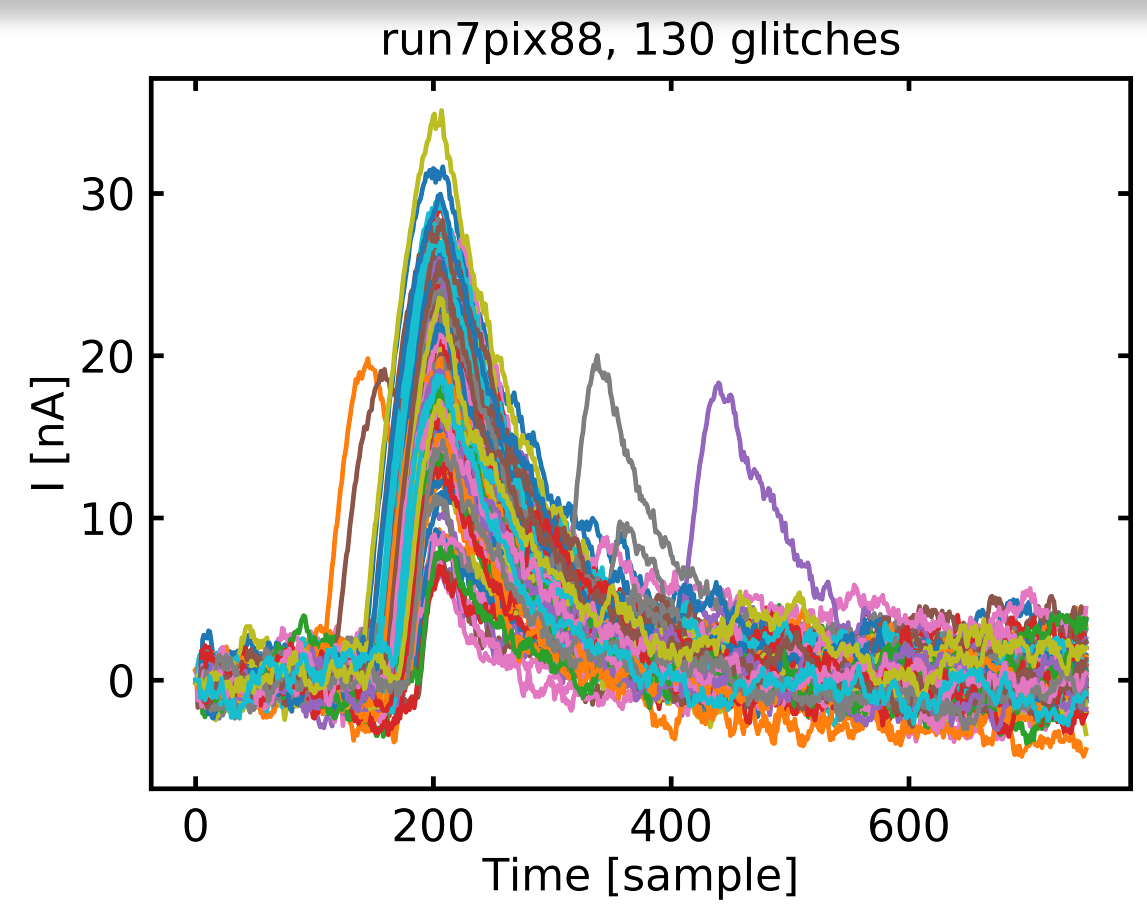

Glitches Processing:

- Median baseline
- Maximum correction

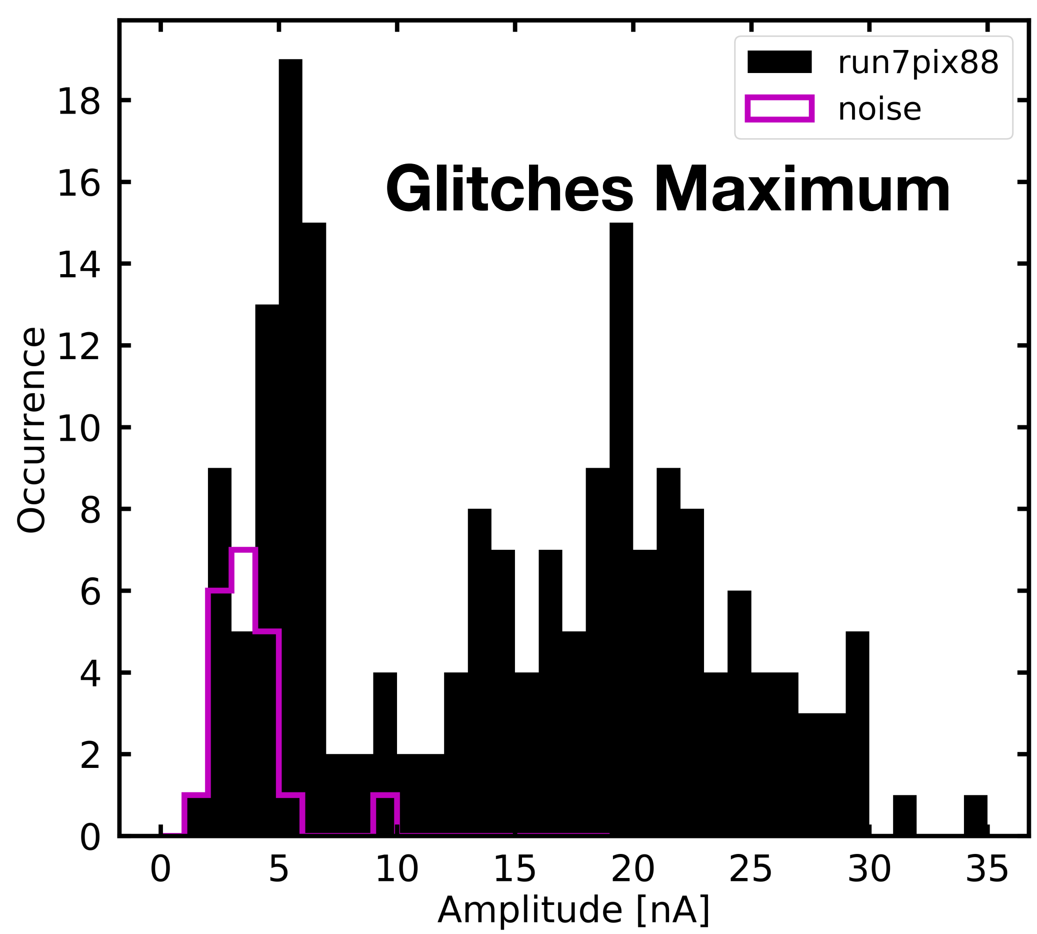

II.4. Template fitting

$$S(t) = a\left(1 - \exp^{-(t-t_0)/\tau_0}\right)\exp^{-(t-t_0)/\tau_1} + c$$

Amplitude **Rising time** **Decay time**

τ_0 : Rising time

τ_1 : Decay time

c : Offset

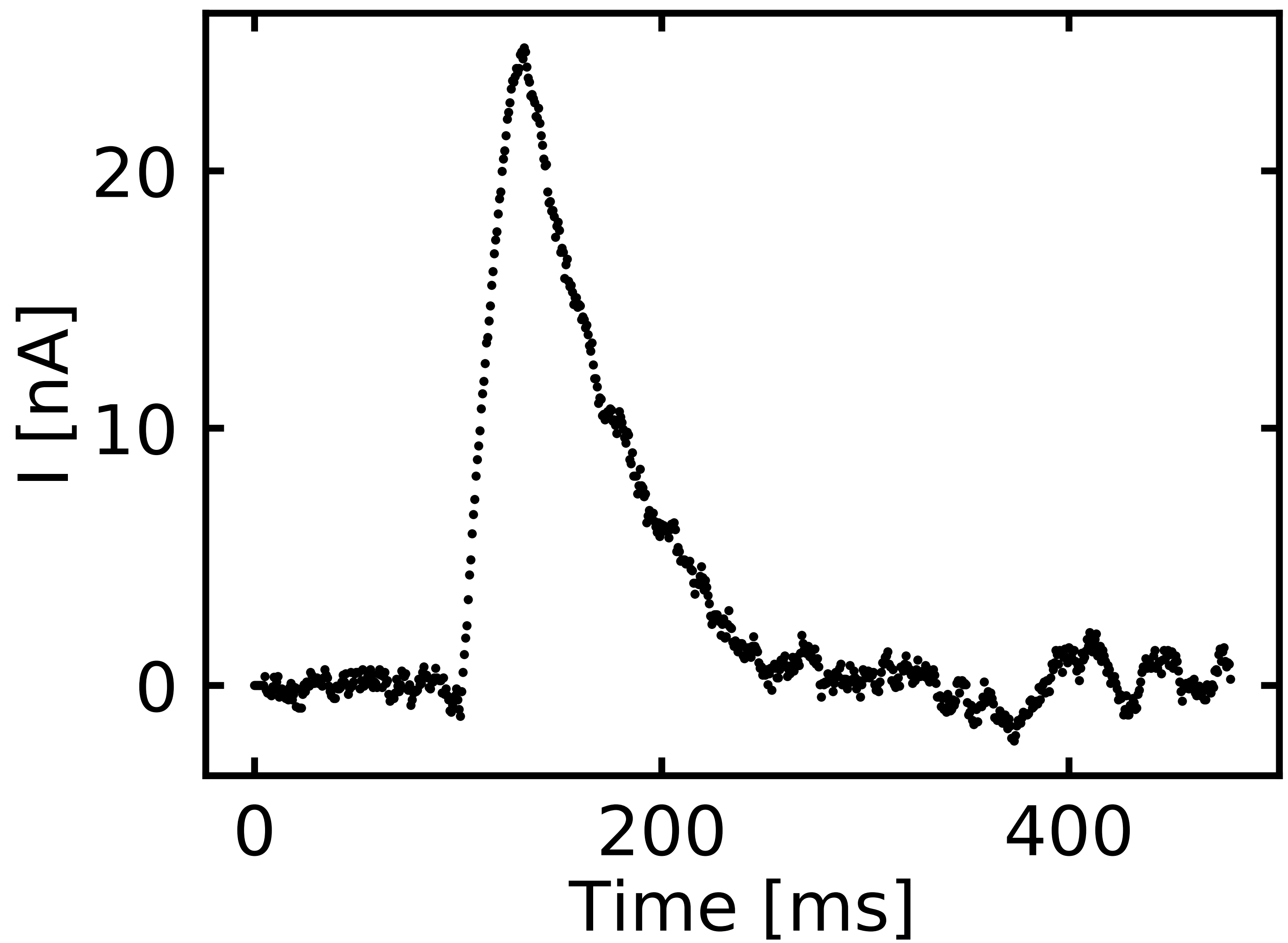

II.4. Fitted glitches, chi2 estimation

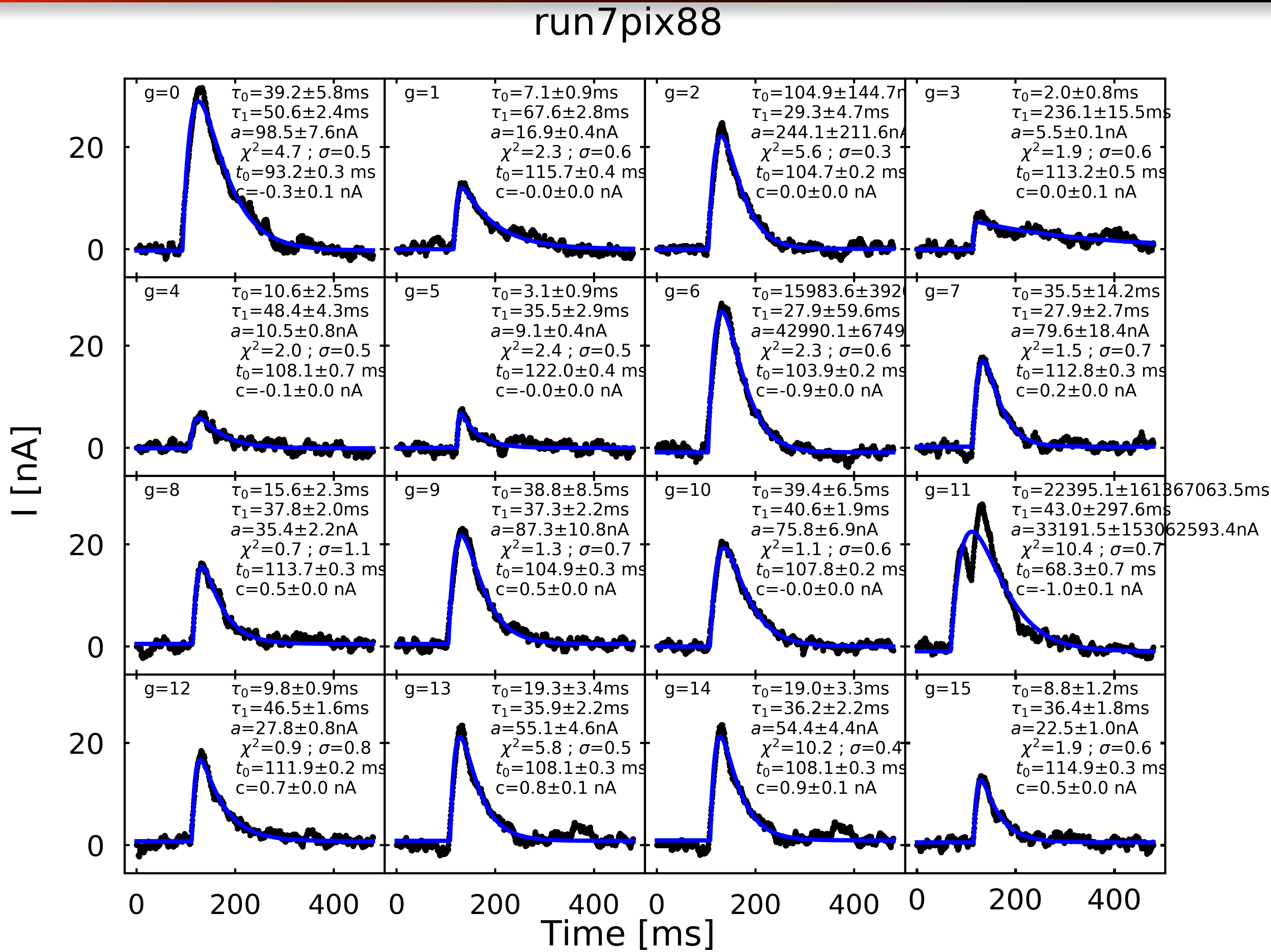

II.4. Time constants distributions

- **Two populations of the rising time constant**

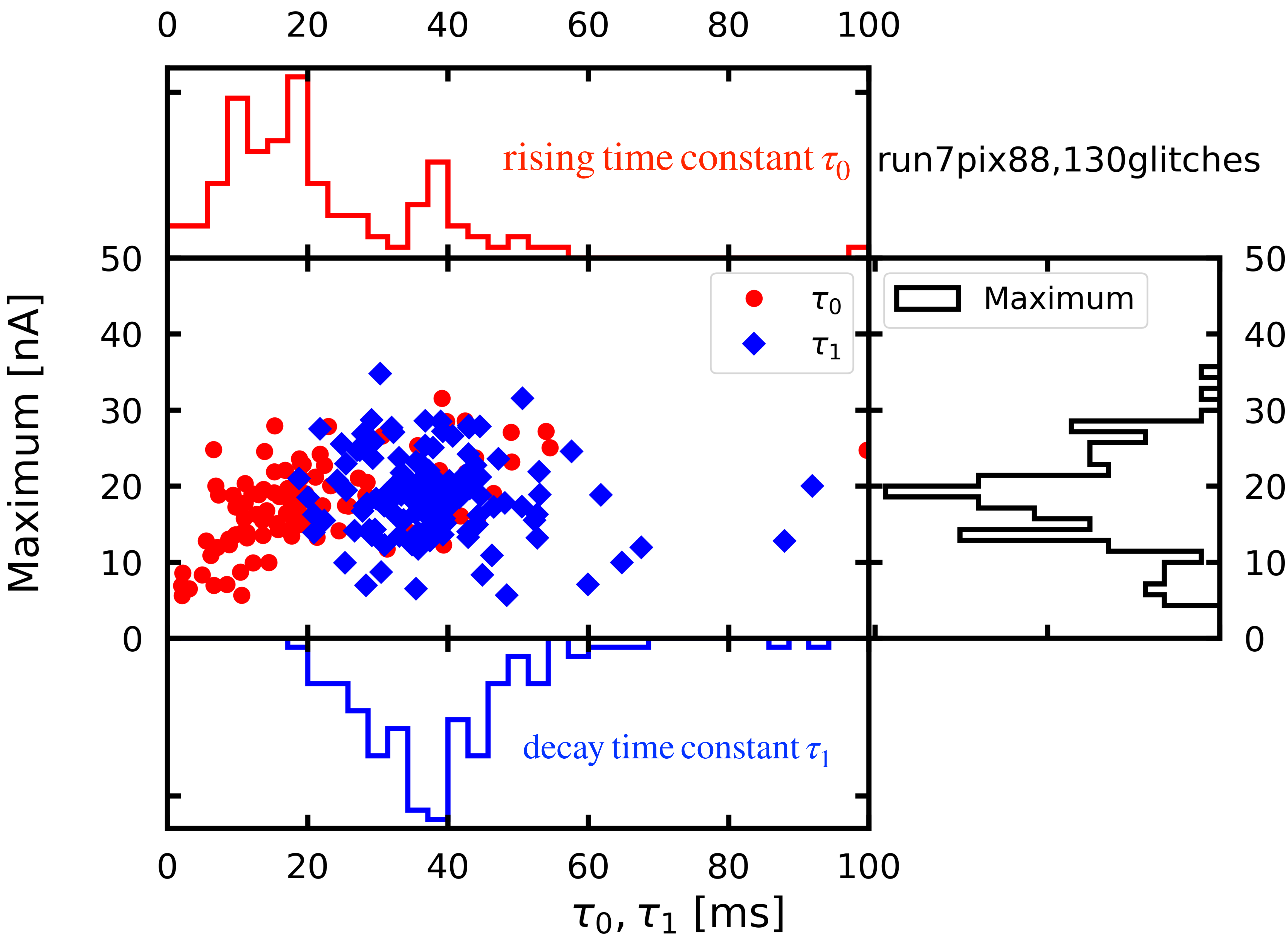

II.4. Time constants distributions

2 populations of the rising time constant:

(1)

$$\tau_0 \sim 10\,\mathrm{ms} \equiv \tau_{\mathrm{elec}}$$

$$\tau_1 \sim 40\,\mathrm{ms} \equiv \tau_{\mathrm{thermal}}$$

(2)

$$\tau_0 \sim 40\,\mathrm{ms} \equiv \tau_{\mathrm{thermal}}$$

$$\tau_1 \sim 40\,\mathrm{ms} \equiv \tau_{\mathrm{thermal}}$$

II.4. Interpretation

- NbSi 293 μm
- Absorber: 50x50 μm holes
- Si substrate 500 μm
- ~3 mm a pixel

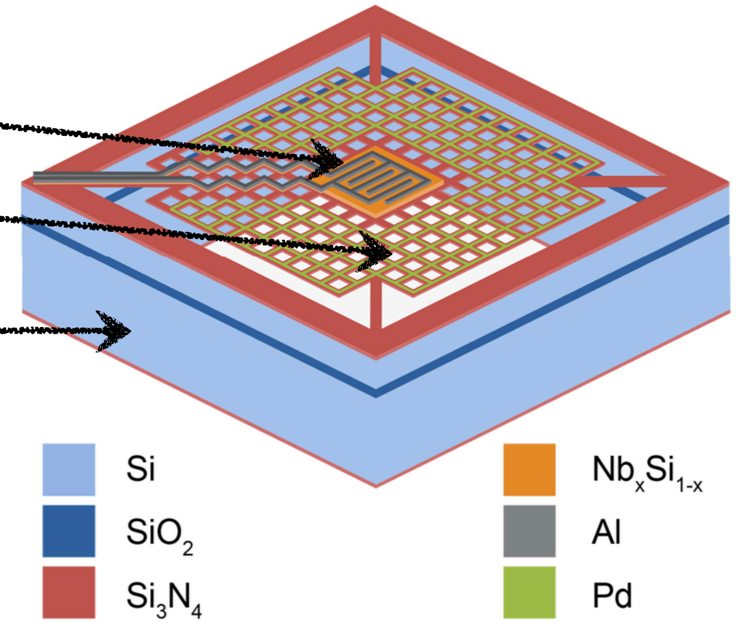

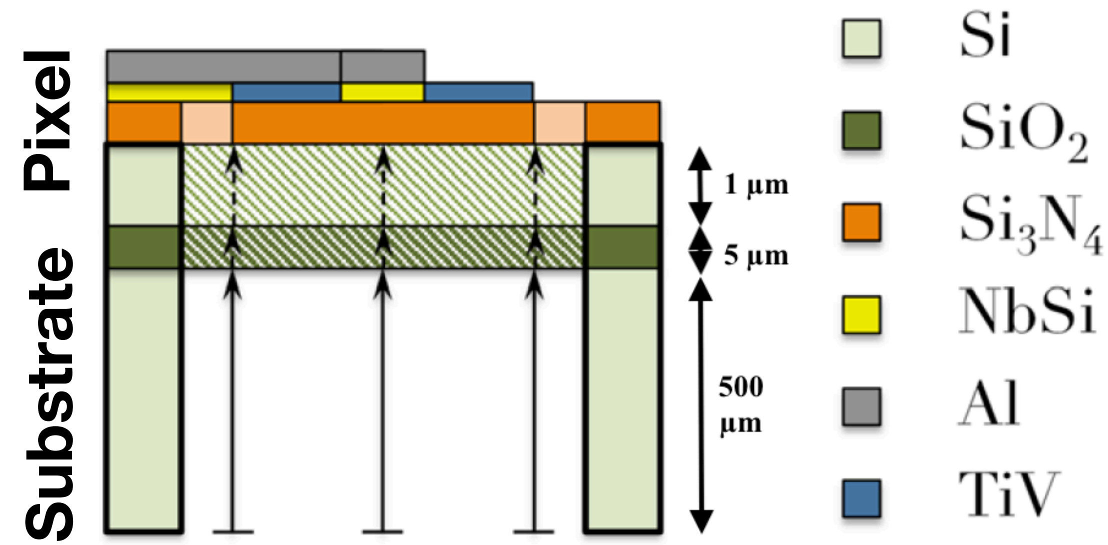

1. **The fist population:** Particles hit directly to *the sensor* (thermometer TES or the absorber), thermal effect propagates very quickly to the thermometer and the rising time constant τ_0 is the *electronic readout* time constant. The thermal equilibrium process is rapidly established due to the deposited energy on the absorber which has a *thickness of 1* μm .

2. **The second population:** Particles could hit the *Si substrate*, the deposited energy is huge due to the *thickness of 500* μm . Because the thermal coupling is *not perfect* between the *Si wafer and the back copper* (thermal bath). *The edge* of the array is *well pressed* over the back copper. However *the center* of the array is *not uniformly pressed* over this copper then the heat flows could transfer slower than the edge. Consequently, these heat flows arise the *increment* of the *background reference temperature* in which is finally *detected* by the sensor through a *rising time*. *Problem: We do not see coincident events in neighbor pixel => cross-talk.*

3. **A proposed solution:** We can add a *gold layer* on the back side of the Si substrate in order to fix and uniform the Si bulk temperature which thus could played better the role of thermal bath.

4. **Space application:** In the aspect of Cosmic Rays and a satellite's focal plane using TES arrays, the *Silicon substrate surface* plays an important role to reduce the impact of CRs.

II.5. Thermal Cross-talk

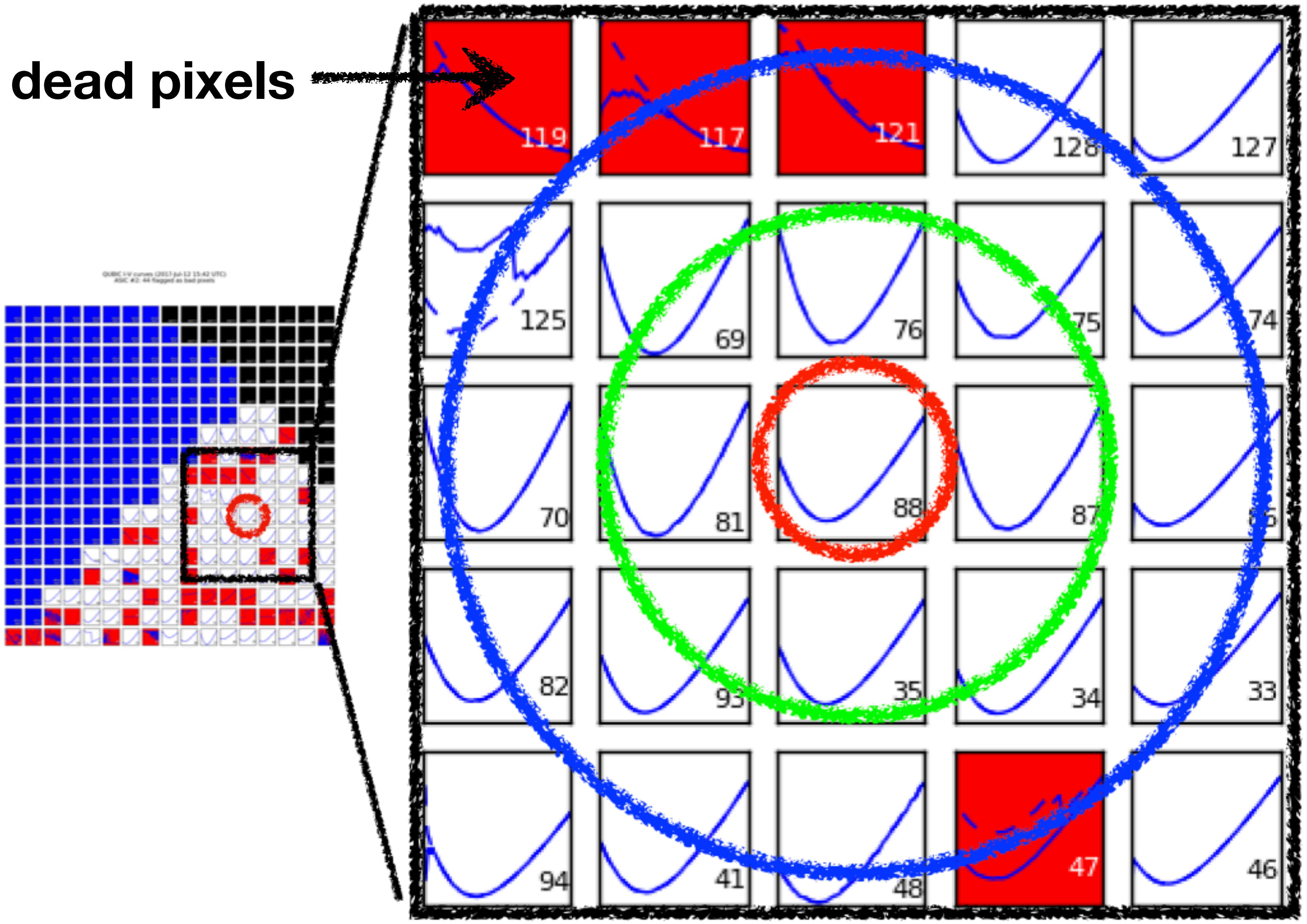

- Fix a reference pixel 88 $d^0_{i(g)}$
- When glitches occur i(g)
- Estimate the thermal elevation among pixels N_j, C1, C2, C
- Estimate baseline noise b

Cross-talk estimator:

Neighbor pixels — Baseline estimation position

$$C(b, \text{pixel area}) = \frac{1}{N_g}\frac{1}{N_j}\sum_{g=1}^{N_g}\sum_{j=1}^{N_j}\frac{d^j_{i(g)} - 0.5d^j_{i(g)-b} - 0.5d^j_{i(g)+b}}{d^0_{i(g)}}.$$

reference pixel

II.5. Thermal Cross-talk

Baseline position b	pixel	$C_1(b)\%$	$C_2(b)\%$	$C(b)\%$
5	88	0.0354	0.0157	-0.0026
20	88	-0.1957	0.1996	0.0565
50	88	-0.2838	0.2842	0.0518
100	88	-0.4423	0.2965	0.0045
200	88	-0.0758	-0.0067	0.017
300	88	0.1725	0.1240	0.1792
400	88	0.1782	0.1338	0.2131
500	88	0.0687	0.2923	0.3047
700	88	0.2157	-0.3502	-0.1325
1000	88	0.3343	-0.3702	-0.0757
1500	88	0.2065	-0.6317	-0.2844

- **The thermal cross-talk is constrained to less than 0.1 %. The low statistic, complex noise do not allow to put a better constraint.**

II.5. Cross-talk of the electronic readout system

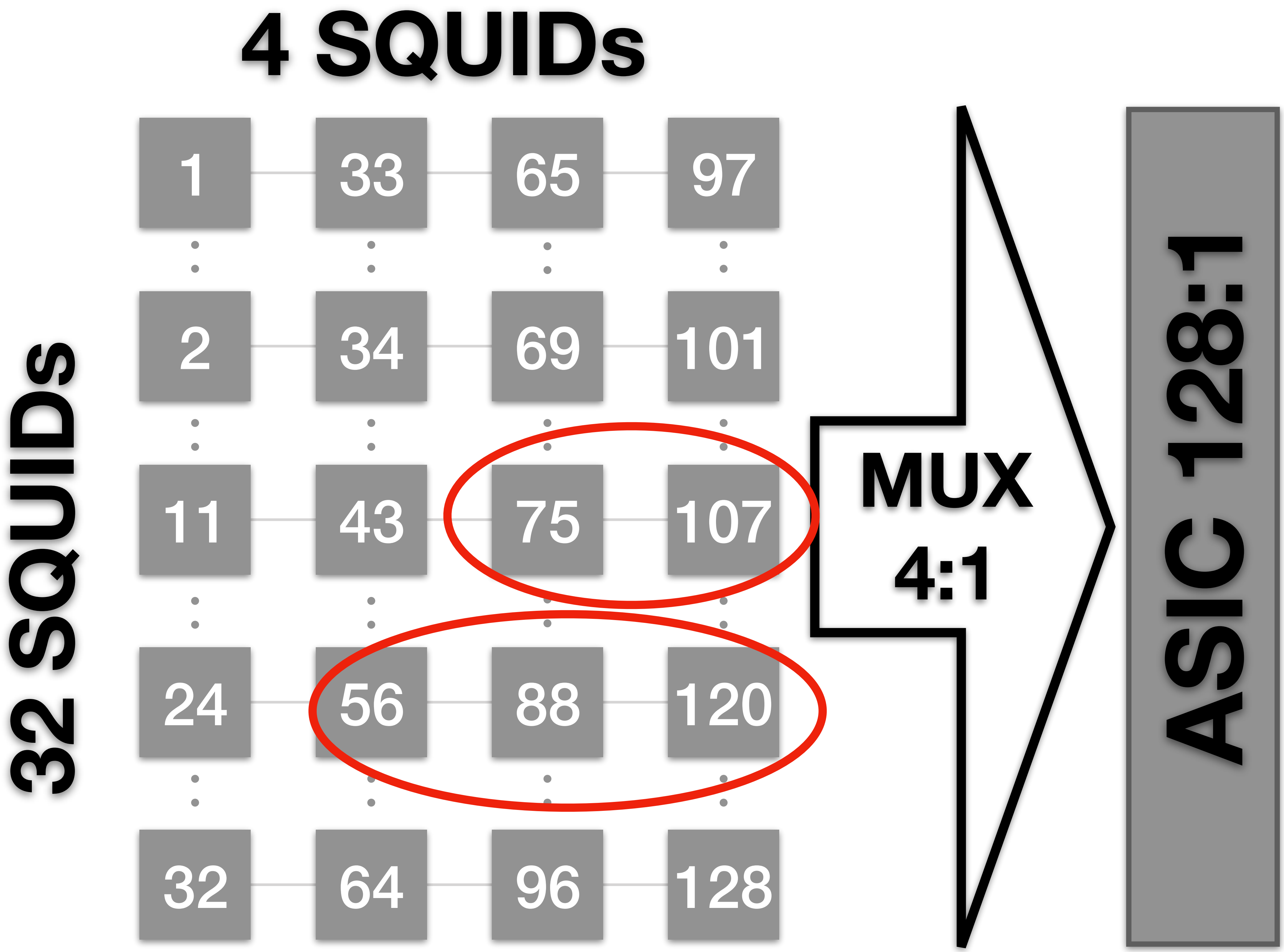

- Time Domain Multiplexing

II.5. Cross-talk of the electronic readout system

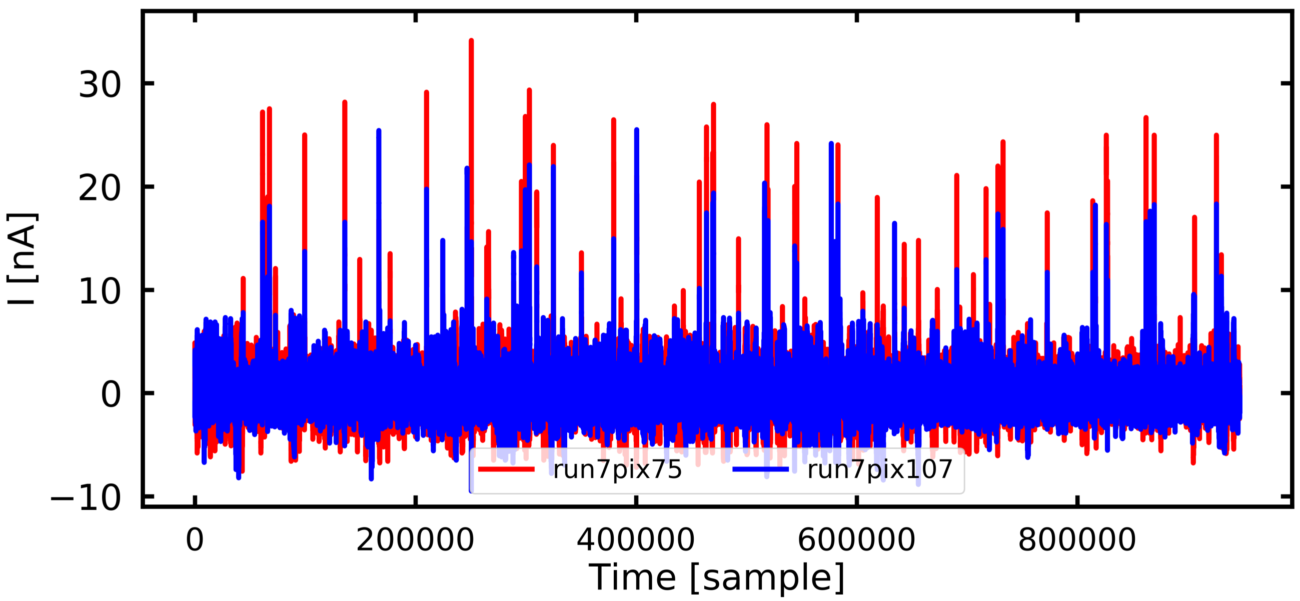

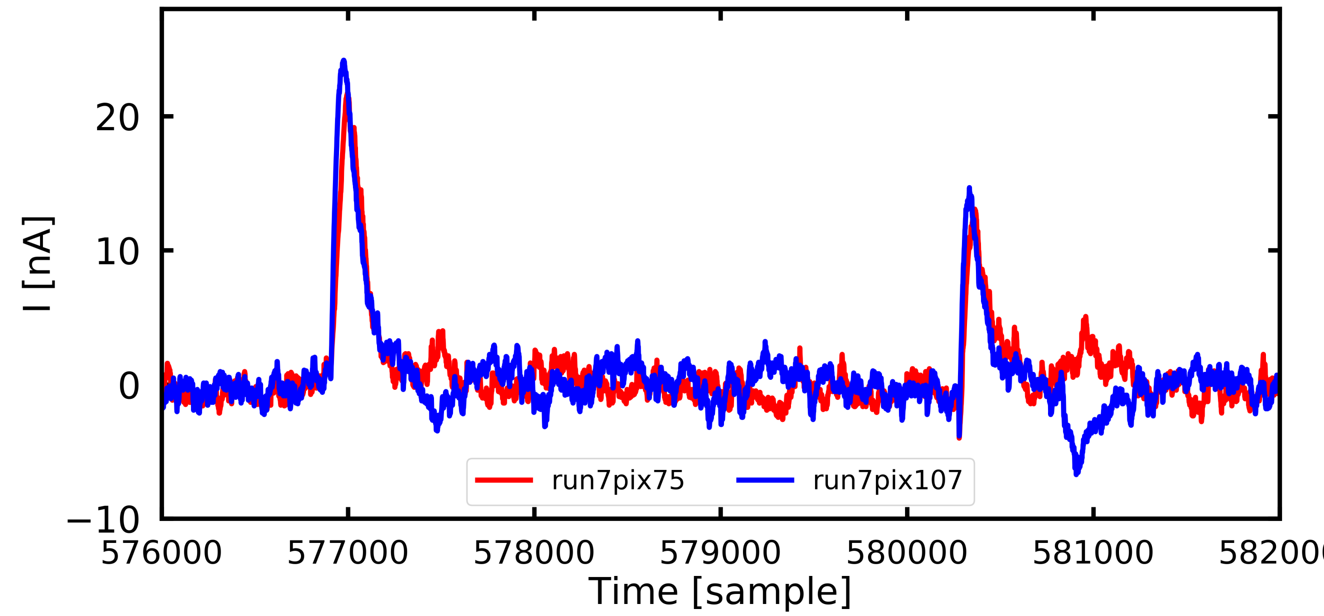

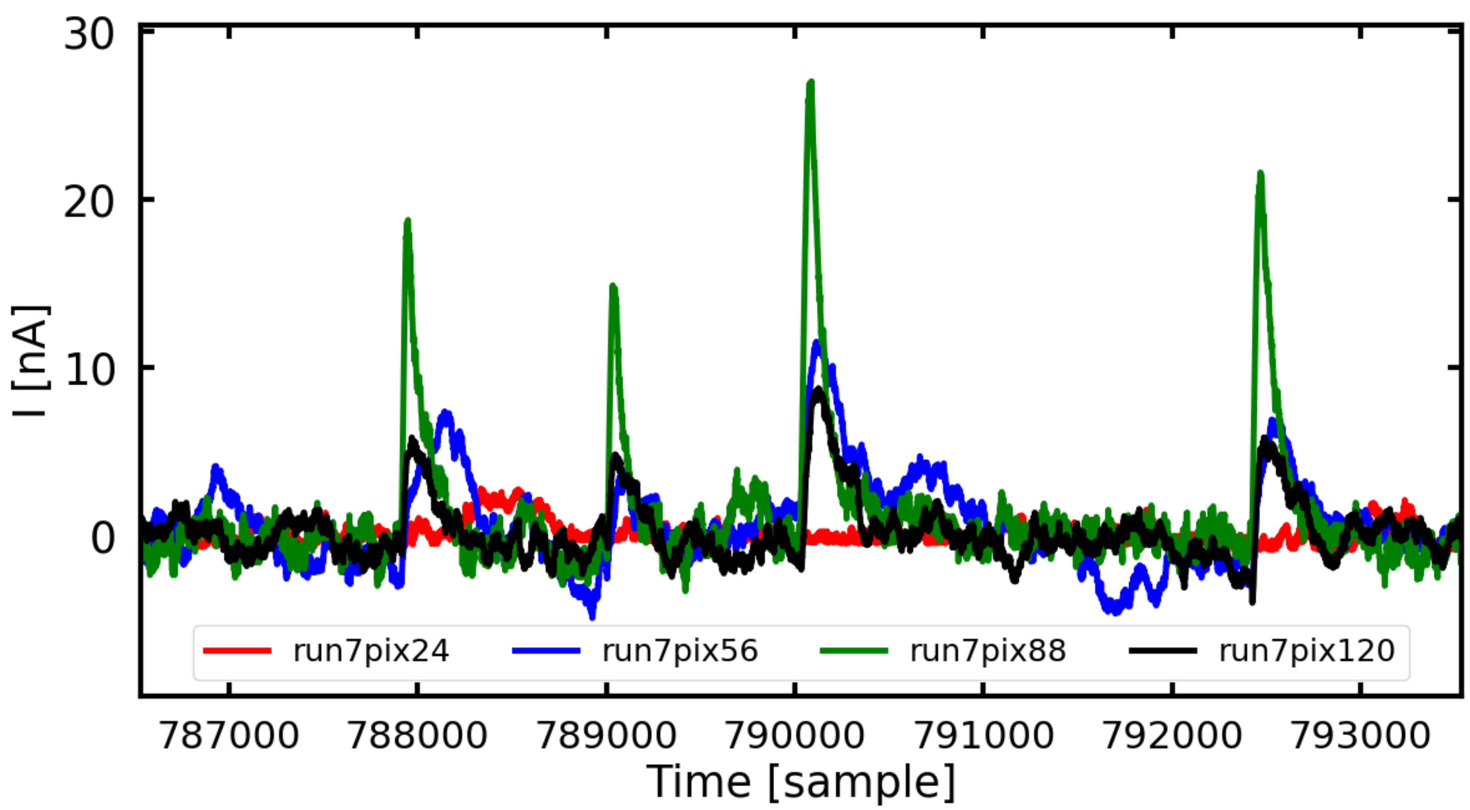

- **We used a fast sampling rate of 0.64 ms (1562.6 Hz)**
- **The frequency acquisition (sample rate) of time domain multiplexing can introduce the cross-talk between two successive pixel.**
- **This study needs a deeper work, => a new topic**

Summary

1. I measured two time constants: The electronic readout chain time constant (7-30 ms) and the thermal time constant (20-60 ms).

2. The possible interpretation of 2 populations of the the rising time constant: Absorber events and Si substrate events.

3. The thermal cross-talk is estimated.

4. I found the cross-talk of the electronic readout system due to frequency acquisition. This study needs a deeper work, => a new topic

Thank you!

BACK UP SLIDES

I. Backup(1) Scanning strategy params $\omega_{\rm prec}/\omega_{\rm spin}$

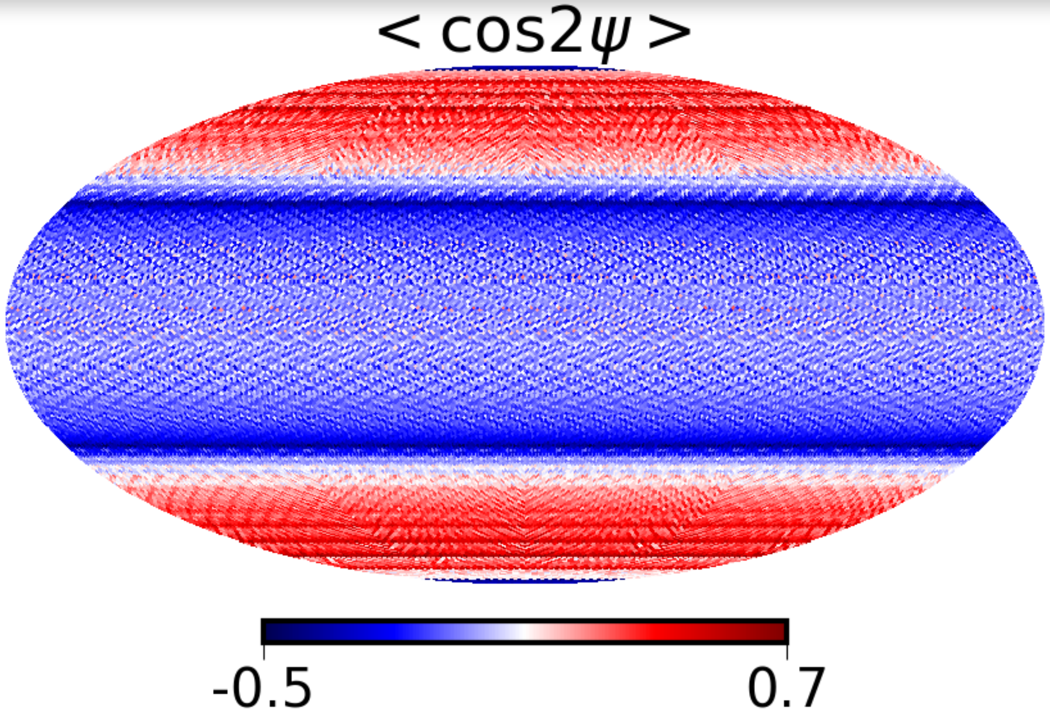

93 minutes, 10 minutes [9,3,3]

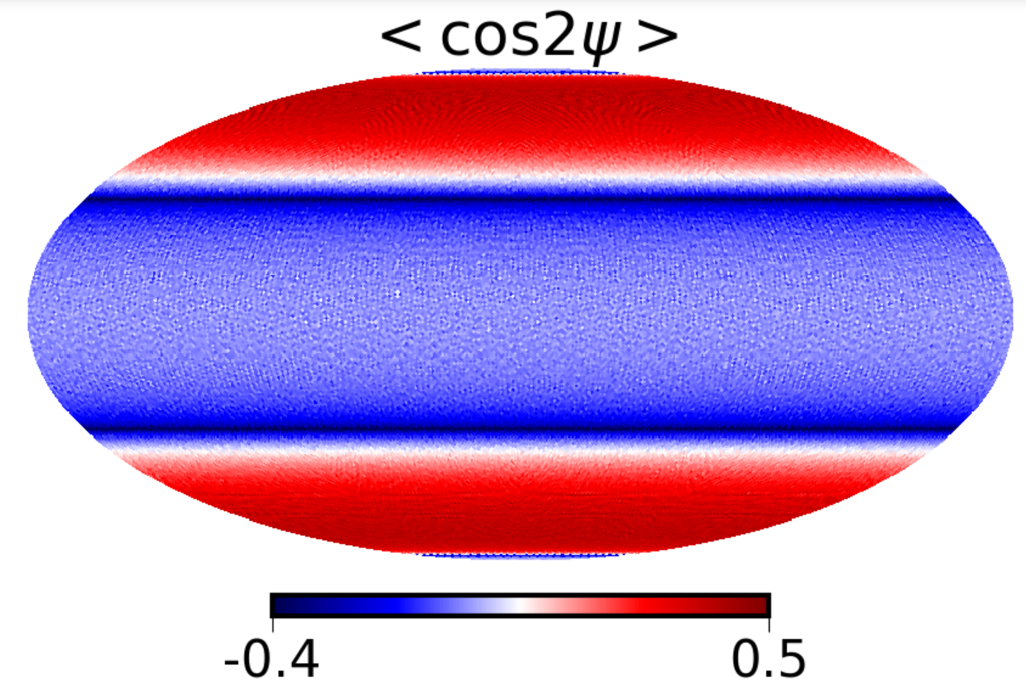

96.61803398 minutes, 10 minutes [9,1,1,1,........]

Mathematically number theory:

$$\omega_{\rm prec}/\omega_{\rm spin} = \theta = [a_0, a_1, a_2, \dots] = a_0 + \cfrac{1}{a_1 + \cfrac{1}{a_2 + \dots}} \quad \textbf{(M.B)}$$

rational number ⟷ (Limited)

irrational number ⟶ (infinite)

The most irrational number: Golden ratio : $\Phi = \dfrac{(1+\sqrt{5})}{2} = 1.61803398875$ **[1,1,1,1,........]**

I. Backup (2) -> Planck leakage

20% masked galactic, 222 detectors and 365 days observation

leakage Q

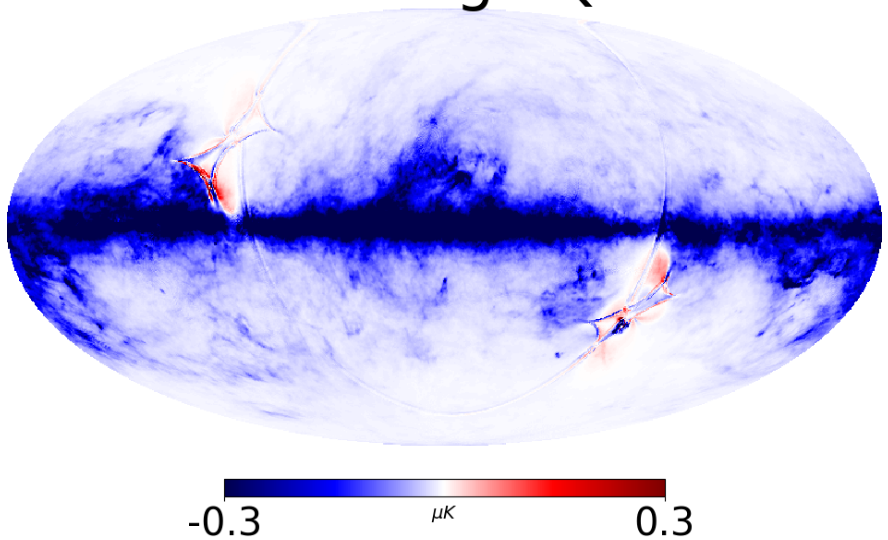

leakage U

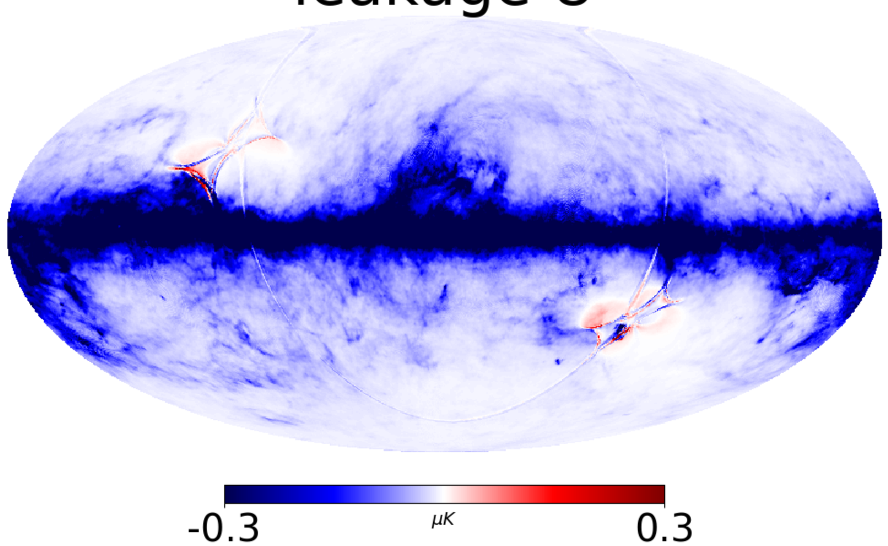

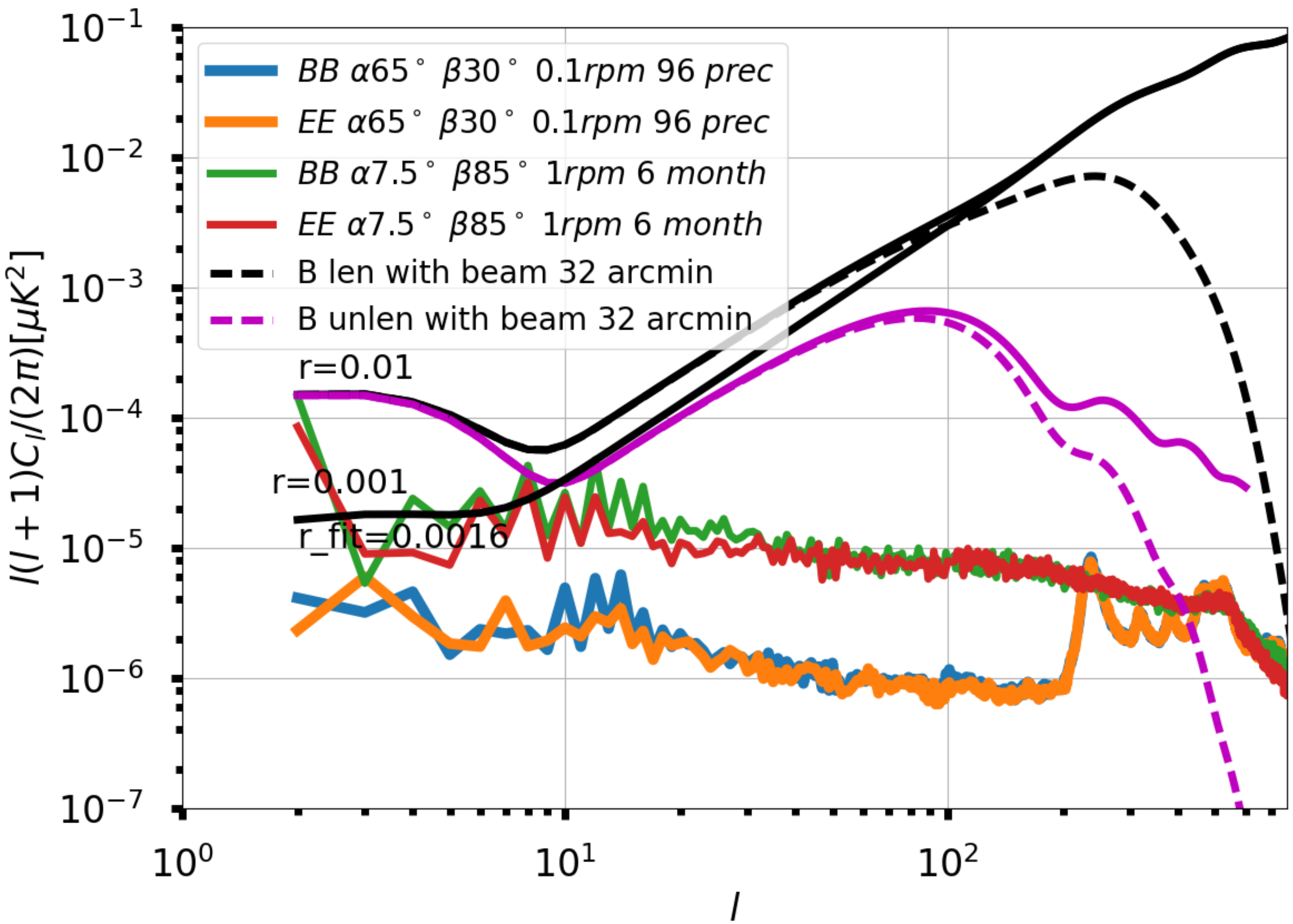

- **Planck scanning strategy is not optimize for polarization measurement**

II.4. Time constants and the PID controller, V_bias

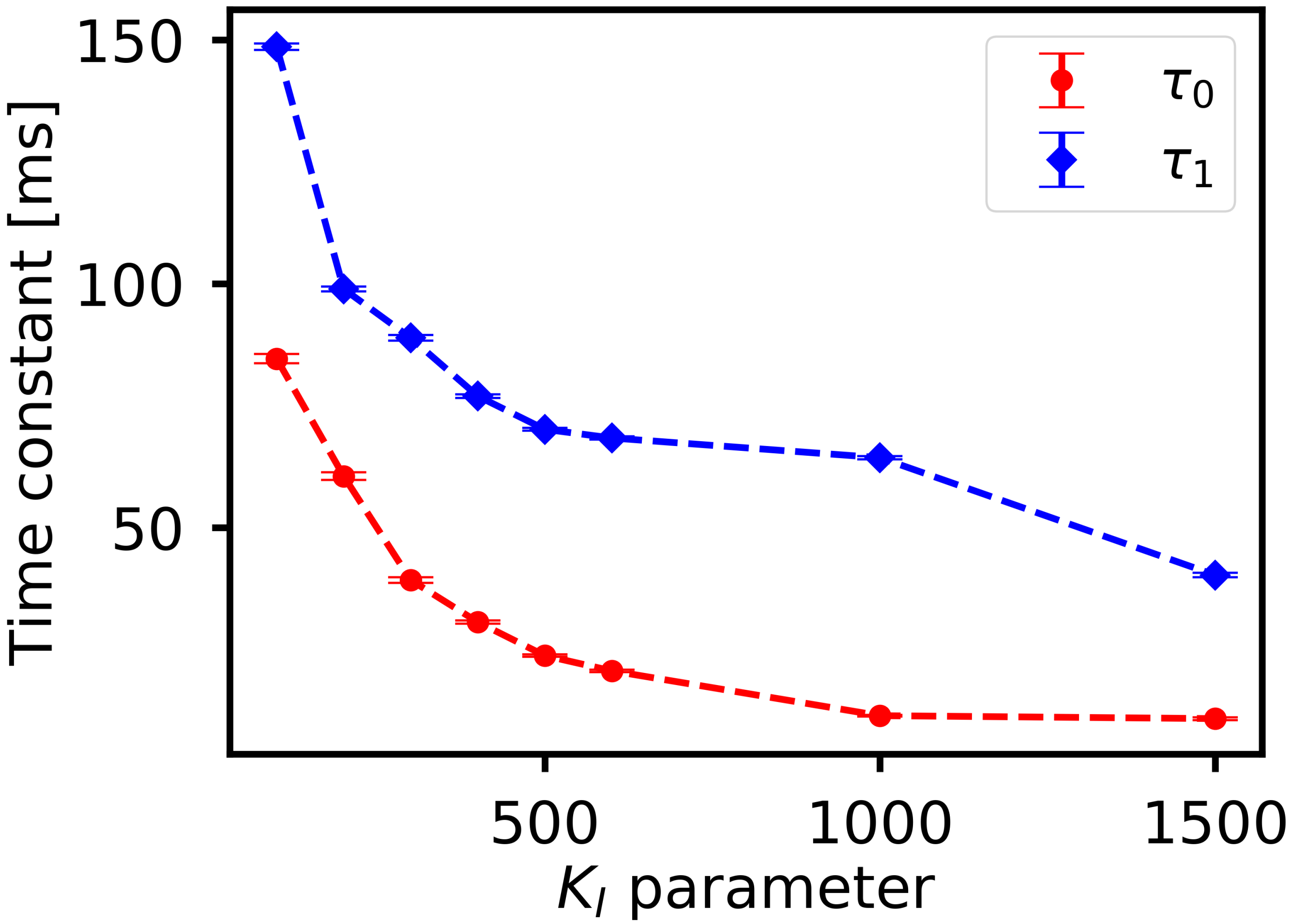

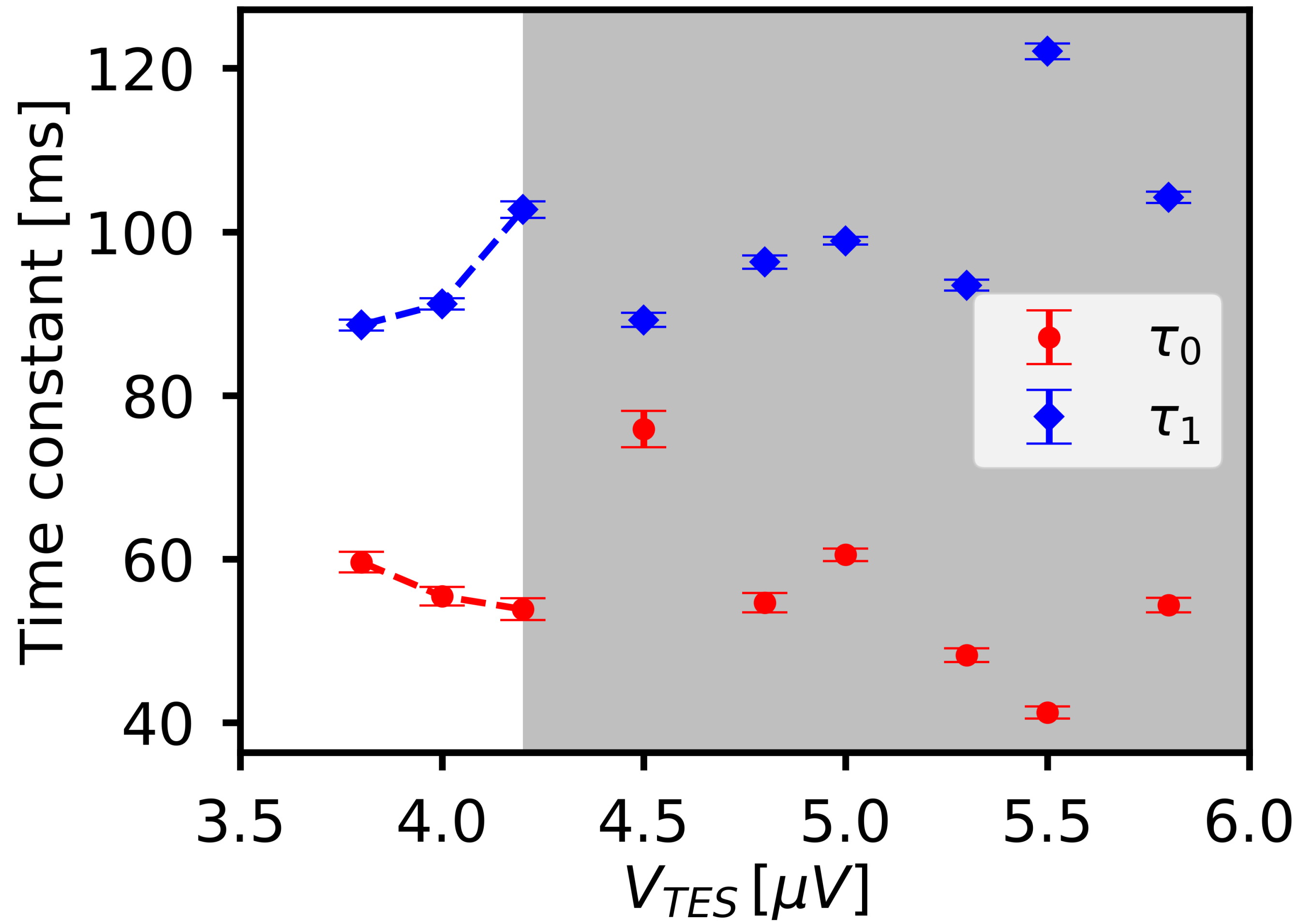

1. *(left)* **When we increase K_I parameter, the time constant corresponding to the readout bandwidth must decrease.**

2. *(right)* **If we increase the voltage bias, the electrical time constant will decrease due to the inverse proportion of the current responsively and the voltage bias.**

3. *(right)* **If we increase the voltage bias, the thermal time constant increase because TES enters to the normal state, the logarithmic sensitivity to temperature parameter is small.**

Time constant & scattering operating point of TESs

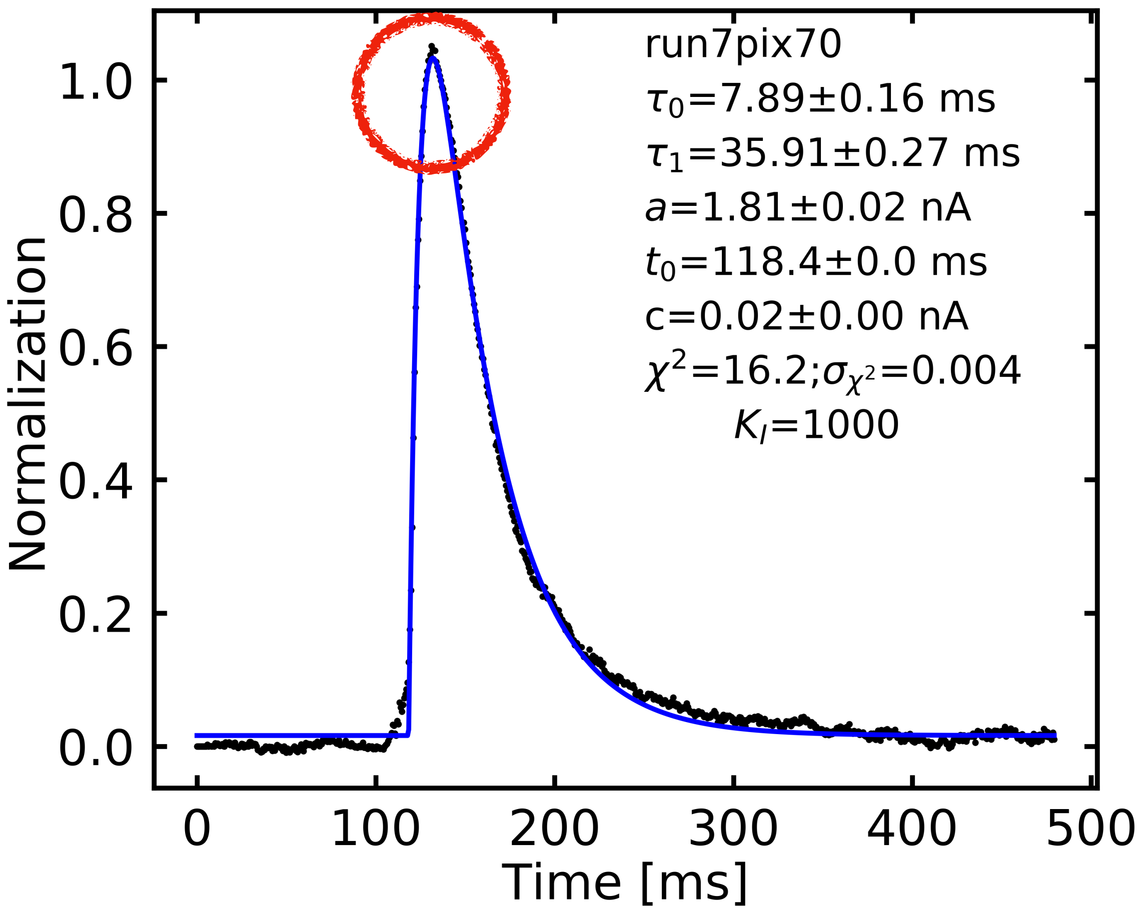

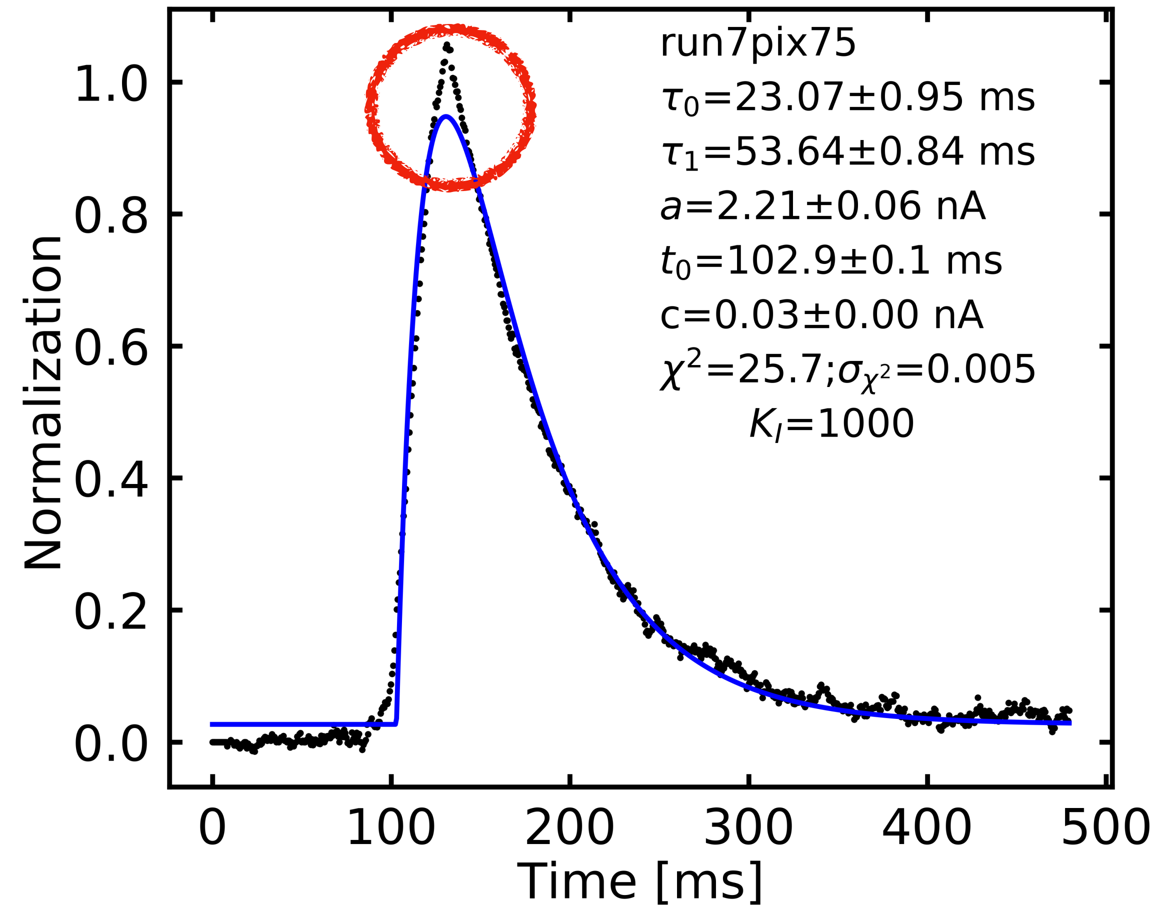

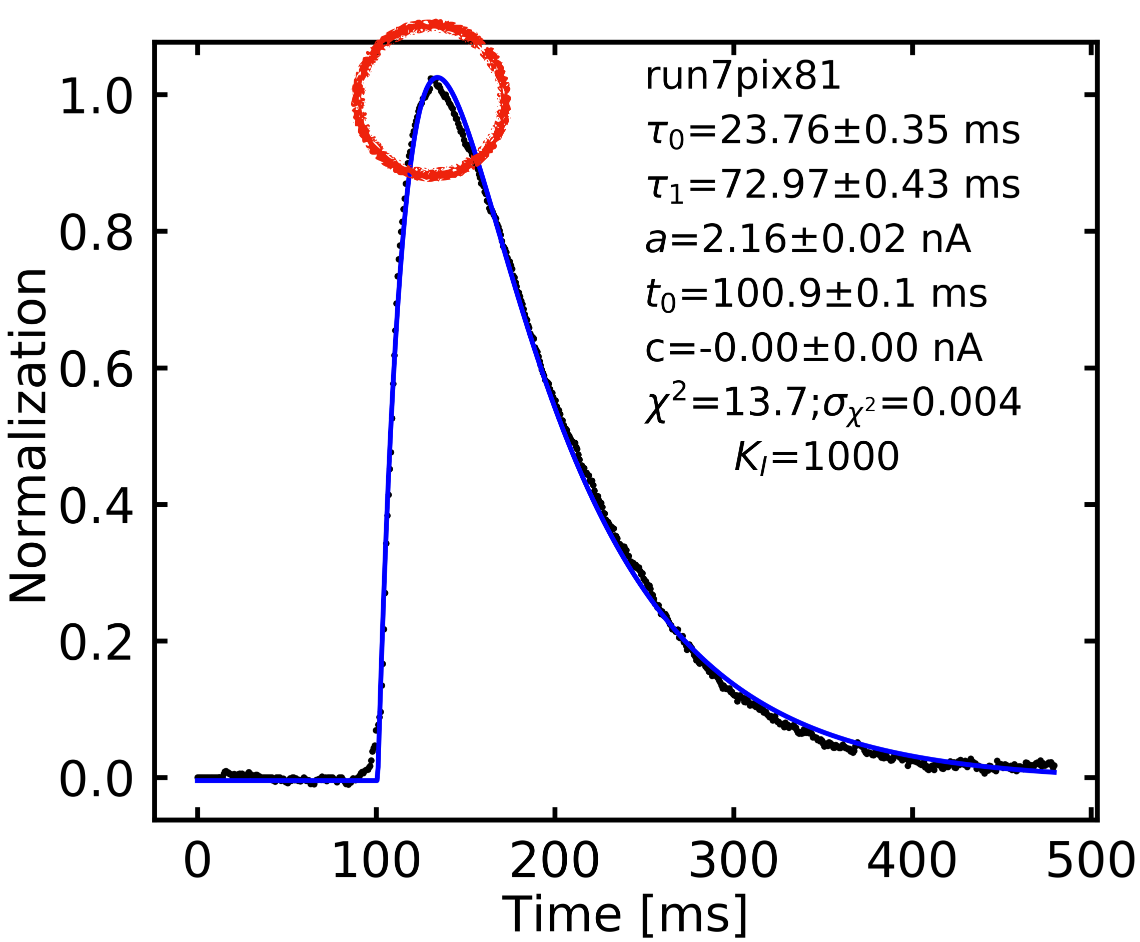

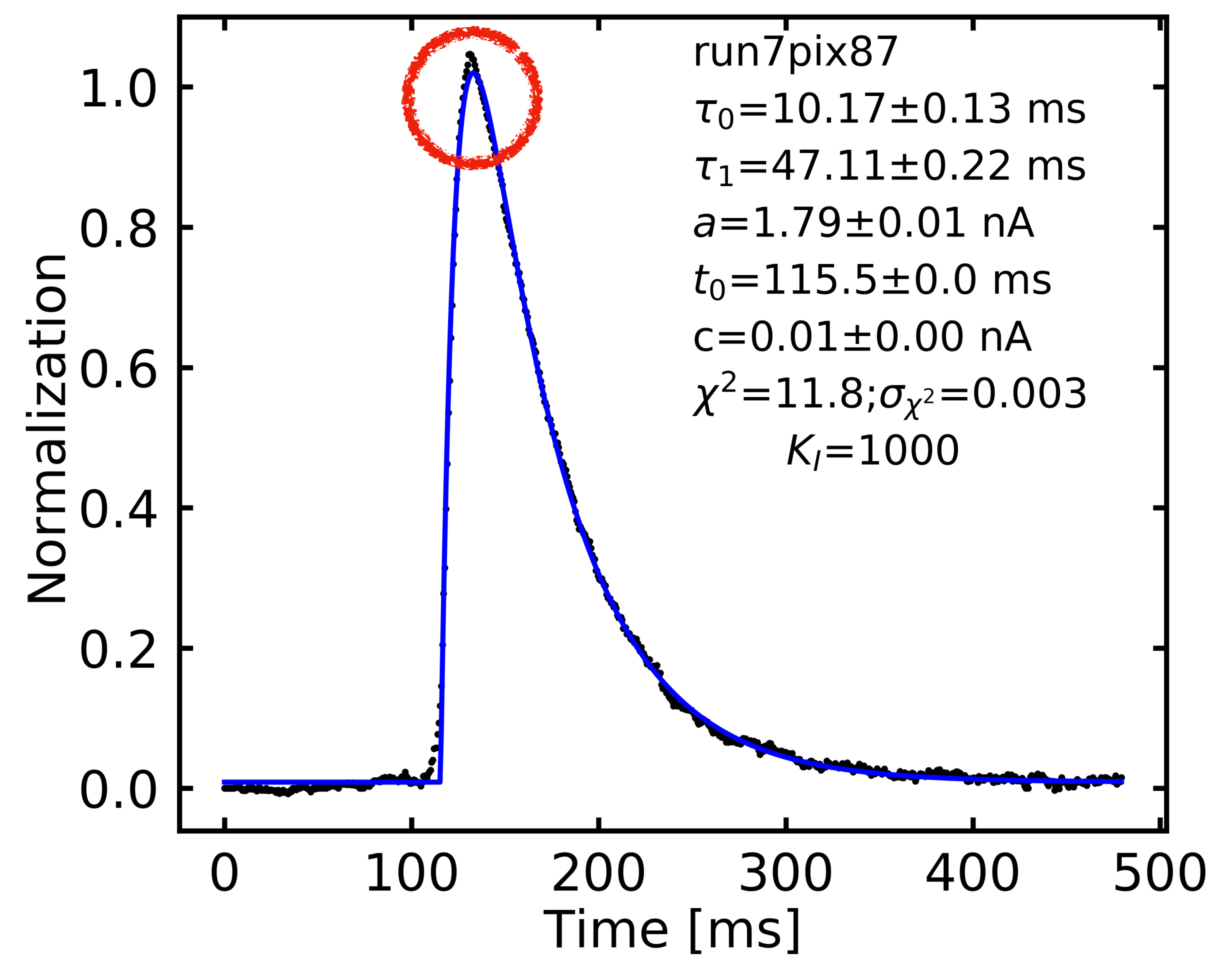

LiteBIRD basic parameter

Table 6.1. LiteBIRD basic parameters

	Low Frequency Telescope (LFT)	High Frequency Telescope (HFT)
Frequency	34 ~ 161 GHz	89 ~ 448 GHz
field of view	> 20 deg ×10 deg	> 20 deg ×10 deg
aperture diameter	400 mm	300 mm
angular resolution	20 ~ 70 arcmin	10 ~ 40 arcmin
rotational HWP	91 rpm	110 rpm (MFT)/ 223 rpm (HFT)
number of detectors	~1000	~2100
data sampling rate	22 Hz	46 Hz
Uncertainty of r	$\delta r < 1 \times 10^{-3}$	
Observation period	3 years	
Scan	L2 Lissajous, precession angle 45 deg, spin angle 50 deg (0.1 rpm)	
Sensitivity	$< 3\mu$K·arcmin	
pointing offset knowledge	< 2.1 arcmin	
focal plane array	bath temperature 100 mK $\mathrm{NET}^{p}_{\mathrm{array}} = 1.7\mu\mathrm{K}\cdot\sqrt{s}$ detector $f_{\mathrm{knee}} < 20$ mHz	
data transfer	7 GByte/day	
mass	2.6 ton	
electrical power	3.0 kW	

7.4. Stacking glitches & Median glitches methods

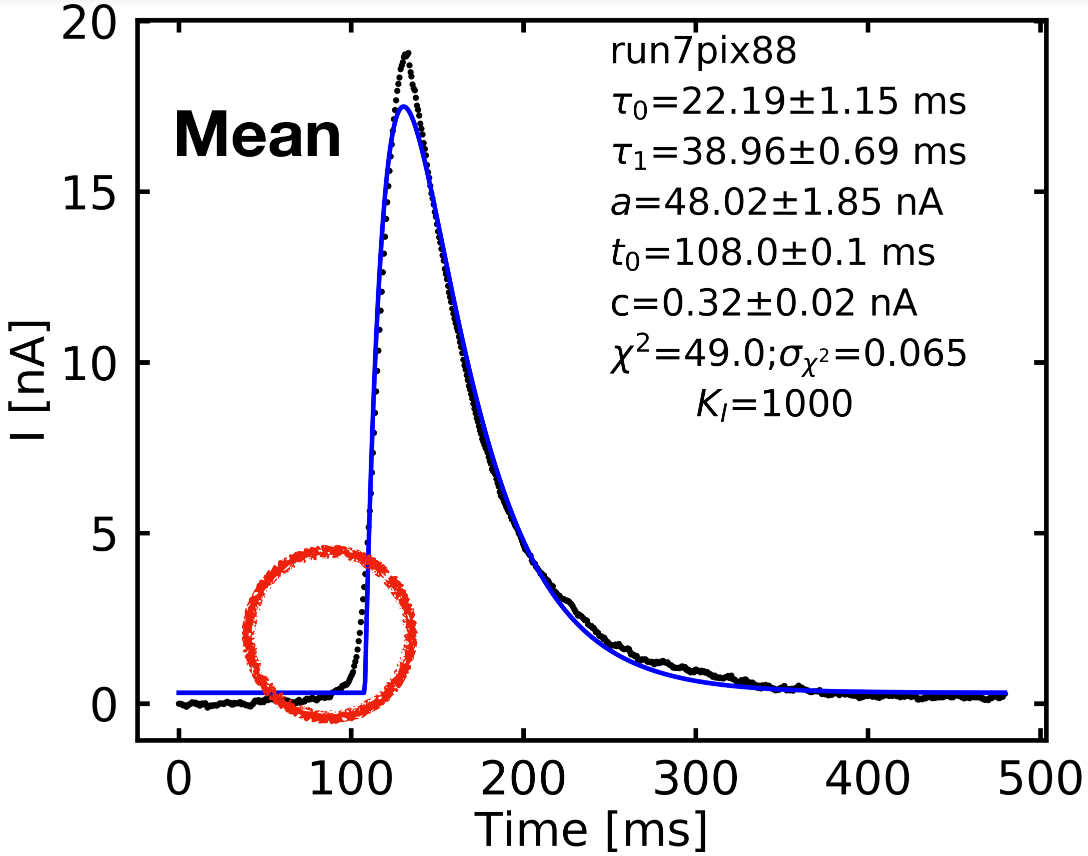

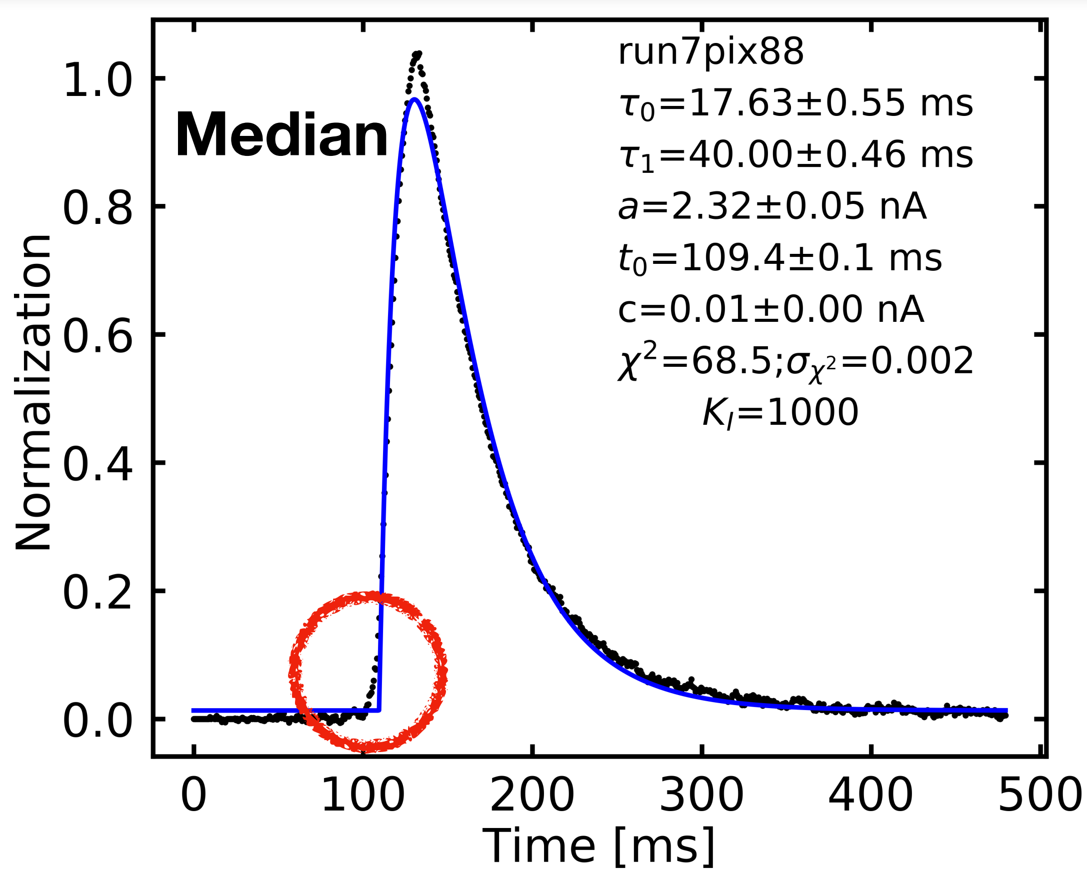

Run	V_{bias} (μV)	K_I	Pixel	Glitches	τ_0 (ms)	τ_1 (ms)	a (nA)
7	5	1000	69	80	11.41±0.15	64.31±0.33	33.28±0.38
7	5	1000	70	54	7.89±0.16	35.91±0.27	54.25±2.08
7	5	1000	75	77	23.07±0.95	53.64±0.84	37.01±1.28
7	5	1000	81	94	23.76±0.35	72.97±0.43	32.15±0.70
7	5	1000	87	70	10.17±0.13	47.11±0.22	36.52±0.53
7	5	1000	88	130	17.63±0.55	40.0±0.46	48.02±1.85
7	5	1000	93	75	15.99±0.36	43.33±0.36	51.14±2.14
7	5	1000	106	23	35.57±1.34	71.84±1.05	86.54±15.32
7	5	1000	107	73	60.72±9.75	39.01±1.35	103.74±60.06

Different values: Scattering operating point TESs => effect of ETF. SQUID non-uniform

Cross talk evidence in the second population of time constant

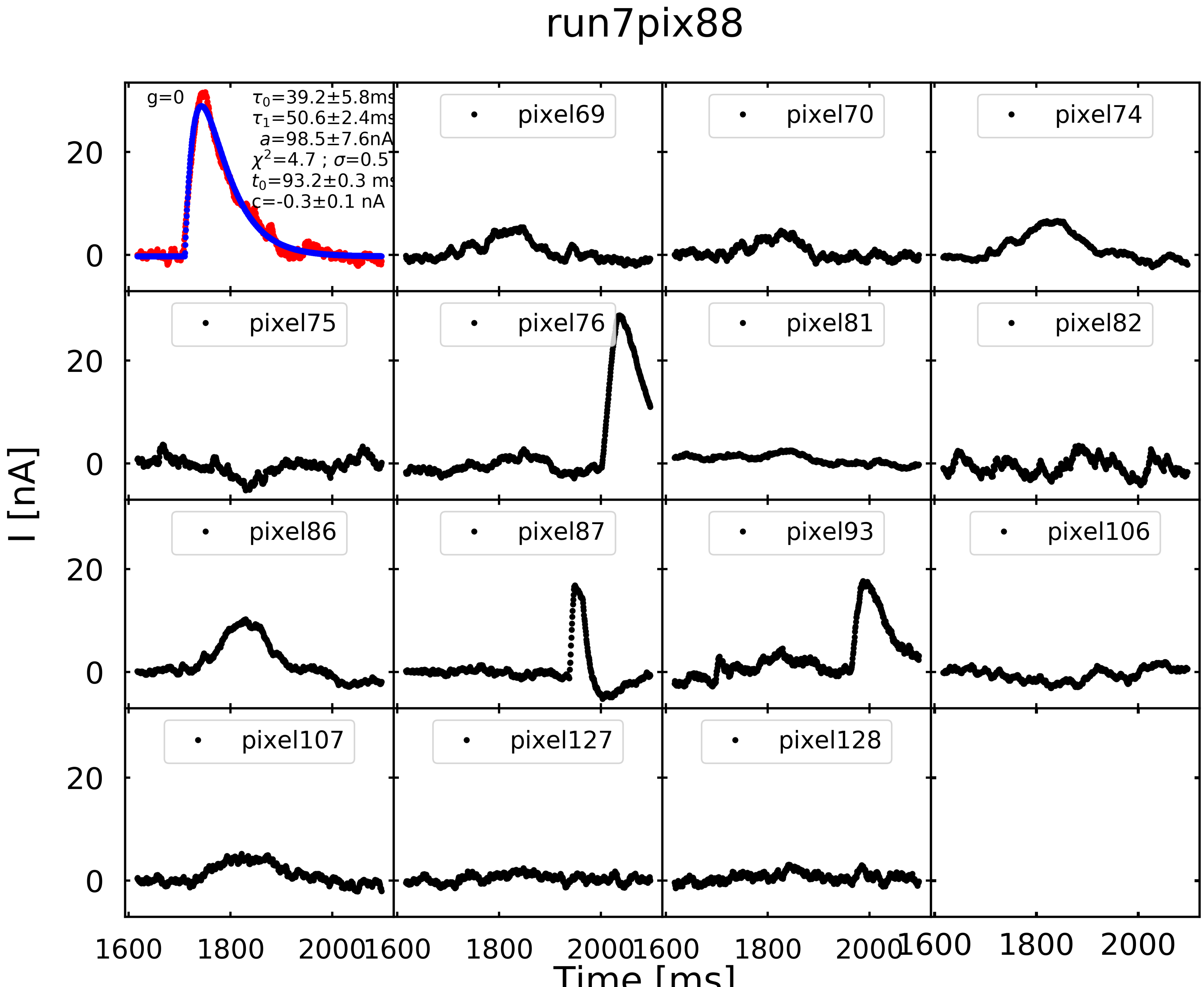

QUBIC general information

Name tag	Information
Instrument Diameter	< 1.6 m
Instrument Height	< 1.8m
Instrument Weight	< 800 kg
Window diameter	39.9 cm
Filters diameters	39.2 cm
Polarizer diameter	32.6 cm
Half-Wave plate diameter	32.7 cm
Back-to-back Horn array	400 (diameter 33.078 cm)
Optical combiner focal length	30 cm
M1 shape and diameter	480mm $\times$ 600 mm
M2 shape and diameter	600 mm $\times$ 500 mm
Frequency channels	150 GHz and 220GHz
Bandwidth	25 %
Primary beam FWHM at 150 GHz, 220 GHz	12.9° , 15°
Blue center peak FWHM 150GHz, 220GHz	23.5 arcmin, 16 arcmin
Number of bolometers / focal plane	1024
Detector stage temperature goal	320 mK
Bolometers NEP	$5 \times 10^{-17} W.Hz^{-1/2}$
Scientific Data sampling rate	100 Hz
Bolometers time constant	< 10 ms
TES size	2.6 mm
Rotation in azimuth	-220° / + 220°
Rotation in elevation	+30° / +70°
Rotation around the optical axis	-30° / +30°
Pointing accuracy	< 20 arcsec
Angular speed	Adjustable between 0 and 5°/s with steps < 0.2°/s

Scanning strategy: We perform azimuth scan of 40 degrees fixing the HWP angle. After we change HWP angle and the elevation (ranging from 45 to 65 degrees) then scan again in azimuth.

The practical TES bias circuit

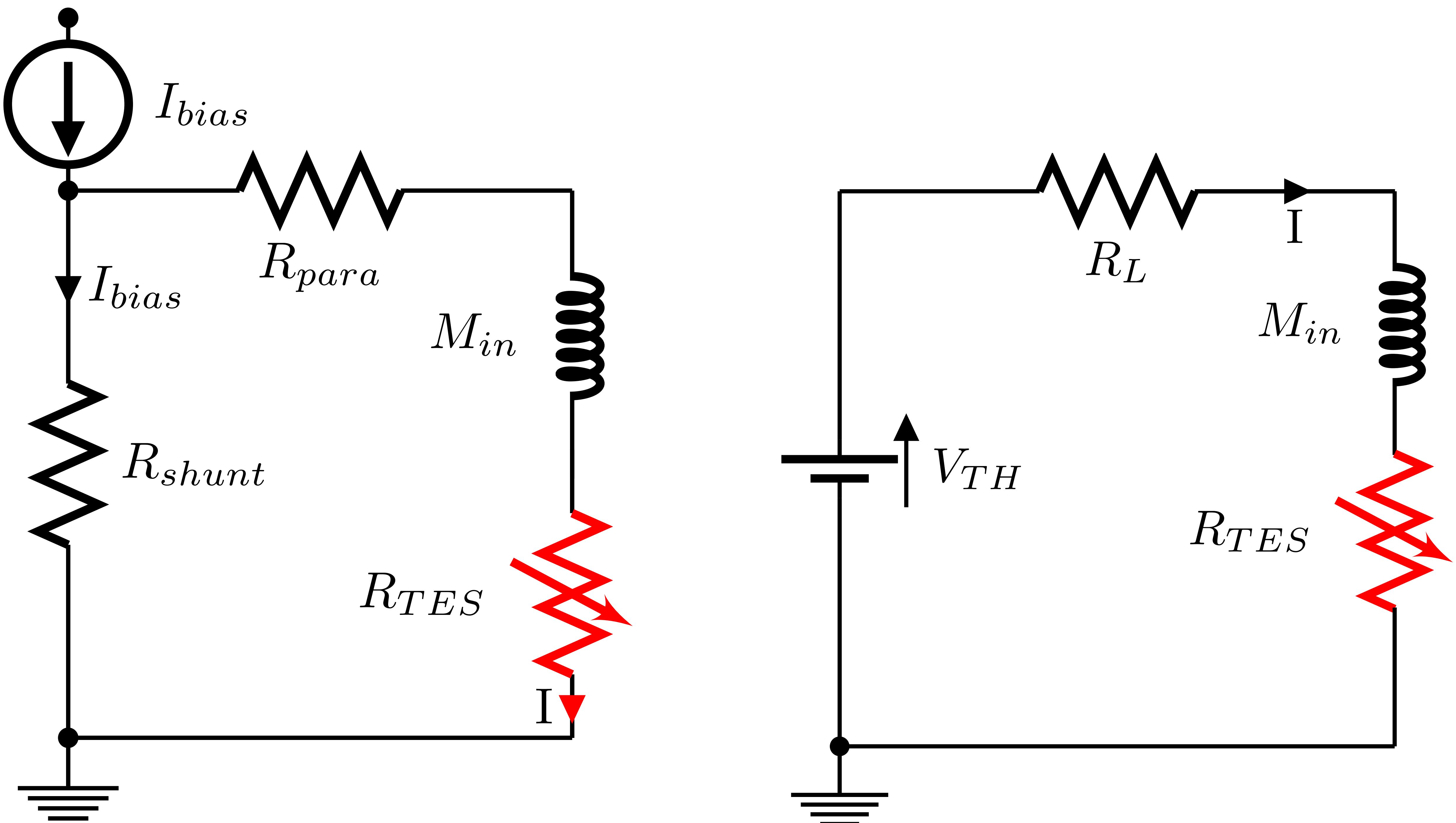

The logarithmic sensitivity to temperature

$$\alpha \equiv \left.\frac{\partial \log R}{\partial \log T}\right|_{I_0} = \left.\frac{T_0}{R_0}\frac{\partial R}{\partial T}\right|_{I_0}$$

$$\mathscr{L} \propto \alpha$$

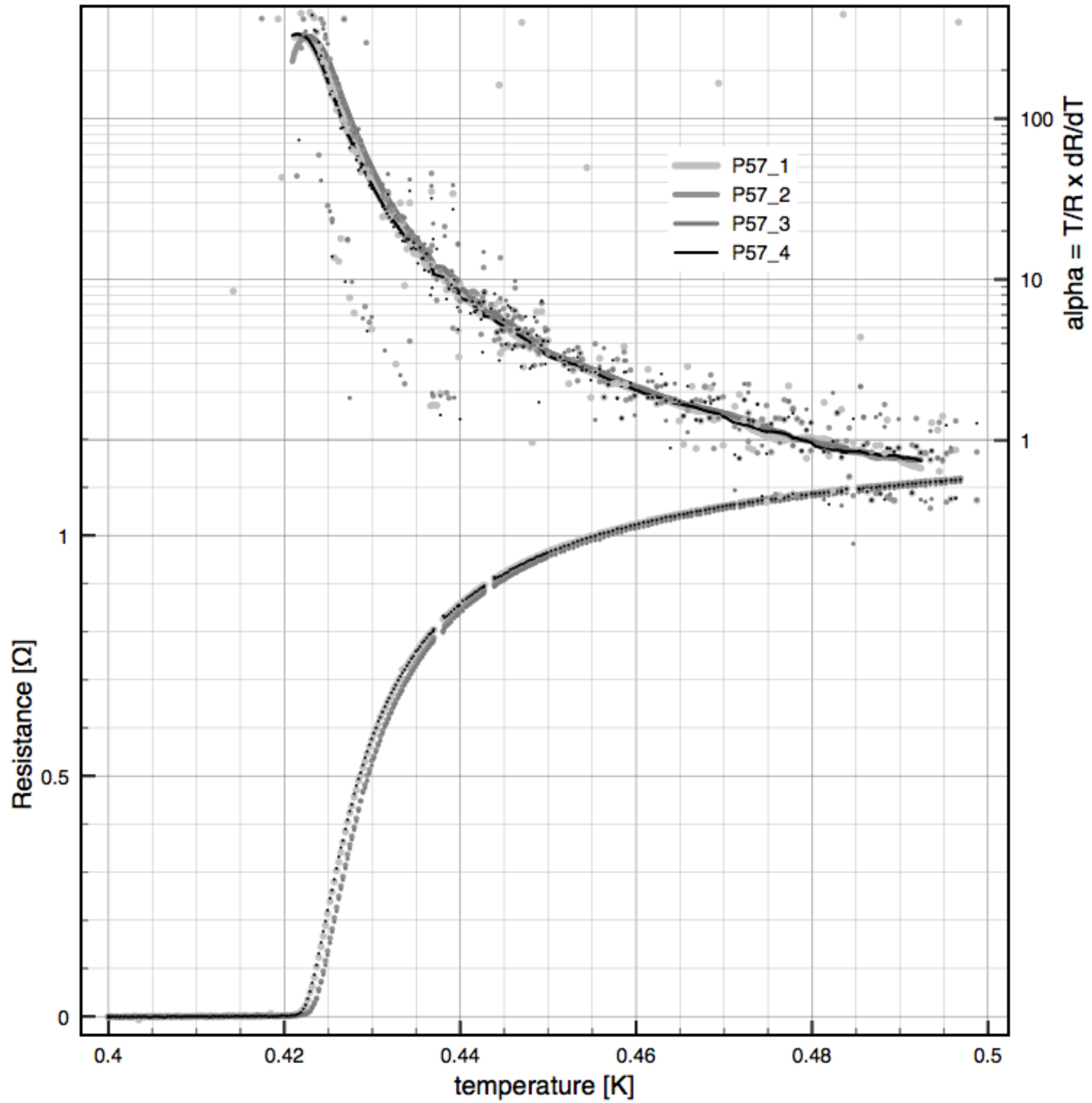

IV curves measurements

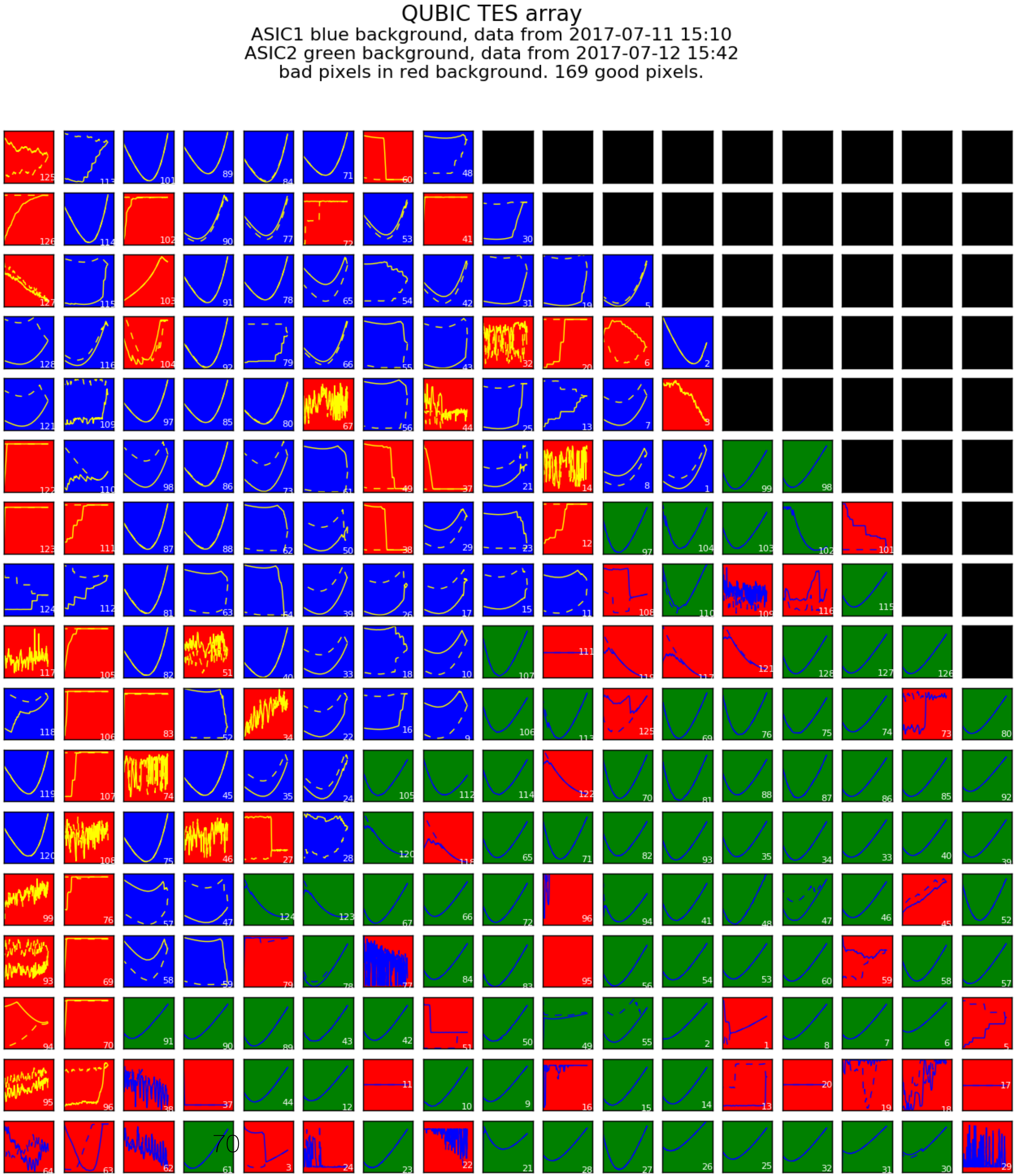

Blue: ASIC1
Green: ASIC2

The scan strategy and possible sky patches

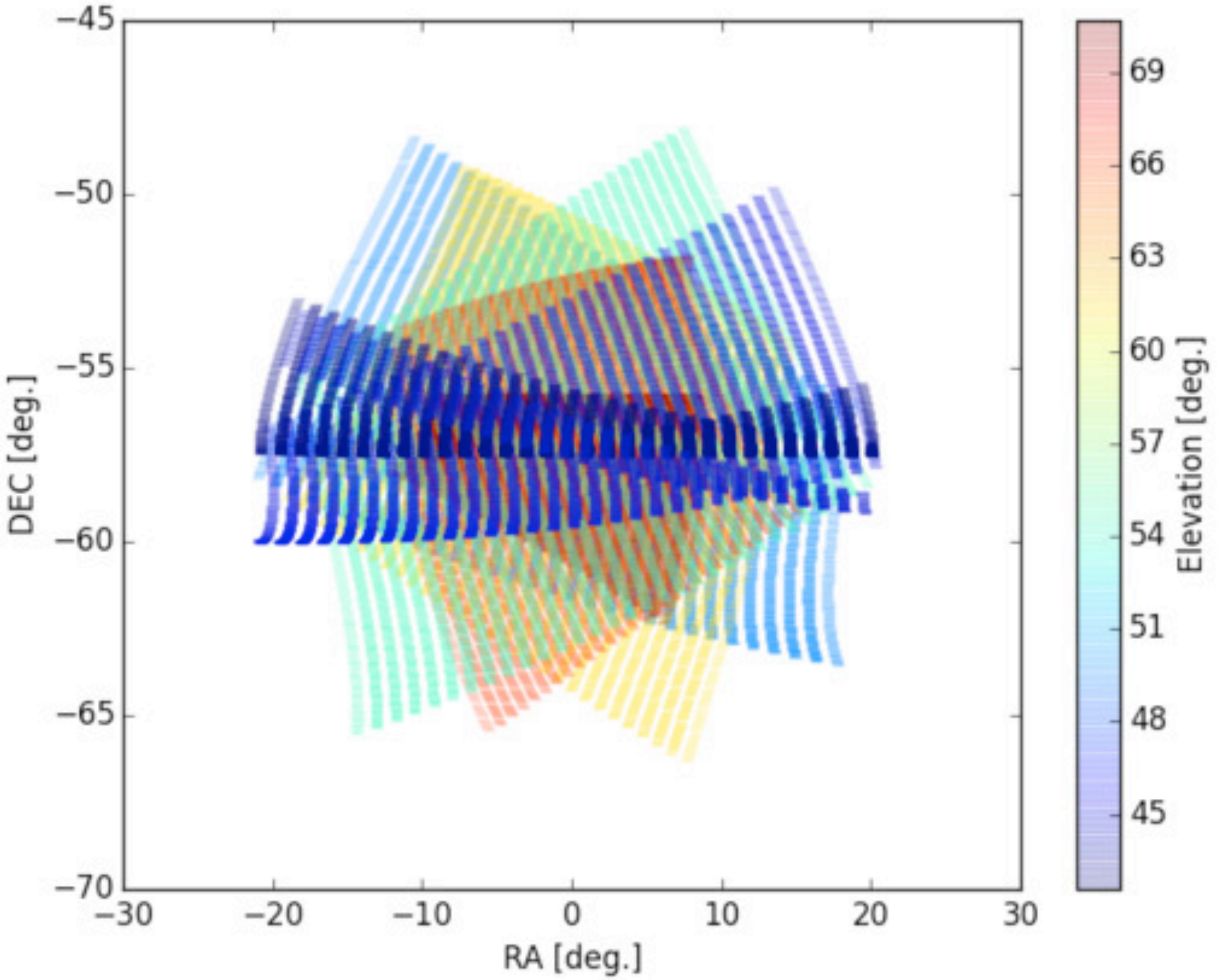

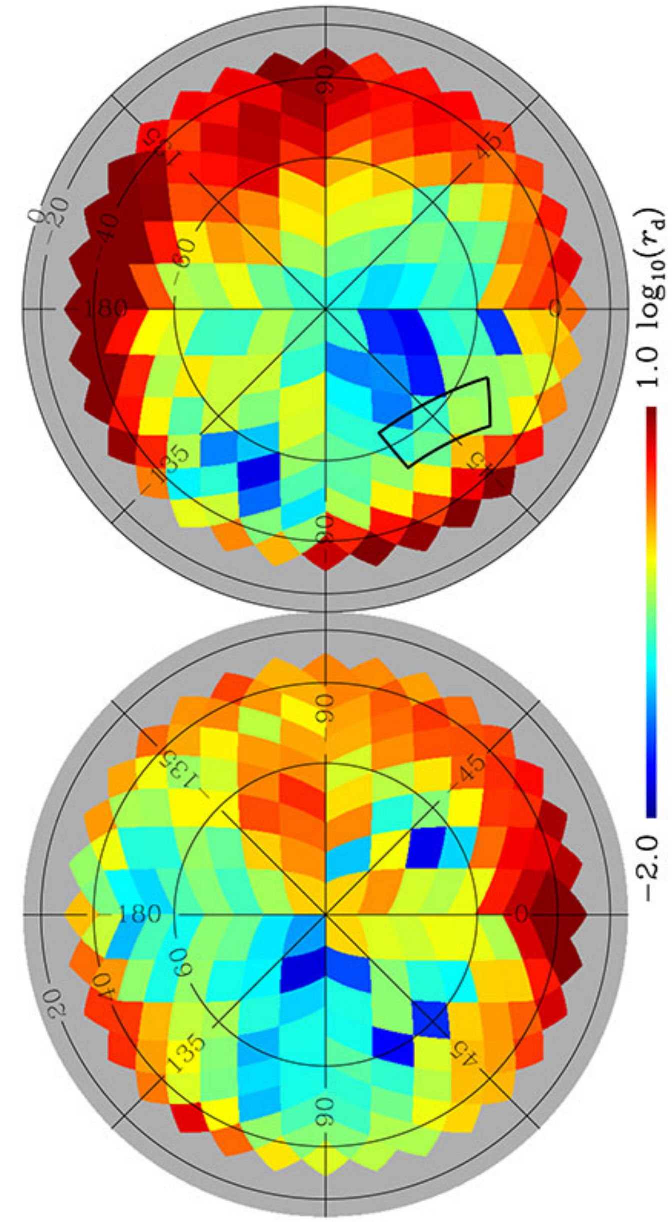

Scanning strategy in local coordinate:

We perform azimuth scan of 40 degrees fixing the HWP angle. After we change HWP angle and the elevation (ranging from 45 to 65 degrees) then scan again in azimuth.

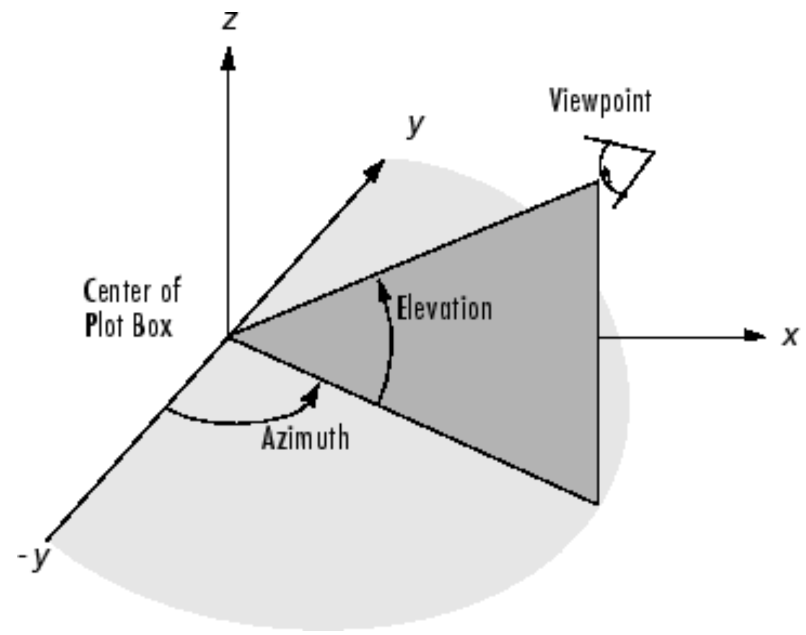

TES technologies

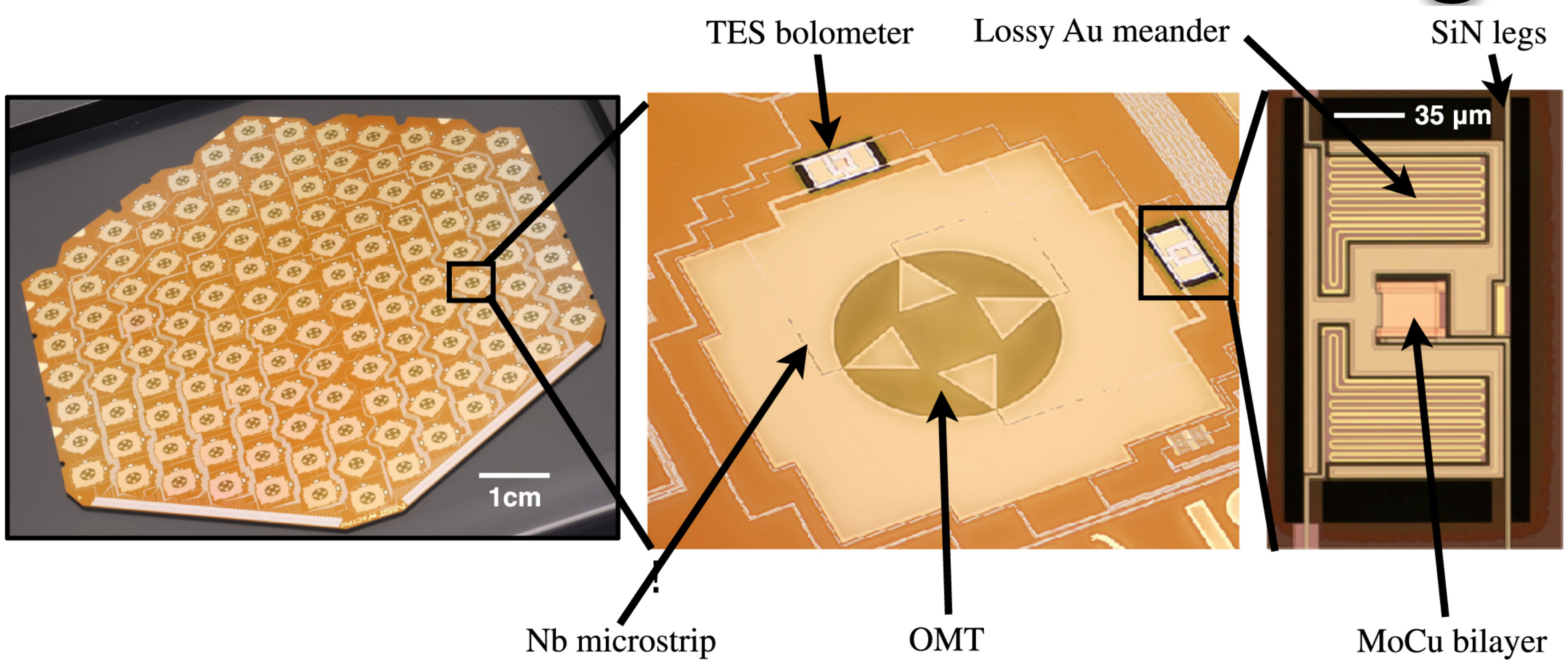

NIST (OMT tech, feed-horn) ACT, SPT, LiteBIRD (High frequency) …

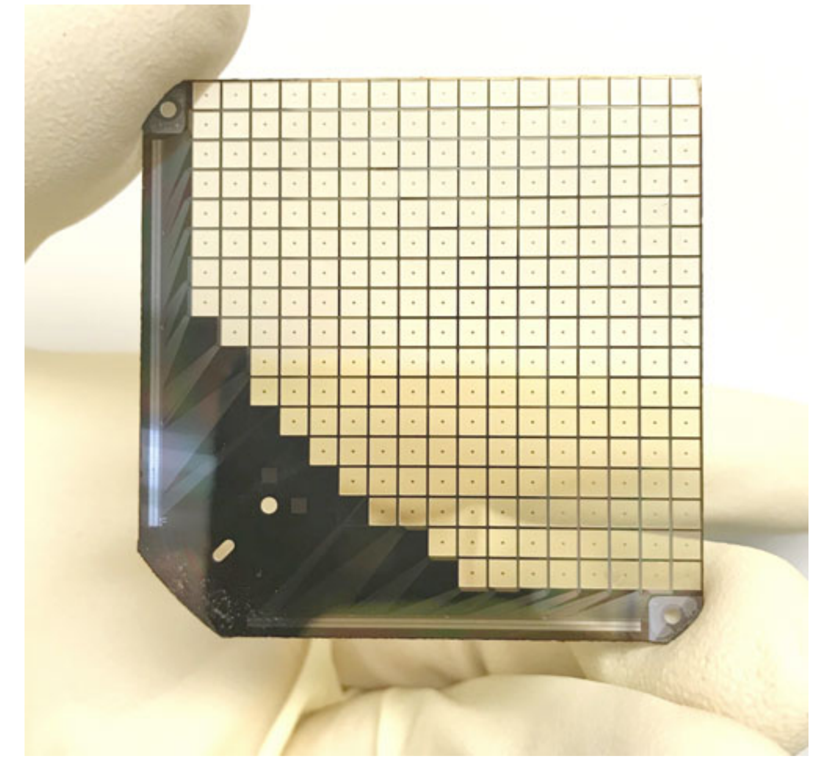

APC (no antenna tech) QUBIC

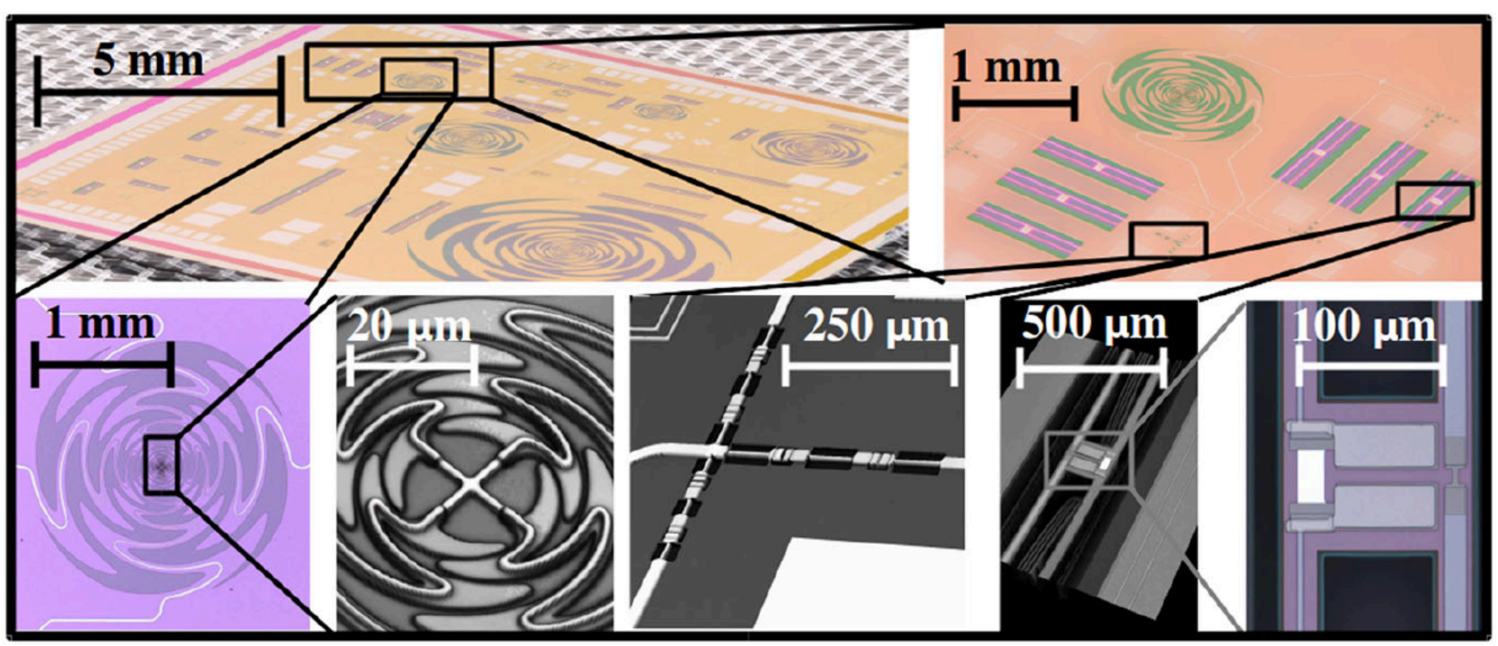

BERKELEY (planar sinuous antenna coupled TES tech) ACT, POLARBEAR, LiteBIRD (low-mid frequency)…

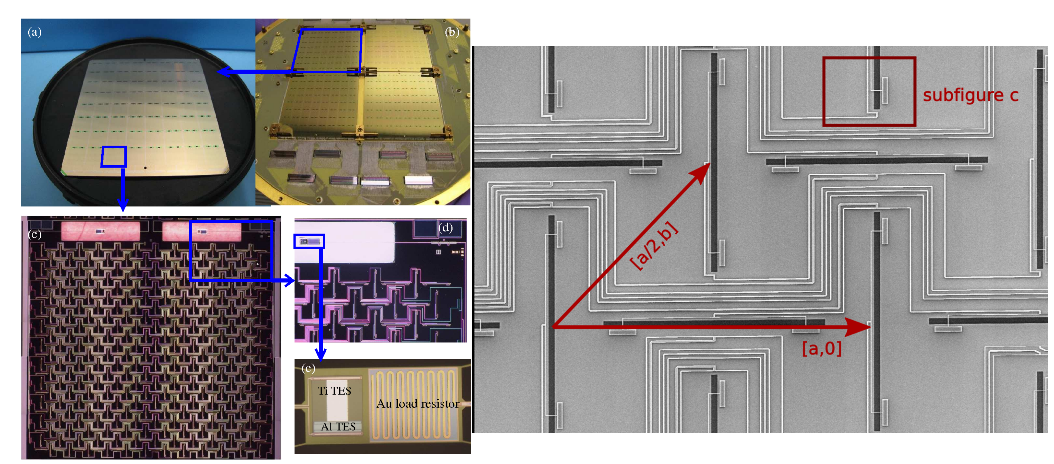

Caltech (planar antenna coupled TES tech), BICEPT

BCS theory

1 Vibrations of lattice are minimal (virtual phonons) below T_c

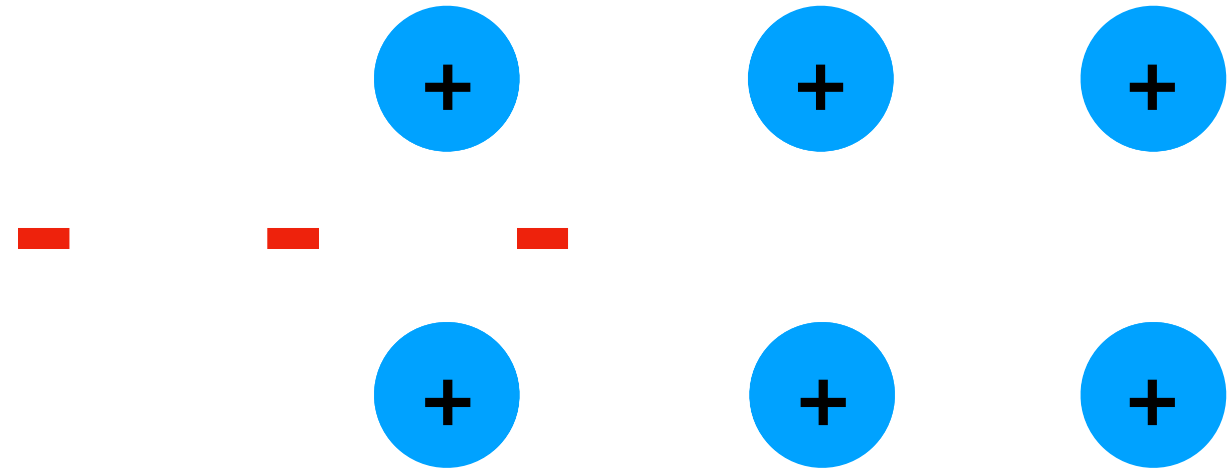

2 Electron traveling in front distorts the lattice

3 Virtual phonons moved closer

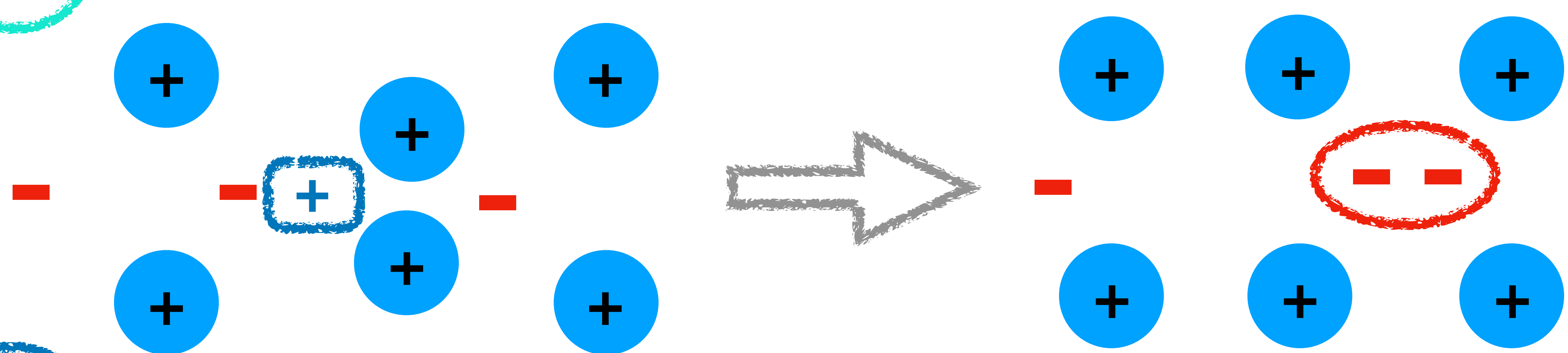

4 A positive region created behind the 1st electron

5 The 2nd electron is attracted to the positive region and the lattice rebounds back into its original shape